

https://dspace.org/

Senecio serratuloides var. in wound healing: efficacy and mechanistic investigations in a porcine wound model

Gould, Alan Nicolas

2015-09-16
http://hdl.handle.net/10539/18679

Downloaded from a DSpace repository. https://dspace.org/

Senecio serratuloides var. in Wound Healing: Efficacy and Mechanistic Investigations in a Porcine Wound Model

Alan N Gould

A dissertation submitted to the Faculty of Health Sciences, University of the Witwatersrand, in fulfilment of the requirements for the degree of Doctorate of Philosophy.



Table of Contents

Acknowledgments iv

Declaration vi

List of Tables vii

List of Figures viii

List of Abbreviations and Nomenclature x

Publications xii

Presentations xiii

Abstract xiv

Chapter 1 - Introduction and Background 1

1.1 Introduction 1

1.2 Background 2

1.2.1 Regions of Origin 2

1.2.2 Wound Models 3

1.2.3 Gross Assessment 11

1.2.4 Process of Wound Healing 11

1.2.6 Histological and Biochemical Analysis 20

1.2.7 Plant Compound Detection and Isolation 21

1.2.8 Current State of Wound Healing Investigations 22

1.2.9 Senecio serratuloides 23

1.3 Aims 25

Chapter 2 - Efficacy and Safety of *Senecio serratuloides* in treating Deep Partial Thickness and Full Thickness Wounds; Macroscopic and Histological Assessment 26

2.1 Introduction 26

2.2 Aims 27

2.3 Materials and Methods 28

2.3.1 Collection and Preparation of Plant Material 28

2.3.2 Animal Model and Test Groups 28

2.3.3 Wound sample Collection and Analysis 29

2.3.4 pH Measurement 29

2.3.5 Skin Biopsy Collection 33

2.3.6 Histological Analysis 33

2.3.7 Deep Partial Thickness Wound Morphometric Analysis 33
2.3.8 Full Thickness Wound Morphometric Analysis 34
2.3.9 Collagen Analysis 36
2.3.10 Safety Analysis of Liver Hepato-toxicity 39
2.3.11 Statistical Analysis 39
2.4 Results 40
2.4.1 Deep Partial Thickness Wound pH 40
2.4.2 Deep Partial Thickness Wound Gross and Histological Analysis 42
2.4.3 Morphometric Analysis 49
2.4.4 Collagen Analysis 56
2.5 Discussion 63
2.5.1 Experimental Wound Model 63
2.5.2 Wound pH 64
2.5.3 Deep Partial Thickness Wound Morphometric Analysis 65
2.5.4 Full Thickness Wound Morphometric Analysis 66
2.5.5 Collagen Deposition 66
2.6 Conclusion 69

Chapter 3 – Mechanistic Investigation of *Senecio serratuloides:* Cytokine, Tyrosine Phosphorylation and Proliferating Cell Nuclear Antigen Quantification 70
3.1 Introduction 70
3.1.2 The Role of Tyrosine Phosphorylation 71
3.1.3 Proliferating Cell Nuclear Antigen 73
3.1.4 Inflammatory Cytokines 73
3.2 Aims 77
3.3 Materials and Methods 78
3.3.1 Animal Model and Test Groups 78
3.3.2 Wound Exudate Collection and Analysis 78
3.3.3 Cytokine Analysis 78
3.3.4 Immunofluorescence Staining and Analysis 79
3.3.5 Section Imaging and Image Analysis 80
3.3.6 Statistical Analysis 81
3.4 Results 83
3.4.1 Cytokine Analysis 83
3.4.2 Tyrosine Phosphorylation and Cellular Proliferation 84
3.5 Discussion 88
3.6 Conclusion 91

Chapter 4 - Plant Extraction, Isolation and Partial Identification through Culture Based Proliferation Assays 92
4.1 Introduction 92
4.1.2 Previous Plant Based Studies 92
4.1.3 Approach to Identifying Potential Compounds of Interest 95
4.1.4 Alkaloid Detection and Characterisation – Gas Chromatography and Mass Spectrometry 95
4.1.5 Approach to Identifying Potential Compounds 98
4.1.6 In-vitro Wound Healing Assays 100
4.1.7 High-Throughput Assay Platform 101
4.2 Aims 103
4.3 Materials and Methods 104
4.3.1 Plant Extraction and Analysis 104
4.3.2 Proliferation Assays 105
4.3.3 Statistical Analysis 108
4.3.4 Extract Analysis 110
4.4 Results 111
4.4.1 Cell Culture and Proliferation Assay 111
4.4.2 Whole Plant Extract Proliferation Assay 113
4.4.3 Plant Fraction Proliferation Assay 115
4.4.4 Real Time Proliferation Assay 124
4.4.5 Gas Chromatography and Mass Spectrometry 128
4.5 Discussion 133
4.5.1 Cell Proliferation Assay 133
4.5.2 Gas Chromatography and Mass Spectrometry 135
4.6 Conclusion 140

Chapter 5 – Final Conclusion and Future Studies 141
5.1 Efficacy and Safety 141
5.3 Mechanistic Investigation 143
5.4 Plant Extraction and Culture 145

Chapter 6 – References 147

Chapter 7 - Appendix 163

Acknowledgments

With the submission of this thesis, it is important to acknowledge and thank a number of people…

- Firstly I would like to thank my parents, John and Lindy Gould. Without their support, I would not have been able to achieve what I have. Their sacrifices have never known any limits. I will always be grateful for the opportunities they have given me and with these I aspire to one day be like them. They are my heroes and biggest supporters.
- To my brother and sister, James and Dominique Gould, thank you for everything you have been through with me. It has been a challenging time but you made it exciting and have always supported me throughout.
- To my girlfriend Hayley Morgan, thank you for putting up with all the late nights in the lab and missing important events. You have been amazing to me all this time.
- To my colleagues Cameron Naidoo, Marlon Germon and Jan Pinchevsky. It has been a great privilege working with you. Thank you for the lengthy discussions, help and support.

From a professional perspective…

- I would like to thank the Central Animal Unit at the University of the Witwatersrand and in particular Sr. Mary-Ann Costello. Without her help the animal work would not have been a success. The lengthy discussions were never in vain.
- Dr. Chetan Patel and Dr. Ridwan Mia need special thanks for taking time from there busy schedules to assist with the animal work.
- I would like to thank the School of Anatomy for the use of the histology laboratory for all the tissue processing and slide preparation. Special thanks needs to be given to Mrs. Mortimer, Mrs. Rogers and Mrs. Ally for teaching and assisting me in this regard.
- I would like to thank Dr. Karolina Kuun for all the assistance in analysing the cytokines. Your help and expertise were invaluable.
- Importantly, I would like to thank Tracy Snyman, from the Department of Chemical Pathology for all her help and assistance in extracting and fractionating the plant. Furthermore the use of the gas chromatograph and mass spectrometer proved invaluable in this project.

- To the Department of Surgery, I would like to thank Professor Veller and Professor Smith for allowing me to pursue my research in the department. To the staff of the department, thank you for all the assistance over this time.
- I would also like to thank and acknowledge the following organisations for assistance with funding the project:
    - The Percy Fox Foundation
    - Investec
    - The David Lurie Trust

To my supervisors…

Dr. Clem Penny has been extremely accommodating in allowing me to work in his laboratory. Without his training in cell culture techniques and immunofluorescence work this project would not have been possible.

Lastly to Professor Geoffrey Candy, my time in the Department of Surgery has been one of the biggest learning experiences of my life. You were willing to take on a student with minimal experience. You entertained any ideas that I had and helped me develop many of the approaches used in this thesis. With all the plans that we discussed, I hope that this project is the beginning of greater things to come. Thank you for everything that you have done and thank you for all the opportunities you have given me.

Declaration

I declare that the work contained in this thesis is my own. It is being submitted for the degree of Doctor of Philosophy in the Faculty of Health Sciences, University of the Witwatersrand, Johannesburg. The work contained here has not been submitted for any degree or examination in this University, or any other University.

……

Alan N Gould

……..day of ……

I certify that the work contained here pertaining to the animal studies have the approval of the Animal Ethics Research Committee, ethics approval number is 2008/15/04 and the clearance certificate can be seen in the appendix.

……

Alan N Gould

……..day of ……

List of Tables

Table 1.1. Pubmed search results for “wound healing” and “traditional medicine”.....4

Table 1.2. Components active in the various stages of wound healing.....14

Table 2.1. Wound pH at specific post-operative days. 40

Table 2.2. Epidermal thickness measurements (µm) at specific post-operative days.....50

Table 2.3. Epidermal thickness ratio at specific post-operative days 50

Table 2.4. Full thickness wound morphological analysis at specific post-operative days. 54

Table 2.5. Collagen content of the deep partial thickness wounds at specific post-operative days.....56

Table 2.6. Full thickness wound collagen analysis at specific post-operative days.. 60

Table 2.7. Screen for potential pyrrolizidine alkaloid toxicity. 62

Table 3.1. Tabulation of the recognised growth factors and associated receptor activity known to be beneficial in the wound healing process. 72

Table 3.2. Flow Cytometer Parameters as run on the FACSArray Flow Cytometer. 79

Table 3.3. Cytokine concentrations at day 5 post-operative.....83

Table 3.4. Epidermal tyrosine phosphorylation (4G10 MFI) at specific post-operative day 84

Table 3.5. Epidermal proliferation (PCNA MFI) at specific post-operative days.....86

Table 4.1. Selected studies where plants used for wound healing have been assessed for potential active compounds. 94

Table 4.2. GCMS data for the relevant alkaloid bases. 99

Table 4.3. Description of the various extractions and resultant fractions. 105

Table 4.4. Percentage reductions of the optimisation of the resazurin based assays. 111

Table 4.5. Percentage reductions of the whole plant extract.....113

Table 4.6. Percentage reduction of Wash 1 fraction of the acidic, neutral and basic extracts. 116

Table 4.7. Percentage reduction of Wash 2 fraction of the acidic, neutral and basic extracts. 118

Table 4.8. Percentage reduction of Elution 1 fraction of the acidic, neutral and basic extracts. 120

Table 4.9. Percentage reduction of Elution 2 fraction of the acidic, neutral and basic extracts. 122

Table 4.10. Real time assay with the two fractions where activity was shown at 4 hours.....125

Table 4.11. Gradient and rate comparison of the fractions where activity was seen. 128

Table 4.12. GCMS results.....132

List of Figures

Figure 1.1. Phases of wound healing. 13
Figure 1.2. Senecio serratuloides. 23
Figure 2.1. Preparation of the dorsum of the pigs. 30
Figure 2.2. A schematic diagram of one of the 2.5 by 2.5 cm deep partial thickness experimental wounds 31
Figure 2.3. Dressings used to hold the treatments in place. 32
Figure 2.4. Representative full thickness wound with the measurements labelled. 35
Figure 2.5. Picrosirius red analysis algorithm. 38
Figure 2.6. Wound pH plotted against time (Days post-operative). 41
Figure 2.7. Wounds viewed on day 2 post-operative 43
Figure 2.8. Wounds viewed on day 5 post-operative 44
Figure 2.9. Wounds viewed on day 7 post-operative 45
Figure 2.10. Wounds viewed on day 9 post-operative 46
Figure 2.11. Wounds viewed on day 12 post-operative 47
Figure 2.12. Wounds viewed on day 16 post-operative 48
Figure 2.13. The mean epidermal thickness of the deep partial thickness wounds plotted against time (Days post-operative). 51
Figure 2.14. Epidermal thickness ratio (mean) of the deep partial thickness wounds plotted against time (Days post-operative). 52
Figure 2.15. Mid-dermal deficit plotted against time (Days post-operative). 55
Figure 2.16. Deep partial thickness wounds post Picrosirius red staining. 57
Figure 2.17. Collagen content of the deep partial thickness wounds plotted against time (Days post-operative). 58
Figure 2.18. Full thickness wounds seen as the entire section above with the corresponding area analysed for collagen deposition below. 59
Figure 2.19. Full thickness wound collagen content plotted against time (Days post-operative). 61
Figure 3.1. Immunofluorescence analysis algorithm 81

Figure 3.2. Epidermal tyrosine phosphorylation (4G10 MFI) plotted against time (Days post-operative).. 85
Figure 3.3. Epidermal Proliferation (PCNA MFI) plotted against time (Days post-operative)..... 87
Figure 4.1. Common alkaloid nuclei making up a major classification system..... 97
Figure 4.2. Reduction of the Resazurin dye..... 101
Figure 4.3 Graphical representation of the optimisation experiments plotted against time (hours). .. 112
Figure 4.4. Graphical representation of the percentage reduction of the whole plant extract at 4 hours post treatment. 114
Figure 4.5. Graphical representation of the percentage reduction of the Wash 1 fraction at 4 hours post treatment. 117
Figure 4.6. Graphical representation of the percentage reduction of the Wash 2 fraction at 4 hours post treatment. 119
Figure 4.7. Graphical representation of the percentage reduction of the Elution 1 fraction at 4 hours post treatment.. 121
Figure 4.8 Graphical representation of the percentage reduction of the Elution 2 fraction. 123
Figure 4.9. Real time assay of the two lead fractions compared to the controls. 126
Figure 4.10. Analysis of the first 4 hours of the real time proliferation assay. 127
Figure 4.11. Gas chromatogram of the 2nd elution of the neutral extract..... 130
Figure 4.12. Gas chromatogram of the 2nd elution of the basic extract…… 131

List of Abbreviations and Nomenclature

4G10 – Trade name for antibodies directed at phosphorylated tyrosine residues

ADD – Average Dermal Deficit

BSA/PBS – Bovine Serum Albumin/Phosphate Buffered Saline

COX - Cyclooxygenase

DMEM – Dulbecco's Modified Eagle's Medium Dulbecco's

DPT – Deep Partial Thickness

EGF – Epidermal Growth Factor

ER – Epidermal Thickness

ERK – Extracellular Signal-Related Kinase

ET – Epidermal Thickness

FGF-10 – Fibroblast Growth Factor - 10

FGF-2 – Fibroblast Growth Factor - 2

FGF-7 – Fibroblast Growth Factor - 7

FT – Full Thickness

GCMS – Gas Chromatography coupled to Mass Spectrometry

HGF – Hepatic Derived Growth Factor

HLB – Hydrophobic Lipophilic

HPLC – High Performance Liquid Chromatography

IGF – Insulin-like Growth Factor

IL-10 – Interleukin - 10

IL-12 – Interleukin - 12

IL-1α and β – Interleukin – 1 alpha and beta

IL-6 – Interleukin - 6

IL-8 – Interleukin - 8

Jak/STAT – Janus kinase / signal transducer and activator of transcription pathway

LFT – Liver Function Test

m/z – Mass to Charge Ratio

MAPK – Mitogen-Activated Protein Kinase Pathway

MFI – Mean Fluorescent Intensity

MMP/TIMP – Matrix Metalloproteinases/Tissue Inhibitors of Metalloproteinases

NGF – Neuronal Derived Growth Factor

NIST – National Institute of Science and Technology

NMR – Nuclear Magnetic Resonance

NO - Nitric Oxide

PCNA – Proliferating Cell Nuclear Antigen

PDGF – Platelet Derived Growth Factor

PE – Phycoerythrin Fluorochrome

PGE – Prostaglandin E

PLC-γ – Phospholipase C-γ Pathway

PSR – Picrosirius Red

PTB – Phosphotyrosine-binding

ROI – Region of Interest

RTK – Receptor Tyrosine Kinase

SH2 – Src homology 2

SPE – Solid Phase Extraction

TGF-β – Transforming Growth Factor - *beta*

TLC – Thin Layer Chromatography

TNF-α – Tumour Necrosis Factor - alpha

VEGF – Vasoendothelial Growth Factor

WHO – World Health Organisation

Publications

Arginine Metabolism and Wound Healing. Gould, AN., Naidoo, CA., Candy, GP. *Wound Healing Southern Africa*. 2008. **1**(1): 48-50.

Matrix Metalloproteinase inhibition and anti-biotics in the treatment of chronic wounds. Naidoo, CA., Gould, AN., Peters, J., Candy, GP. *Wound Healing Southern Africa*. 2009. **2**(2): 71-73**.**

The role of advanced glycation end products in the hyperinflammatory response of diabetic wounds. Candy, GP., Gould, A., Naidoo, C., Kruger, D. *Wound Healing Southern Africa. 2011.* ***4****(1):25-28.*

Enhanced Cutaneous Wound Healing by *Senecio serratuloides* (DC) in a Pig Model. Gould, AN., Penny, CB., Patel, CC., Candy, GP. South African Journal of Botany. Submitted for review, 2014.

Presentations

2008

Bert Myburg Research Day, Department of Surgery, University of the Witwatersrand, Johannesburg.

2009

Surgical Research Symposium, Department of Surgery, University of the Witwatersrand, Johannesburg.

Interfaculty Research Symposium, University of the Witwatersrand.

Bert Myburg Research Day, Department of Surgery, University of the Witwatersrand, Johannesburg.

2010

Surgical Research Symposium, Walter Sisulu University, East London.

Faculty of Health Sciences Research Day, University of the Witwatersrand.

SA Society for Basic and Clinical Pharmacology, Cape Town.

2011

Surgical Research Symposium, University of Pretoria, Pretoria.

Bert Myburg Research Day, Department of Surgery, University of the Witwatersrand, Johannesburg.

2012

Bert Myburg Research Day, Department of Surgery, University of the Witwatersrand, Johannesburg.

2014

Surgical Research Symposium, University of Kwazulu Natal, Durban.

Bert Myburg Research Day, Department of Surgery, University of the Witwatersrand, Johannesburg.

Abstract

Introduction

Senecio serratuloides is widely used for wound healing in South Africa but minimal information regarding its efficacy is available. Furthermore toxic pyrrolizidine alkaloids may be present. The following investigation sought firstly to evaluate the efficacy and safety of *Senecio serratuloides* in a porcine wound model*;* secondly to assess for a potential mechanism and finally isolate and identify fractions in *in-vitro* assays.

Assessment of Efficacy and Safety

Materials and Methods: Deep partial thickness and full thickness wounds were created on 9 pigs. Treatment included an occlusive dressing (negative control), activated carbon, or the *Senecio* preparation. Wounds were monitored using photographic documentation, pH measurement and histological analysis (skin thickness and collagen content). Toxicity was monitored on blood and liver samples.

Results and Discussion: Efficacy of *Senecio serratuloides* was established with a significantly thicker epidermis, maximal at day 7 post-operative, 2 days before the controls. Effects on collagen content was negligible with no toxicity detected.

Mechanistic investigation

Materials and Methods: Wound fluid was analysed for IL-10, IL-12, IL-1β, IL-6, IL-8, TNF-α using flow cytometry based assays. Tyrosine phosphorylation and cellular proliferation was assessed using dual immunofluorescence staining.

Results and Discussion: IL-1β levels were significantly greater in the *Senecio* treatment. Tyrosine phosphorylation increased to day 9 post-operative where it stabilised in all groups. In the same period, cellular proliferation was sustained in the *Senecio* treated wounds but not in the controls. Keratinocyte proliferation was identified as the target for *in-vitro* assays.

Extraction, Isolation and Partial Identification using In-vitro Proliferation Assays.

Materials and Methods: The plant was fractionated using solid phase extraction cartridges. Keratinocytes were grown under standard conditions in 96-well plates. Cellular proliferation was assessed spectrophotometrically using a resazurin dye technique. Active fractions were analysed using gas chromatography and mass spectrometry.

Results and Discussion: Identified fractions increased the rate of proliferation by 300-400%. Potential lead compounds were identified. Importantly, pyrrolizidine alkaloids could not be detected.

Conclusion

Senecio serratuloides is efficacious in treating deep partial thickness wounds without inducing liver toxicity. Sustained keratinocyte proliferation linked to tyrosine phosphorylation may be an underlying mechanism. Although successful, *in-vitro* detection of active fractions requires further characterisation.

Keywords: Senecio serratuloides, Wound healing, Porcine Wound Model, Deep partial thickness wound, Epidermal thickness, Collagen, Inflammatory cytokines, Tyrosine phosphorylation, Proliferating cell nuclear antigen, Plant extraction and fractionation, Proliferation assays, Gas chromatography and mass spectrometry, Alkaloids.

1.1 Introduction

Traumatic injury and surgical interventions create a wound that normally heals in an acceptable time period, leaving a scar that diminishes over time. Although most wounds can be treated at a modest cost, wounds in sick or diabetic patients can become infected and take longer to heal. Some of these may develop into a chronic wound that fails to heal. These wounds are therefore difficult to treat, can impact on the well-being of the patient, and delay the discharge of the patient from hospital with an associated cost to the patient or health care provider. The cost of caring for wounds to ensure healing in a developed country such as the United States of America was estimated to be approximately 16 billion dollars in 2012 (1). The increasing prevalence of non-communicable diseases of lifestyle, such as diabetes, will result in more diabetic wounds being treated and that often take longer to heal (2). Treating these chronic wounds will add significantly to the costs to the health care providers. Therefore considerable effort is being invested to find substances that will accelerate or improve outcomes in wound healing.

Sophisticated treatments have been developed in first world countries that are simply unaffordable and consequently unavailable in poorer developing countries. In these countries, the World Health Organisation (WHO) has reported that patients still rely heavily on traditional remedies and knowledge when caring for wounds (3). Such remedies are readily accessible at a low cost and are widely accepted by the community. However, as the treatment of wounds with unregistered remedies is seldom recorded by traditional healers, there is a lack of reliable information of the burden and the cost of treating wounds on health care systems in these countries.

There has always been an interest in traditional remedies from a personal consumer level, and more recently from the multinational pharmaceutical companies (4). It is well known that the origins of many pharmaceutical companies were based on traditional or folk remedies. For example, the original product of the pharmaceutical giant Bayer AG's, acetylsalicyclic, was marketed as Aspirin. Aspirin is derived from salicyclic acid, a folk remedy for headaches found in willow bark. Another instance, Metformin, was originally extracted from the French lilac plant, *Galega officinalis*, and used since the 1400s in the treatment of type 2 diabetes (5). It can therefore be seen that traditional remedies offer a potential source of lead compounds to treat disease and symptoms, including wound healing (6).

However, despite the major efforts invested in identifying novel agents which enhance wound healing, the very complexity of the wound healing process makes elucidating the effect of a single active compound difficult to determine. Although gross effects of a substance on wound healing may be measured, there is often a lack of evidence with regard to the mechanism of action to substantiate the use of these products, even when these products are produced by major industry players. A recent article has suggested this issue is being addressed (7). Furthermore the approach of measuring gross parameters would not be subtle enough to detect the effect of a single candidate compounds which acts at a particular point in time, or one that is effective only within a narrow concentration range during wound healing (8).

The complexity of wound healing and with somewhat limited samples available from experimental animal models, has resulted in a reductionist and simplified approach to determining the effects of novel compounds. Parameters and variables (to be discussed at a later time point) investigated in many studies describing the wound healing process often do not encompass the process entirely and this may simply be due to the overall complexity not permitting in-depth analysis (8). Therefore the question posed in the present study queries the ideal model with the appropriate variables for evaluation to screen for the efficacy of plant based therapeutic agents.

1.2 Background

The literature regarding traditional medicine for the use of wound healing using Mesh search including the phrases “wound healing” and “traditional medicine”, yielded 190 search results over a time period from 1991 to 2012. Table 1.1 summarises the results arranged by 1) geographical region, 2) the wound healing model, including the animal used and the type of wound created, 3) the gross, histological and biochemical parameters used to analyse the efficacy of the plant and 4) investigations to determine the plant constituents.

1.2.1 Regions of Origin

A vast majority of studies reporting on the efficacy of plant based therapies were sourced from developing countries, where, as noted previously, up to 80% of people are reliant on traditional medicines. Most reports were from India and Turkey, with reports from Africa, including Ghana, Uganda, Ethiopia, and South Africa. Relatively standardised protocols appear to have been used, perhaps due in part to previous success, costs and simplicity of the experimental approaches. However, two studies from South Africa will be discussed further below as the experimental approach was different (9, 10).

1.2.2 Wound Models

To determine the efficacy of a plant based therapies on wound healing in a human, the ideal experimental model would be human test subjects. However, obvious ethical considerations prohibit this, and therefore alternative models are required. Both *in-vitro* and *in-vivo* models have been developed. *In-vitro* models are often culture-based experiments, using either individual keratinocyte or fibroblast cell cultures, or as co-cultures of these cell types (11).

Alternatively *In-vivo* models rely on an "ideal" test animal wherein experimental conditions can be controlled. Additional factors in determining such an approach include the cost, the number of animal's required and available veterinary expertise. Furthermore, available analytical reagents must be biologically compatible with the chosen models (11).

Rodent models, including the Sprague-Dawley rat, Swiss Albino mouse, Wistar Albino rat and Guinea pig, are preferred because of their small size, cost, availability and surgical/operational procedure (12). However, a particular disadvantage of rodent models is the primary mechanism whereby their cutaneous wounds heal; in rodents, full thickness wounds contract such that the free edges oppose, whereas in human skin, wound closure is mediated by active keratinocyte migration these cells being derived from both the wound edges and hair follicles (13).

Table 1.1. Pubmed search results for "wound healing" and "traditional medicine". Emphasis was placed on the experimental design and "o" indicates that these variables and models were used in these studies.

Plant	Area	Continent	Animal	Model		Gross		Histological							Biochemical										Compound Detection	Reference
				Main	Additional	Wound Contraction	Tensile Strength	Epithelialisation	Epidermal Remodelling	Dermal Remodelling	Fibroblast proliferation	Inflammatory infiltrate	Neo-vascularisation	Collagen deposition	Hydroxyproline	Hexosamine	DNA	Protein	Uronic Acid	Elastase/Collagenase	Anti-oxidant	Cytokines	Growth Factors	Other		
Achyranthes aspera L.	Ethiopia	Africa	Rat	Incision / Excision		o	o		o	o	o	o	o	o			o									(14)
Ficus asperifolia Miq.	Ghana	Africa	NA	Culture	Anti-microbial																o					(15)
Gossypium arboreum L.	Ghana	Africa	NA	Culture	Anti-microbial																o					
Flabellaria paniculata	Nigeria	Africa	Rat	Excision	Anti-microbial	o		o																		(16)
Bulbine Natalensis	RSA	Africa	Pigs	Excision		o	o	o					o	o		o	o	o					VEGF, TGF-βR1, TGF-βR1			(9) (10)
Bulbine frutescens	RSA	Africa	Pigs	Excision		o	o	o					o	o		o	o	o					VEGF, TGF-βR1, TGF-βR1			
Urtica urens	RSA	Africa	NA	Culture	Anti-microbial																o					(17)
Capparis tomentosa	RSA	Africa	NA	Culture	Anti-microbial																o					
Dicoma anomala	RSA	Africa	NA	Culture	Anti-microbial																o					
Leonotis leonorus	RSA	Africa	NA	Culture	Anti-microbial																o					
Xysmalobium undulatum	RSA	Africa	NA	Culture	Anti-microbial																o					
Helichrysum foetidum	RSA	Africa	NA	Culture	Anti-microbial																o					
Pterocarpus angolensis	RSA	Africa	NA	Culture	Anti-microbial																o					
Terminalia sericea	RSA	Africa	NA	Culture	Anti-microbial																o					

Plant	Area	Continent	Animal	Model		Gross		Histological							Biochemical										Compound Detection	Reference
				Main	Additional	Wound Contraction	Tensile Strength	Epithelialisation	Epidermal Remodelling	Dermal Remodelling	Fibroblast proliferation	Inflammatory infiltrate	Neo-vascularisation	Collagen deposition	Hydroxyproline	Hexosamine	DNA	Protein	Uronic Acid	Elastase/Collagenase	Anti-oxidant	Cytokines	Growth Factors	Other		
Gunnera perpensa	RSA	Africa	NA	Culture	Anti-microbial																o					
Zantboxylum chalybeum	Uganda	Africa	Rat	Excision		o		o				o		o											o	(18)
Warbugiaugandensis	Uganda	Africa	Rat	Excision		o		o				o		o											o	
MEND	Zimbabwe	Africa	Guinea Pig	Excision		o								o												(19)
Shibao powder	China	Asia	Rabbit	Excision																			TGF - β, b-FGF			(20)
Siegebeckia pubescens	China	Asia	Rat and Culture	Incision / Excision		o	o				o		o	o	o											(21)
Jatyadi Taila	India	Asia	Rat and Rabbit	Excision		o			o	o	o	o	o		o	o									o	(22)
Acalypha indica	India	Asia	Rat	Excision		o	o								o		o		o			TNF-α	TGF-β	Col 1 α, Col 3 α		(23)
Semecarpus anacardium	India	Asia	Rat	Incision / Dead Space		o	o	o						o											o	(24)
Tridax Procumbans	India	Asia	Rat	Excision			o											o			o					(25)
Euphorbia caducifolia	India	Asia	Mouse	Incision / Excision		o	o								o		o								o	(26)
Trichosanthes dioica	India	Asia	Rat	Incision / Excision		o	o	o			o		o	o	o										o	(27)
Glycosmis arborea	India	Asia	Rat	Excision / Incision / Dead Space	Toxicity	o	o								o										o	(28)
Hypericum patulum	India	Asia	Rat	Incision / Excision		o	o							o											o	(29)
Leucus lavandulaefolia	India	Asia	Rat	Incision / Excision		o	o																			(30)

Plant	Area	Continent	Animal	Model		Gross		Histological							Biochemical										Compound Detection	Reference
				Main	Additional	Wound Contraction	Tensile Strength	Epithelialisation	Epidermal Remodelling	Dermal Remodelling	Fibroblast proliferation	Inflammatory infiltrate	Neo-vascularisation	Collagen deposition	Hydroxyproline	Hexosamine	DNA	Protein	Uronic Acid	Elastase/Collagenase	Anti-oxidant	Cytokines	Growth Factors	Other		
Thespesia populnea	India	Asia	Rat	Incision / Excision		o	o								o											(31)
Plagiochasma appendiculatum Lehm. et Lind.	India	Asia	Rat	Incision / Excision	Anti-microbial	o	o								o						o				o	(32)
Sesamum indicum (L.)	India	Asia	Rat	Incision / Excision / Dead Space		o	o	o				o	o	o	o		o				o				o	(33)
Ghee based formulation	India	Asia	Rat	Incision / Excision		o	o								o											(34)
Terminalia arjuna	India	Asia	Rat	Incision / Excision		o	o								o										o	(35)
Dendrophthoe falcata (L.f) Ettingsh	India	Asia	Rat	Incision / Excision	Anti-microbial	o	o								o	o					o				o	(36)
Holoptelea integrifolia	India	Asia	Rat	Incision / Excision	Anti-microbial	o	o	o			o		o		o						o				o	(37)
Aristolochia bracteolata Lam.	India	Asia	Rat	Incision / Excision / Dead Space	Toxicity		o	o						o	o						o					(38)
Lithospermum erythrorhizon	Korea	Asia	Culture	Migration																						(39)
Murraya koenigii L.	Malaysia	Asia	Rat	Excision		o		o			o	o	o	o												o	(31)
Sphaeranthus indicus	Pakistan	Asia	Guinae Pig	Excision		o																					(40)
Opuntia ficus-indica	South Korea	Asia	Rat	Incision		o																					(41)
Memecylon edule Roxb.	Thailand	Asia	NA	Culture																		IL - 10					(42)
Abies cilicica subsp. cilicica	Turkey	Asia	Rat and Mouse	Incision / Excision		o	o		o	o	o	o	o	o													(43)

Plant	Area	Continent	Animal	Model		Gross		Histological							Biochemical										Compound Detection	Reference
				Main	Additional	Wound Contraction	Tensile Strength	Epithelialisation	Epidermal Remodelling	Dermal Remodelling	Fibroblast proliferation	Inflammatory infiltrate	Neo-vascularisation	Collagen deposition	Hydroxyproline	Hexosamine	DNA	Protein	Uronic Acid	Elastase/Collagenase	Anti-oxidant	Cytokines	Growth Factors	Other		
Abies nordmanniana subsp. bornmulleriana	Turkey	Asia	Rat and Mouse	Incision / Excision		o	o		o	o	o	o	o	o												
Abies nordmanniana subsp. equitrajani	Turkey	Asia	Rat and Mouse	Incision / Excision		o	o		o	o	o	o	o	o												
Abies nordmanniana subsp. nordmanniana	Turkey	Asia	Rat and Mouse	Incision / Excision		o	o		o	o	o	o	o	o												
Cedrus libani	Turkey	Asia	Rat and Mouse	Incision / Excision		o	o		o	o	o	o	o	o												
Picea orientalis	Turkey	Asia	Rat and Mouse	Incision / Excision		o	o		o	o	o	o	o	o												
Cichorium intybus L.	Turkey	Asia	Rat and Mouse	Incision / Excision		o	o		o	o	o	o	o	o					o	o	o				o	(44)
Daphne oleoides	Turkey	Asia	Rat	Incision / Excision			o		o	o	o	o	o	o		o				o	o				o	
Ranunculus pedatus	Turkey	Asia	Rat and Mouse	Incision / Excision		o		o	o	o	o	o	o	o	o										o	(45)
Ranunculus constantinapolitanus	Turkey	Asia	Rat and Mouse	Incision / Excision		o		o	o	o	o	o	o	o	o										o	
Michauxia campanuloides:	Turkey	Asia	Rat and Mouse	Incision / Excision		o		o	o	o	o	o	o	o							o			Anti-inflammatory	o	(46)
Michauxia laevigata	Turkey	Asia	Rat and Mouse	Incision / Excision		o		o	o	o	o	o	o	o							o			Anti-inflammatory	o	
Michauxia tchihatchewii	Turkey	Asia	Rat and Mouse	Incision / Excision		o		o	o	o	o	o	o	o							o			Anti-inflammatory	o	
Michauxia thyrsoidea	Turkey	Asia	Rat and Mouse	Incision / Excision		o		o	o	o	o	o	o	o							o			Anti-inflammatory	o	
Michauxia nuda	Turkey	Asia	Rat and Mouse	Incision / Excision		o		o	o	o	o	o	o	o							o			Anti-inflammatory	o	(46)

Plant	Area	Continent	Animal	Model		Gross		Histological							Biochemical										Compound Detection	Reference
				Main	Additional	Wound Contraction	Tensile Strength	Epithelialisation	Epidermal Remodelling	Dermal Remodelling	Fibroblast proliferation	Inflammatory infiltrate	Neo-vascularisation	Collagen deposition	Hydroxyproline	Hexosamine	DNA	Protein	Uronic Acid	Elastase/Collagenase	Anti-oxidant	Cytokines	Growth Factors	Other		
Pinus halepensis Mill	Turkey	Asia	Rat and Mouse	Incision / Excision		o		o	o	o	o	o	o	o	o											(47)
Pinus pinea L	Turkey	Asia	Rat and Mouse	Incision / Excision		o		o	o	o	o	o	o	o	o											
Pinus sylvestris L	Turkey	Asia	Rat and Mouse	Incision / Excision		o		o	o	o	o	o	o	o	o											
Pinus nigra Arn	Turkey	Asia	Rat and Mouse	Incision / Excision		o		o	o	o	o	o	o	o	o											
Pinus brutia Ten	Turkey	Asia	Rat and Mouse	Incision / Excision		o		o	o	o	o	o	o	o	o											
Salvia cryptantha	Turkey	Asia	Rat and Mouse	Incision / Excision		o					o	o	o	o							o			Tyrosinase activity		(48)
Salvia cyanescens	Turkey	Asia	Rat and Mouse	Incision / Excision		o					o	o	o	o							o			Tyrosinase activity		
Multiple Plants	Turkey	Asia	Rat and Mouse	Incision / Excision																						(49)
Anglo Saxon	Britain	Europe	NA	Culture	Anti-microbial																					(50)
Phyllanthus muellerianus (Kuntze) Exell.	Germany	Europe	NA	Culture																						(51)
Calendula officinalis and more	Germany	Europe	NA	Culture																						(52)
Compound R	America	North America	Guinea Pig	Burns		o																				(53)
Croton zehntneri	Brazil	South America	Mouse	Excision		o					o	o	o	o											o	(54)
Vernonia scorpioides	Brazil	South America	Guinea Pig	Excision		o																				(55)
Multiple plants	Brazil	South America	NA	Culture																	TNF - α		Cell signalling			(56)

Plant	Area	Continent	Animal	Model		Gross		Histological							Biochemical										Compound Detection	Reference
				Main	Additional	Wound Contraction	Tensile Strength	Epithelialisation	Epidermal Remodelling	Dermal Remodelling	Fibroblast proliferation	Inflammatory infiltrate	Neo-vascularisation	Collagen deposition	Hydroxyproline	Hexosamine	DNA	Protein	Uronic Acid	Elastase/Collagenase	Anti-oxidant	Cytokines	Growth Factors	Other		
Arrabidaea chica	Brazil	South America	Rat	Excision and Culture		o	o								o											(57)
Peperomia galioides	Peru	South America	Mouse and Culture	Incision / Excision	Proliferation		o																			
Mentzelia cordifolia	Peru	South America	Mouse and Culture	Incision / Excision	Proliferation		o																			
Mutisia acuminata	Peru	South America	Mouse and Culture	Incision / Excision	Proliferation		o																			
Himatanthus sucuuba	Peru	South America	Mouse and Culture	Incision / Excision	Proliferation		o																			
Spondias mombin	Peru	South America	Mouse and Culture	Incision / Excision	Proliferation		o																			(58)
Eleutherine bulbosa	Peru	South America	Mouse and Culture	Incision / Excision	Proliferation		o																			
Muehlenbeckia tamnifolia	Peru	South America	Mouse and Culture	Incision / Excision	Proliferation		o																			
Anredera diffusa	Peru	South America	Mouse and Culture	Incision / Excision	Proliferation		o																			
Jatropha curcas	Peru	South America	Mouse and Culture	Incision / Excision	Proliferation		o																			
Anredera diffusa	Peru	South America	Rat	Incision			o																		o	(59)
Hamelia patens	El Salvador	South America	Rat	Incision			o																			(60)

A more comparable animal model is porcine skin with Sullivan, *et al.* (13) highlighting the similarities between the human and porcine skin from both an anatomical and functional perspective, as well as the similarities in wound healing. Important similarities highlighted by the authors include firstly from a gross anatomical perspective a similar pattern of hair distribution. Secondly, at a micro-anatomical level, the comparison between the porcine and human dermis shows similarities in dermal thickness, number and distribution of blood vessels and the presence of rete-ridges and dermal papillary bodies. Furthermore the epidermal layers in both species have a similar keratinocyte turnover time and expression of native proteins. With regards to wound healing while both human and porcine skin heal by similar processes, the response to treatment modalities correlates only 78% of the time. This however is greater than that of smaller rodent based models and *in-vitro* culture assays which correlate with the human response 53% and 57% of the time respectively. Porcine models have previously been used in wound healing studies, but quite infrequently to evaluate plant based therapies. Recently, two studies from the University of the Witwatersrand utilised the porcine model to evaluate the effects of *Bulbine natalensis* and *Bulbine frutensis* and followed a similar protocol to that used for rodent models of wound healing (9, 10).

It is evident that the model animal chosen will dictate the type of wound which can be created experimentally and how the resultant wound can be analysed. Most studies have employed incisional and excisional wounds created on the dorsum of the rodents. Incisional wounds usually produced using a scalpel, extended from the epidermis to the fascial planes and may be allowed to close by either primary intention, that is with sutures, or by secondary intention, that is, without sutures. In the majority of studies, sutures were removed up to one week later, and often used in tensiometer assays to measure wound breaking strength. The excisional wounds were usually created with punch biopsies, and harvested at various timepoints allowing for gross anatomical, histochemical and biochemical analyses of these samples. Other models used in wound healing experiments include burn models and deep partial thickness wounds. Deadspace models have been used to evaluate *Semecarpus anacardium* (24), *Glycosmis arborea* (28), *Sesamum indicum (L.)* (33), *Aristolochia bracteolata Lam.* (38). In these models, an artificially created subcutaneous space was made with an implant made from various materials and was allowed to be infiltrated by the cellular and connective tissue components which can be analysed thereafter (61). This technique is best suited to rodents as the skin of these animals is loose and easily manipulated for this purpose.

1.2.3 Gross Assessment

Billingham and Russell (62) stated that contraction of wounds was the generally accepted method by which tissue continuity and functionality could be restored. They based their findings on a rabbit model which included a full thickness excisional wound coupled with sequential planimetric measurements of the wound area. Although this study did not evaluate any traditional remedy, it identified important determinants of wound contracture. These included the depth of the wound, shape of the wound, age of the animal, species of the animal and type of skin (loose or fixed). The driving mechanism behind wound contraction was not proposed in this study.

Subsequently a wound healing sequence was proposed that included 1) a raised marginal tissue pressure due to inflammation, 2) migrating embryonal fibroblasts carrying the wound margins, 3) circumferential collagen fibres acting as a sphincter and the 4) contractibility of regenerating tissue opposing wound margins. More recent consensus, from publications in 1995 and 2007, is that fibroblast populations infiltrate the wounded area, where some deposit collagen and some differentiate into myofibroblasts which are contractile in nature, thus explaining the contractile nature of the wound healing process (63, 64).

Wound tensiometry or determination of the tensile strength is a technique that was proposed as a surrogate marker of wound healing and was originally described in 1929 by Howes, *et al.* (65). It has been shown to correlate with collagen content and is also related to structural orientation (66). However, White, *et al.* (66) showed that although maximal collagen formation was measured 17-20 days after injury, maximal tensile strength was only reached months after wounding. Tensile strength is therefore not entirely related to collagen production, but rather a multitude of additional factors including non-collagenous skin constituents, such as the epidermis, fibroblasts, endothelia, inflammatory cells, keratins and mucopolysaccharides (67). Despite these findings, this approach has been sensitive enough to detect differences between different treatment modalities and has become a widely utilised technique in many of the studies seen in Table 1.1 and include *Hypericum patulum* (29), *Achillea biebersteinii Afan*. (68), and in herbal formulations containing extracts of *Terminalia arjuna* (69).

1.2.4 Process of Wound Healing

Wound healing is required to effectively stabilize and repair injury (2, 70). In an optimal system, the process of wound healing occurs in an orderly and controlled series of overlapping phases, including, haemostasis, inflammation, proliferation, and remodelling (71, 72). To understand the rationale behind measuring other possible parameters in models of wound healing, it is

important to comprehend the sequence of events and factors regulating the process of wound healing.

Cutaneous wound healing is a highly dynamic and complex process and in an optimal system, is orchestrated to not only effectively and timeously re-establish the homeostatic properties of the integument but also to be functionally similar to intact (non-wounded) tissues (8). However, when the normal process or aspects of the process are altered either by the body's own system or by external factors (73), aberrations occur that may be detrimental to wound healing and in extreme cases lead to complete degradation of the skin and progression to non-healing wounds. On the other hand, careful manipulation of the right biochemical pathways could lead to accelerated healing with the eventual aim of attaining the formation of an aesthetically and physiologically normal epithelium. This poses a challenge as biochemical pathways in the healing wound have been shown to be highly variable with synergistic, agonistic and antagonist effects of many key constituents.

Multiple reviews summarise the physiology of wound healing describing four distinct phases of haemostasis, inflammation, proliferation and remodelling (64, 71, 74, 75). These phases are classically described as overlapping and are depicted by Figure 1.1. Additionally multiple factors seen in Table 1.2 adapted from Baum and Arpey (76) summarise the soluble factors affecting wound healing which are also important targets for investigation. Each of these phases, together with key associated growth factors are described below.

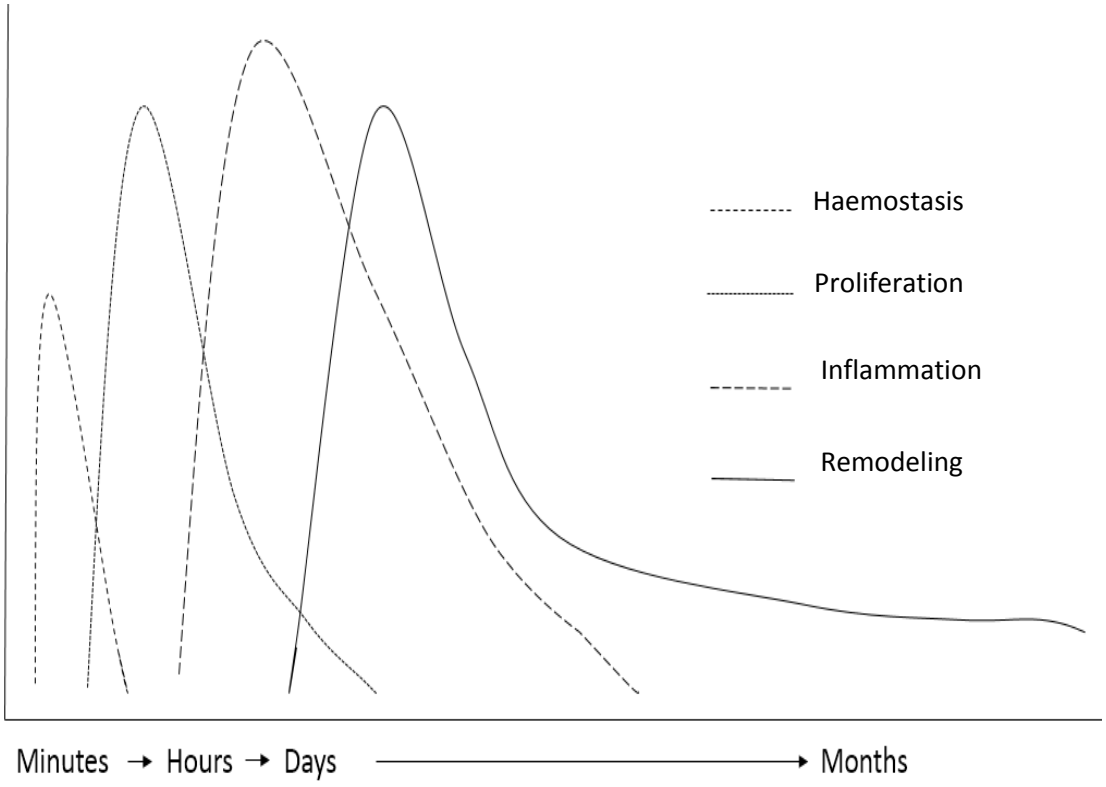


Figure 1.1. Phases of wound healing.

Table 1.2. Components active in the various stages of wound healing (adapted from Baum and Arpey, (76)*.*

Phase	Timing	Cellular Components	Non-Cellular Components	Regulators
a) Haemostasis	Injury to 15-30 minutes	Endothelial Cells	Fibrin	Prostagalandins
		Platelets	Fibronectin	Thromboxanes
				Thrombin
b) Inflammatory	15-30 minutes to 1 week	Endothelial Cells	Fibrin provisional matrix	Cytokines: TNF-α, IL-1α and β, IL-6, IL-8
		Neutrophils		Growth Factors: TGF-β, PDGF
		Macrophages		Others: Histamine, Leukotrines, Complement
		Lymphocytes		
c) Proliferative	2 days to a few weeks	Endothelial Cells	Provisional matrix	Growth Factors: FGF-2, FGF-7, FGF-10, VEGF, EGF, TGF-β, PDGF
		Macrophages	Collagen	
		Fibroblasts	Proteoglycans	Others: MMP/TIMP, Nitric Oxide, Angiopoietin
		Keratinocytes		
d) Remodelling	Weeks to months	Myofibroblasts	Collagen	Growth Factors: TGF-β, PDGF
		Fibroblasts	Proteoglycans	Cytokines: IL-1, IL-10
		Macrophages		Others: MMP/TIMP
		Lymphocytes		

a) ***Haemostatic Phase****:* Restoring homeostasis must occur rapidly and occurs directly after a traumatic or intentional surgical insult. Blood vessels respond by contracting and activating the clotting cascade. The resultant fibrin plug forms from fibronectin and fibrinogen and associated platelet aggregation. Platelets are an important component of this process as they contain growth factors, cytokines, coagulation factors and protease inhibitors in their α-granules (77). Importantly, the fibrin plug forms the provisional matrix necessary to promote and support cell infiltration into the wounded area (78). It further, serves as a temporary repair mechanism before the following repair phases can come into effect (79). It is this early infiltration of cells that, through their production of appropriate cytokines, regulate the subsequent phases of wound healing.

b) ***Inflammatory Phase:*** In response to cytokine, chemokine and other signals, inflammatory cells migrate into the wounded area. The predominant cell types are initially the short-lived polymorphonuclear leukocytes or neutrophils which are slowly replaced by the macrophage population (64). During this phase there is a release of soluble factors of multiple origins and functions and has been extensively reviewed by Werner and Grose (80). As is listed inTable 1.1, several soluble factors were investigated with regards to plant based therapies. These factors include the growth factors, transforming growth factor–β (TGF–β), basic fibroblast growth factor (bFGF), vasoendothethial growth factor (VEGF); and the cytokines, tumor necrosis factor–α (TNF-α) and interleukin 10 (IL–10). The factors listed here are by no means comprehensive in terms of the overall number of factors described by Werner and Grose (80), but rather represent the factors analysed when considering plant based therapies and will be further discussed at a later stage.

c) ***Proliferative Phase*****:** In an extensive review by Baum and Arpey (76), two important components of this phase were identified as 1) the formation of granulation tissue following the migration and proliferation of fibroblasts, with the subsequent production of collagen, 2) re-epithelialisation where the granulation tissue is covered by migrating keratinocytes. The migration and proliferation of these various cellular components is due to chemotactic signals generated within the wound.

The source of these fibroblasts is from neighbouring unwounded tissue and from undifferentiated mesenchymal cells (76) and respond to signals by TGF-β, bFGF and PDGF (80). In culture based experiments, within the first 24 hours, these factors have similar effects on the migration of fibroblasts within the first 24 hours but thereafter

differential effects are seen with PDGF having the greatest effect and TGF- β the least (81). Additional factors have been linked to the migration and proliferation of fibroblasts namely epidermal growth factor (EGF), FGF and Insulin like growth factor (IGF) (80). The role of EGF to some degree is that of a modulating one as reported by Ware, Wells and Lauffenburger (82). Together with a matrix ground substance as a migratory surface, the speed and direction of fibroblast migration is manipulated by various concentrations of EGF (82).

Re-epithelialisation is achieved by the migration, proliferation and differentiation of keratinocytes (83). Keratinocytes are derived from the adjacent non-wounded sites and if the hair follicles are intact, cells from these appendages are also mobilised. Keratinocytes migrate as sheets of cells and cease migrating on contact with opposing migratory keratinocytes. These migratory sheets of keratinocytes are fed by proliferating cells immediately posterior to the leading edge (84).

To analyse these specific features of re-epithelialisation various markers present in the skin can be analysed using histochemical staining techniques of epidermal keratins. Migratory keratinocytes express and show a reorganisation of keratins 6 and 16 in response to wounding (83), proliferating cells express keratins 5 and 14 (85) and the differentiating suprabasal cells express keratins 1, 10 and K2 (83). Re-epithelialising tissue shows variation in differentiation state but evaluation of the keratin sub-types does not feature in the studies seen in Table 1.1.

Various key factors regulate keratinocyte migration, proliferation and differentiation. In addition to calcium, magnesium, pH and hypoxia, growth factors involved in migration include neuronal growth factor (NGF) and hepatocyte growth factor (HGF), both of which are linked to tyrosine kinases and tyrosine phosphorylation (86, 87). Additionally (Table 1.2) factors affecting keratinocytes can be viewed as migratory stimulators and include FGF-2, 7, 10 and TGF-β, as well as those stimulating proliferation including NGF, HGF, IL-6, nitric oxide, leptin, and others (76). Although analysis of many of these factors is mostly absent from studies focussing on plant based therapies, it is clear that their roles are important in wound healing.

d) ***Remodelling Phase*****:** The remodelling phase is the synthesis and remodelling of the extracellular matrix which starts early with the deposition of granulation tissue and continues for months after the wound has been closed (70). Key to this phase is the synthesis and enzymatic breakdown of collagen fibres (88) by matrix

metalloproteinases (MMP's) (64). However the activity of MMP's is not only limited to the remodelling phase as they are directly involved with cell migration, cytokine and growth factor release from the cells producing them, in concert with the degradation of these factors (64). This phase is under the control of factors such as IL-1β and TNF-α which up-regulate expression and down-regulate their natural antagonists, the tissue inhibitors of metalloproteinases (TIMP) (74).

Few studies, utilising either plant based therapies or commercially available products, have followed the wound healing process in its entirety. Limited data suggests that the final strength of the wounds is only about 80% of non-injured skin several months post-treatment (70). It would appear that this phase is not well documented in the literature and neither has it been well investigated as opposed to the prior phases.

1.2.5 Soluble Growth Factors

The following factors described are those analysed by the authors in Table 1.1. Although by no means an extensive list, the factors presented here are those reported when considering the roles or mechanisms of plant based products in wound healing.

Transforming growth factor–β (TGF- β). TGF- β is a ligand superfamily that is further divided into five sub-families designated TGF- β 1-5 (89). The membrane receptors of these ligands are linked to serine and threonine kinases that phosphorylate to transduce the ligand signal (89). Whereas the Epidermal Growth Factor (EGF) family ligand transmembrane receptors are coupled to tyrosine kinase activity a link between the TGF and EGF families exist where the former enhances the mitogenic effects of the later (80). The significance of these signalling mechanisms within the context of the present study is further reviewed in Chapter 3.

TGF-β acts throughout all the wound healing phases by exerting mostly chemotactic and proliferative signals on monocytes, endothelial cells, fibroblasts and keratinocytes (89). Faler, *et al.* (89) emphasized that the role of this factor differs in some instances, where it could be anti-proliferative when endothelial cells and keratinocytes are involved, possibly due to the wound models used. However, with regards to experimentally assessing the efficacy of traditional medicines, TGF-β was found to be beneficial in wound healing studies reported by Zhao, *et al.* (20), Ganeshkumar, *et al.* (23), and Pather and Kramer (10) and are described below.

The study by Zhao, *et al.* (20) was conducted using rabbit full thickness wounds to assess the effects of Shibao powder on soft tissue healing, where the authors evaluated the expression

of bFGF and TGF-β in the granulation tissue of these wounds. In response to the treatments there was an increased expression of bFGF at 6 days post operatively and increased levels of TGF-β at days 10 and 14, all of which were significant.

Similarly, Ganeshkumar, *et al.* (23) showed elevated levels of TGF- β at day 7 post-operatively when the effects of ethanolic extracts of the plant *Acalypha indica* were assessed on full thickness excisional rat wounds. In association with raised TGF- β levels were increased rates of wound contraction, epithelialisation and tensile strength (23). As the approach taken here was to quantify ribonucleic acid (RNA) expression levels from harvested wound tissue, no distinction was made as to the specific cellular localisation of the expression of TGF- β.

Conversely, Pather and Kramer (10), assessed the expression of TGF- β by utilising immunohistochemical staining of the tissues harvested from porcine full-thickness models, where extracts of *Bulbine natalensis* and *Bulbine frutensis* were used. Compared to the controls *Bulbine natalensis* and *Bulbine frutensis* treated wounds showed an increase in TGF-β expression which was linked to earlier epithelialisation of the wounds compared within the different treatment groups.

Basic fibroblast growth factor (bFGF). bFGF is a member of the fibroblast growth factor family, whose signal is similarly transduced via transmembrane receptors coupled to tyrosine kinases, producing proliferative signals in endothelial, fibroblastic and keratinocyte cell lines (80, 90). McGee, *et al*. (91) reported that recombinant bFGF increased tensile strength and breaking energy but not collagen content in a full thickness incisional rat wound model. It was suggested that its effects may be more related to increased numbers of fibroblasts or their contractile counterparts, myofibroblasts. There is a paucity of data regarding plant based therapies and their potential effects on bFGF expression. Zhao, *et al.* (20) however reported significantly increased levels of bFGF expression, altered composition of the granulation tissue with regards to collagen content and organisation in response to Shibao powder in a rabbit tendon incisional wound model.

Vasoendothethial growth factor (VEGF). VEGF is a growth factor whose receptors are also linked to transmembrane tyrosine receptor kinases (80). VEGF has been shown to be produced by multiple cells active in the wound healing process, including neutrophils, macrophages, endothelial cells, fibroblasts, myofibroblasts and keratinocytes (92) and exerts effects throughout the entire wound healing process. Additionally VEGF has also been implicated in scarless wound healing (93), an attractive aesthetic variable in wound healing. From the articles documented in Table 1.1, the expression and localisation of VEGF was demonstrated with the use of *Bulbine natalensis* and *Bulbine frutescens* full thickness wounds

in a pig model (10). Here, increased VEGF expression in the basal layers of the regenerating epidermis as well as scattered expression through the granulation tissue was established. Further, this increased expression correlated with an elevated break strength and angiogenesis.

Interleukin-10. IL-10 has been shown to be a prominent anti-inflammatory cytokine active in the skin. Berg, *et al.* (94) demonstrated the role of IL-10 in Croton oil irritated skin in a mouse model. The effects of IL-10 were assessed based on its potential to reduce the inflammatory induced necrosis of skin tissue in wild type mice as well as IL-10 knockout mice. It was seen here that the inflammatory response based on macrophage infiltration, oedema and ulcer formation. Furthermore, the extent of damage was greater, with an increased inflammatory response in the knockout mice. In addition levels of other inflammatory cytokines, specifically IL-1β and IL-6, were also shown to decrease in response to IL-10. Other responses included an inhibition of chemotaxis of neutrophils and macrophages to the affected site (95).

Nualkaew, *et al.* (42) investigated the anti-inflammatory effects of *Memecylon edule Roxb*. showed various fractions of the plant, in a macrophage culture model combined with a rabbit ear oedema model, produced an elevation of the IL-10 with a corresponding decrease in oedema suggesting a beneficial effect. In contrast, Eming, *et al.* (72) found that in IL-10 knockout mice decreased levels of IL-10 accelerated wound closure in a mouse model where accelerated epithelialisation and wound contraction was observed. This suggests that cytokines inhibited by IL-10 may have a beneficial contribution to the wound healing process and these pro-inflammatory agents but quite possibly act as chemotactic agents for cells active in the wound healing process.

Tumour necrosis factor-α (TNF-α). In contrast to the anti-inflammatory effects of IL-10, TNF-α has more of a detrimental role and has indeed been linked to non-healing chronic wounds (96). TNF- α is a cytokine that is primarily produced by activated macrophages (97) but has also been shown to be produced by neutrophils (98). Its role in wound healing is a complex one, as its beneficial effects may be dose dependent, with roles in inflammation, mitogenicity and angiogenesis. Its role is however better explained as a synergistic molecule with regards to platelet derived growth factor (PDGF), but shows antagonistic effects with respect to TGF-β (99).

In utilising both a rat dead space and *in-vitro* cell culture wound models, Rapala (97) assessed the effects of TNF-α. In the dead space model, TNF-α decreased wound associated collagen production, but only with the continual addition of the cytokine and more specifically, only at days 4-7. In fibroblast cultures, TNF-α also reduced the production of collagen. While in culture

the effects of TNF-α are easily seen, the impact in animal models is not as great. Added to this, evidence from TNF-α null mice show that without the cytokine, expression of TGF-β expression is uncontrolled leading to excessive granulation tissue production and ineffective epithelialization (100). In light of this, the Brazilian study by Schmidt, *et al.* (56) where a multitude of plants were examined only *Xanthium cavanillesii* was capable of reducing the expression of TNF- α significantly (up to 70%) in fibrolast cultures after lipopolysacharide stimulation.

1.2.6 Histological and Biochemical Analysis

Determining the mechanism whereby a plant based therapeutic agent enhances healing requires the simultaneous measurement of a number of parameters. Interpreting concentrations of chemokine, cytokines and other parameters which orchestrate optimal wound healing has been made in the context of the wound healing phases. However such inferences may not be valid as measures may not be specific to one phase and may overlap with other phases. What is apparent is that the histological and biochemical variables that are commonly measured are in essence the outcomes of multiple underlying processes which are never fully evaluated when investigating a potential plant based therapy. They describe the wound in general terms but may not be adequate for mechanistic descriptions of the investigated plants. In light of this, histological and biochemical investigations are relatively cheap, remain the basis of wound healing investigations and therefore require further elaboration.

Histological measures in wound healing including inflammatory infiltration, neovascularisation, fibroblast infiltration, epithelialisation, collagen deposition and remodelling are common variables determined when evaluating the efficacy of plant based therapies. Although these measures provide qualitative assessment of wound healing, the assays are mostly operator dependent. While there was a correlation between experienced observers and histological measurements, automated tissue processing was proven superior since it removes both inter/intra observer error and was more reproducible (101).

In contrast, biochemical assays reduce the subjectivity associated with the histological analyses. An example is the reproducible colorimetric determination of hydroxyproline concentrations, which have been widely used to determine collagen content in connective tissues (102). Correct sampling appears to be a drawback of the assay. Additional biochemical parameters assessed when evaluating traditional medicines are DNA concentrations, elastase and collagenase activity, total protein and the frequently measured assessment of anti-oxidants in plants.

Free radicals (i.e. superoxide's and hydroxyls) are produced in healing wounds and have potent antimicrobial activity (103). They are also involved in signalling mechanisms within the wound environment (104). Excessive release of free radicals result in an elevated pain response and are responsible for excessive viable tissue damage (105). Concentrations of free radicals at micromolar concentrations enhance the wound healing process, whereas millimolar concentrations result in uncontrolled damage, to cause prolonged wound healing and possible formation of a chronic wound (106). Elevated free radical concentrations have been demonstrated in vascular insufficiency, diabetes and advanced age, conditions wherein chronic wounds are more common (107). Therefore anti-oxidants in traditional medicines may be important variables in the context of chronic wounds rather than in acute wound healing.

Few studies have determined the toxicity of plant derived compounds. While, for example, the toxicity of orally administered extracts of *Glycosmis arborea* (28) and *Aristolochia bracteolate Lam* (38) have been determined, there is a lack of information relating to toxicities of topically administered natural plant products to wounds.

1.2.7 Plant Compound Detection and Isolation

Given the complexity of the wound healing process, measuring panels of variables and determining interactions between these variables, should lead to a more complete understanding of wound healing and allow for the elucidation of some mechanisms of action of plant based therapies. In this regard, the isolation of the individual active compounds would better disclose the mechanism and the potential effects of concentration variability. Beneficial synergistic and antagonistic interactions between such compounds could also be elucidated (108). Indeed most beneficial outcomes may be from individual compounds isolated from different plants or even polyherbal pharmacy (109).

The studies listed in Table 1.1 indicate the wound healing potential of many relevant plants although the underlying mechanisms remain largely unknown. This may be due to the the limited number of variables that can be measured in a single experiment in the highly complex setting. If an outcome can be identified from the variables easily assessed such as wound closure, high throughput assays can be employed to identify the active fractions, component or components which affect the measured variable.

From the studies reviewed in Table 1.1, it can be seen that a number of authors have documented potential components of the plants based on previously documented protocols seen in Trease and Evans (110), and here the majority of the authors employed the phytochemical screen. Furthermore chromatographic techniques including high performance

liquid chromataography (HPLC) and gas chromatography coupled with mass spectrometry (GCMS) have been used to identify potential compounds. Nagappan, *et al*. (31), for example, identified essential oils from *Murraya koenigii by* GCMS and isolated a carbazole alkaloid, mahanimbicine with potential anti-inflammatory properties. This was shown to increase both collagen depositon and organisation. β-Sitosterol from *Cichorium intybus* (L.) was firstly isolated by column chromatography and then identified by nuclear magnetic resonance (NMR) It's benefit in wound healing was due to its anti-oxidant and anti-inflammatory properties (47).

1.2.8 Current State of Wound Healing Investigations

The complexity of the wound healing process has led investigators to determine general screening outcomes such as the wound tensile strength and contracture, as well as qualitative histological measures, including inflammatory cell infiltrate and epithelialisation of the wounds. Relatively few studies have continued to further determine molecular mechanisms of action of these plant remedies. Such molecular studies may allow for the development of rapid screening techniques of potential extracts, ultimately identifying lead compounds of benefit in wound healing (6).

1.2.9 Senecio serratuloides

Senecio serratuloides, a plant widely used for wound healing. It is referred to by the traditional healers of South Africa as “umsukumbili” or the “2 day cure” and belongs to the family Asteraceae/ Compositae. Although the plant is widespread throughout South Africa, information available on *Senecio serratuloides* is recent and mainly derived from books published on the various plants utilized in South African traditional medicine settings. The indications for this plant are for cutaneous cuts, sores, and burns (111, 112). The plant is simply prepared for use as dried leaves which are then burnt, crushed and applied directly to the affected areas.



Figure 1.2. Senecio serratuloides. Leaves that are routinely used for wound healing are clearly defined from the stem. (Image taken from iSpot web page: http://www.ispot.org.za/node/195582).

Although little information is available as to the efficacy of the plant some beneficial effects have been described by Fawole, *et al.* (113) including anti-inflammatory properties (COX-1/2 assays), anti-cholinesterase, and anti-oxidant activity. These attributes were determined directly from plant preparations including 50% methanol, dichloromethane, petroleum ether and ethanolic extracts.

A major limitation with this plant is that the genus is known to contain pyrrolizidine alkaloids (114, 115). Although these have not been specifically identified in this particular plant, there are reports of hepatic and pulmonary disorders observed with pyrrolizidine alkaloid poisoning

(116, 117). *Senecio serratuloides* was included in a screen of South African medicinal plants for genotoxicity using the AMES and VITOTOX® test where toxicity was only seen at high concentrations in the VITOTOX® assay (118). Since these *in-vitro* assays do not take into account the hepatic and pulmonary toxicity secondary to pyrrolizidine alkaloid poisoning, it would be an expansive leap to infer toxicity of the plant this warranting further investigation.

Importantly, in most reports of pyrrolizidine alkaloid poisoning, the route of entry into the body is through the accidental contamination and consumption of food (119). In contrast as a wound healing remedy, this plant is applied topically on the wounded areas of the skin and there appear to be no reports of toxicity following this application. Thus the route of administration of the plant appears to have toxicological implications.

The practice of charring the plant introduces the question of delivery and availability of the active ingredients. Traditional healers gently char this plant during preparation and this produces a slow release system known as biochar (120). Mawera, *et al.* (19) report an "ashened" local plant used for wound healing in Zimbabwe. Although the name of the plant was not disclosed, it is the first report of plant material prepared in this way.

In summary, inappropriate wound healing and the development of a chronic wound can be a costly complication of simple surgical procedures. Interventions which accelerate the process are continually being sought and investigated. Although the efficacies of traditional wound healing remedies have been reported anecdotally, few have been subjected to any rigorous scientific investigation. *Senecio serratuloides* is one such local South African remedy which will be the subject of the present investigation. As accidental ingestion of this plant has resulted in hepatic failure, the question whether this plant is safe to use topically requires thorough testing. Moreover, the molecular mechanism whereby this plant accelerates the healing process has not been investigated.

It is clear that multiple issues are present. Firstly the wound healing process that is described as being complex allows for multiple targets to be manipulated in order to accelerate the process and so assaying one particular target loses the sensitivity needed to identify lead compounds. Secondly very little is known about *Senecio serratuloides* with regards to efficacy, mechanism by which the plant works, and toxicity. It can therefore be seen that there is no indication as to how the plant works and if it is safe. There is additionally little indication as to what compounds in the plant could be active.

1.3 Aims

In this investigation, the aim was to develop an objective set of parameters to assess wound healing that:

a) Could be reproducibly measured to describe the overall effect of the plant in question;
b) May identify suitable end-point parameters to elucidate the mode of action of the active compounds in the healing process;
c) Identify a suitable *in-vitro* assay that could be used in high throughput screening assays when screening for active substances in the plant material.

Chapter 2 - Efficacy and Safety of Senecio serratuloides in treating Deep Partial Thickness and Full Thickness Wounds; Macroscopic and Histological Assessment

2.1 Introduction

Treating and caring for wounds places an enormous, and escalating burden on hospital and health care resources, with an estimated cost in 2010 of $15.3 billion in the USA alone (2). Sophisticated care is often unaffordable and unavailable in developing countries, where many patients rely on familiar, readily accessible and inexpensive traditional wound healing remedies.

In South Africa, the plant, *Senecio serratuloides* (DC; *Asteraceae/ Compositae*), the "2 day cure", has been anecdotally reported by traditional healers to promote the healing of cuts, sores, and burns (112). Traditional healers apply fresh, dried or even charred leaves directly onto the wound, that may then be covered with pig or zebra fat. Despite being used widely, its wound healing efficacy has yet to be fully evaluated particularly as there are reports of deliberate or accidental oral consumption of this plant causing hepatic, renal and pulmonary dysfunction and death in stock animals.

This toxicity has been attributed to the presence of pyrrolizidine alkaloids (116) found within plants of the genus *Senecio*, although these have not specifically been reported from *Senecio serratuloides*. However, we are unaware of reports of cases of pyrrolizidine alkaloid poisoning following the topical application of *Senecio serratuloides* to cutaneous wounds. AMES and VITOTOX® assays of solvent extracts of this plant have shown no signs of mutagenicity, except at concentrations exceeding 2000 µg/ml (118). Despite these reports, Fawole, *et al.* (113) have demonstrated anti-oxidant and other beneficial properties in the plant to partly explain the beneficial wound healing properties. As the plant is widely used by traditional healers, a more detailed investigation of the wound healing potential and safety of *Senecio serratuloides* is required.

2.2 Aims

Therefore the aims of this Chapter where to:

a) Establish the efficacy of *Senecio serratuloides* in the healing of deep partial and full thickness cutaneous wounds in a porcine model, by assessing the effect of the treatment on wound closure, contraction and collagen infiltration;

b) Determine changes in the pH, epidermal thickness and collagen infiltration of the recovering wound to provide potential mechanisms responsible for accelerating the healing process;

c) Determine the toxicity and safety of topically applied *Senecio serratuloides* preparation in the porcine model.

2.3 Materials and Methods

2.3.1 Collection and Preparation of Plant Material

The plant material was purchased between 2008 and 2010 from the Mooi Street Traditional Market, Johannesburg, and was identified and deposited at the C.E. Moss Herbarium of the School of Animal, Plant and Environmental Sciences, University of the Witwatersrand. Specimen voucher numbers include 08/05/2009, 09/08/2009, 09/05/2009, and 27/02/2010. For simplicity *Senecio serratuloides* will be referred to as *Senecio* from this point forward.

The material was air dried and stored at -20 ^{o}C until used. The preparation and application of the plant material was according to the traditional healer's instructions. Leaves were dried in an oven at 40 ^{o}C overnight, after which they were crushed to a fine powder using a pestle and mortar and heated on a hot plate until charred to a black "ash". The material was ground again, and the resultant powder placed directly on the wounds (described below).

2.3.2 Animal Model and Test Groups

Large white pigs (*Sus scrofa domesticus*) were selected for experimentation due to the similarities to human skin (13). Ethical clearance was obtained from the Animal Ethics Committee (Clearance number: 2008/15/04) of the University of the Witwatersrand.

Surgery and Wound Generation: Nine (n = 9) female pigs (±30 kg) were anaesthetized using injectable midazolam (0.3 mg/kg) (Dormicum, Roche) and ketamine (11 mg/kg) (AnaketV; Bayer HealthCare). Anaesthesia was maintained by Isofor (Bayer HealthCare) as a volatile agent. Dr. Patel performed the surgery at the Central Animal Unit within the Faculty of Health Sciences. Deep partial thickness wounds were created with an electric dermatome, set to 800µm (Aesculap HH Dermatome Ga 630) to remove six square sections of skin (2.5 cm by 2.5 cm) spaced 4 cm apart, and either side of the midline of the dorsum of each pig. Additional to the deep partial thickness wounds, full thickness punch biopsies were created adjacent to the partial thickness wounds (Figure 2.1 and Figure 2.2).

Treatment and Dressing: Wounds were treated with one of the following: 1) prepared *Senecio* material (0.2 g); 2) activated carbon (0.2 g, Merck South Africa; Cat. No. 102186), as the positive control; or 3) left untreated as the negative control. Each treated wound was also dressed with separate standard occlusive dressing, with an integrated absorptive pad (3M Tegaderm® Cat. No. 3584) (Figure 2.3). The test area of each pig was wrapped in a stocking to hold the dressings in place. Each pig was housed separately in the Central Animal Unit and

buprenorphine (0.3 - 0.6 ml) (Temgesic, Reckitt Benckiser Pharmaceuticals) was administered as post-operative analgesia.

2.3.3 Wound sample Collection and Analysis

The dressings were changed on days: 2, 5, 7, 8, 9, 12, and day 16, based on the schedule of the Central Animal Unit. At each dressing change photographs of the wounds were taken to record the overall healing pattern. Wound surface pH was measured, the wound fluid was collected from the absorptive pads and jugular venous blood was taken. Wound and control biopsies were taken as has been described in a later chapters. Liver biopsies were collected one month post-completion of the experiments.

2.3.4 pH Measurement

On the days of sample collection, the wound pH was measured using a surface electrode (Separations Scientific ST P17-BNC) and the average of three measurements plotted against the post-operative time in days. Before measuring the pH the wounds were cleaned with de-ionised water and the electrode was rinsed in de-ionised water between measurements to negate any potential effects on the pH that could be ascribed to the treatments or cleasing regimen.

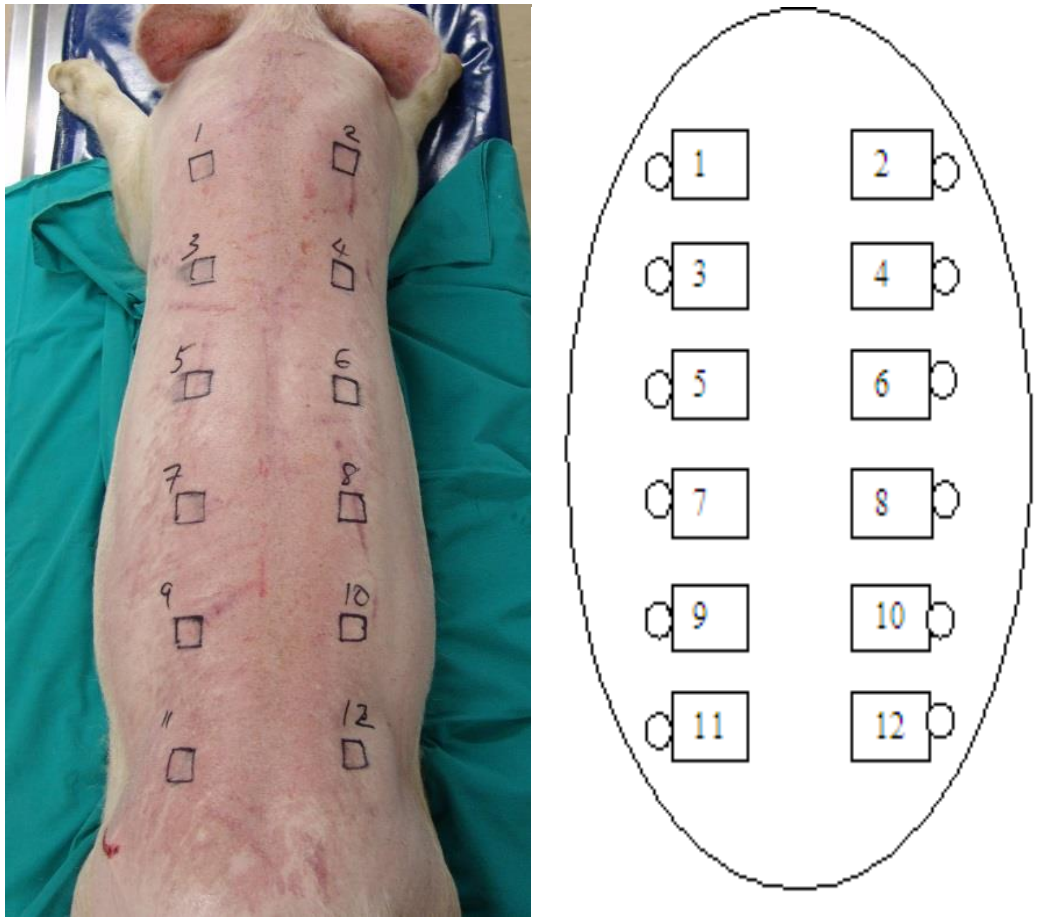


Figure 2.1. Preparation of the dorsum of the pigs. Left: the animals were shaved and the demarcated areas outlined with a permanent marker. Right: a schematic diagram of the 2.5 cm by 2.5 cm deep partial thickness wounds with adjacent full thickness wounds created with a 6 mm core biopsy. Wounds 1, 4, 7, 10 were treated as the negative control. Wounds 2, 5, 8, 11 were treated with activated carbon. Wounds 3, 6, 9, 12 were treated with the test plant, Senecio.

A.

B.

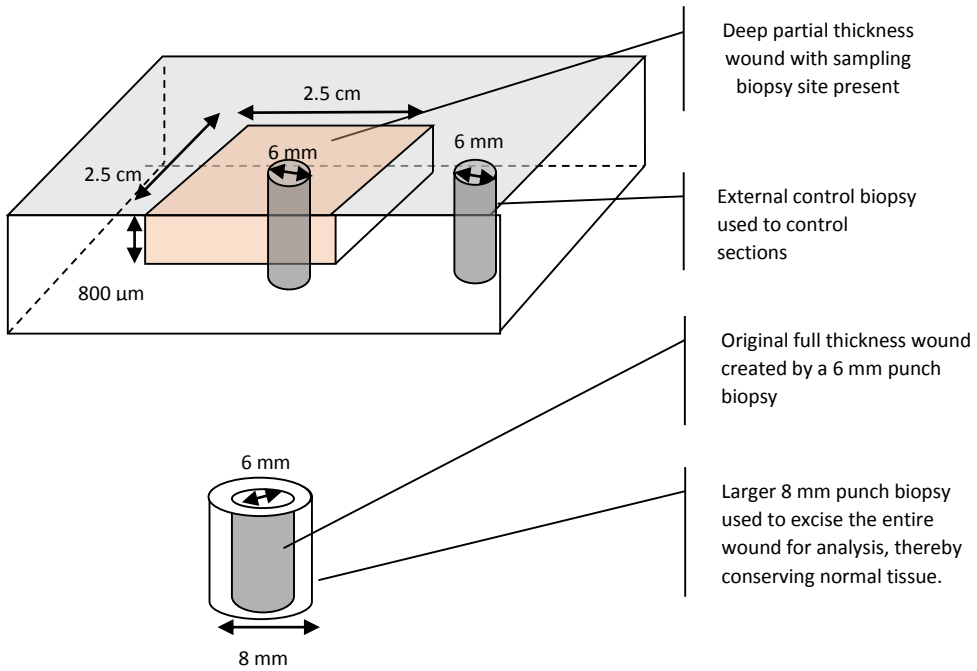


Figure 2.2. A schematic diagram of one of the 2.5 cm by 2.5 cm deep partial thickness experimental wounds, 800 µm in depth, created on the back of the pig. The location of the core biopsy sites, relative to the wound area are illustrated. A biopsy of normal uninjured skin, outside the wound area, was taken as the control external reference tissue. B. Schematic diagram of samples taken from a full thickness wound.



Figure 2.3. Dressings used to hold the treatments in place. The image above shows the animal's dorsum once all the wounds were treated as per protocol. The wounds were dressed with the occlusive dressings which were held in place with zinc-oxide tape and a surgical stocking (not shown).

2.3.5 Skin Biopsy Collection

The remaining wounds were dressed and covered as described above and biopsied on subsequent days according to the schedule. This process was repeated for the three treatment groups on these days. Full thickness wounds (Figure 2.2) were completely excised with a 8 mm punch biopsy.

2.3.6 Histological Analysis

The skin biopsies obtained for histological analysis were immediately placed in 10% buffered formalin. The biopsies were subsequently dehydrated through a graded ethanol series, followed by clearing in Xylene and embedded in paraffin wax; and sections were cut at a thickness of 5µm on a sledge microtome. Sections were floated on a water bath pre-heated to 50 ^{o}C, containing premixed Sta-On (Leica Biosystems, Cat. No.3803105). Sections retrieved on alcohol washed microscopy slides were heat adhered to the slides at 60 ^{o}C overnight in preparation for subsequent histological analyses.

All basic histology, including tissue processing, sectioning and staining was conducted in the School of Anatomical Sciences, situated within the Faculty of Health Sciences at the University of the Witwatersrand. The staining procedures included routine haematoxylin and eosin (H and E) staining of biopsy material for morphometric analysis and Picrosirius red staining for evaluating collagen deposition. The same biopsy specimens provided source material for the immunofluorescence studies, as described in Chapter 3.

Sections were imaged at 100x magnification on a Zeiss Axioskop 2 microscope and images captured with a Sony 3CCD camera. For each wound, 2 representative sections were chosen with further morphometric analysis being performed with the planimetric software package IMAGE J (version 1.4.3.67).

2.3.7 Deep Partial Thickness Wound Morphometric Analysis

To account for the variability of the epidermal thickness along the dorsum of the pigs (13) control biopsies were made immediately adjacent to the wounds. Ten measurements of the newly forming epidermis were taken along both sections (five measurements per slide) for each wound and adjacent control samples. A ratio was then determined from the measurements inside the wound to that for the adjacent control epidermal thickness. To avoid bias that could arise from determining the ratio from highly variable tissues, the measurements for each section were ranked from largest to smallest and from this series the ratios were calculated. The largest measurement in the wound was equated with the largest measurement

in the control samples. An average of the ten measurements per wound was determined and plotted against time. The approach was summarised as:

Step 1: 10 measurements from inside wound and ranked from largest to smallest.

Step 2: 10 measurements from adjacent skin considered “normal” and ranked from largest to smallest.

Step 3: Ratio determined by the equation:

$$\text{Epidermal Thickness Ratio (ETR)} = \frac{\text{Wound Skin Thickness (μm)}}{\text{Adjacent Normal Skin Thickness (μm)}}$$

Corresponding ranked measurements where used at this point to determine the ratio, i.e. rank number 1 of the wounded skin thickness and rank number 1 of adjacent normal skin thickness.

Step 4: Average epidermal thickness ratio was calculated for each wound.

Step 5: Calculated epidermal ratio was used as the final descriptive parameter for each wound.

The results were reported as the epidermal thickness (ET) of the epidermis and the calculated epidermal thickness ratio (ETR).

2.3.8 Full Thickness Wound Morphometric Analysis

Full thickness wounds were analysed using the measurements illustrated in Figure 2.4 below. Measurements include; 1) Epidermal Tongue Length, 2) Inter-Epidermal deficit as a proxy of wound epithelialisation and 3) Mid-Dermal Deficit. Full thickness wounds were analysed on days 8 and 16 post-operative and results plotted against time (days post-operative).

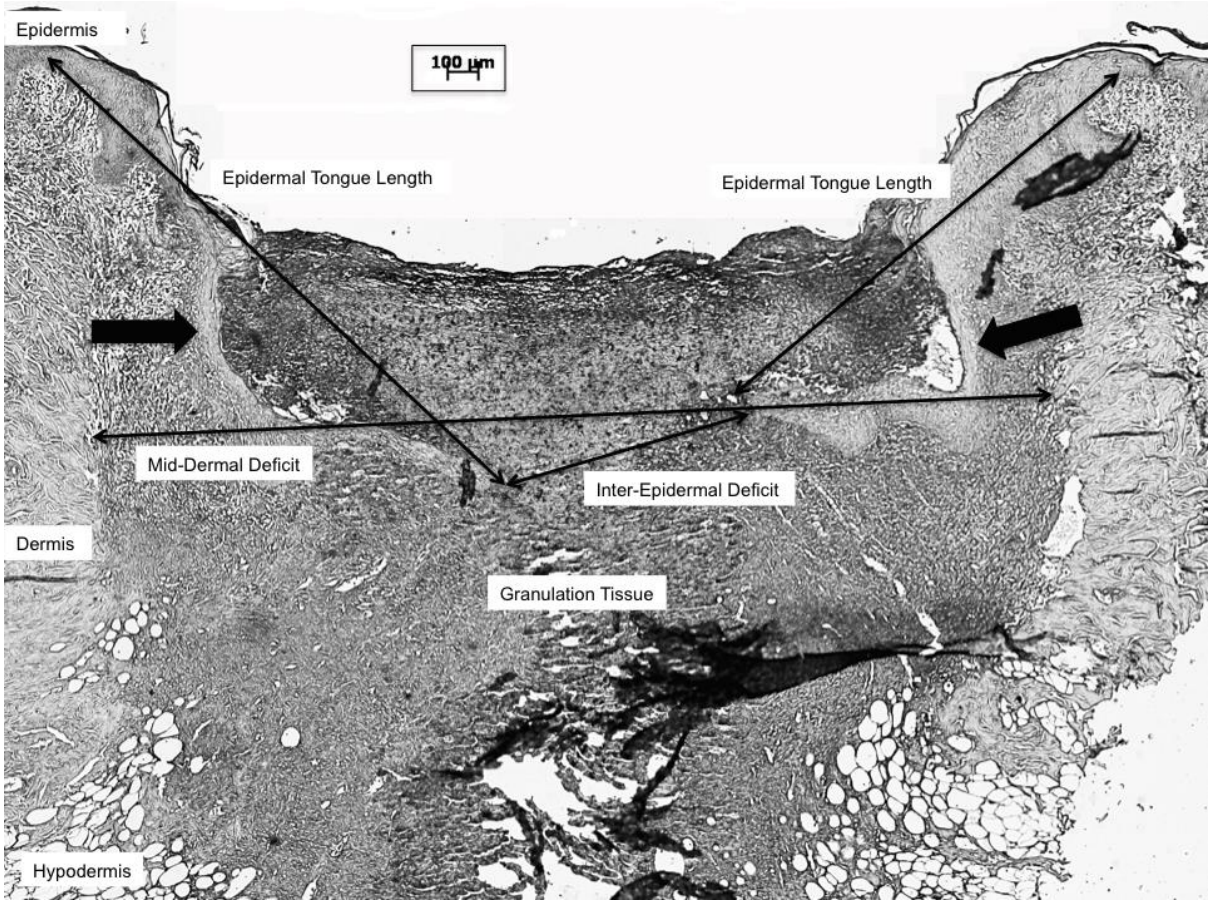


Figure 2.4. Representative full thickness wound with the measurements labelled. Black arrows indicate the epidermal tongues that migrate into the wounded area. Inter-epidermal deficit was used as an indication of whether or not the wounds were epithelialized. (Original H & E image at 100x magnification)

2.3.9 Collagen Analysis

Picrosirius Red (PSR) Staining Procedure

To determine the effect of the treatments on collagen infiltration, a Picrosirius red (PSR) stain was employed to stain for collagen in an *in-situ* form of analysis. Prepared histological sections were immersed in 500 ml of saturated picric acid containing 0.5 g of Sirius or Direct red dye (SIGMA, St Louis, Mo) for an hour. Sections were then washed in 2 changes of 1% glacial acetic acid for 10 minutes at each interval. After the 2 washes in 1% glacial acetic acid (AnalaR, BDH; UK) the sections were dehydrated through a graded series of alcohols, infiltrated with Xylene and mounted using Entellen (SIGMA).

PSR Section Imaging and Image Analysis

The prepared sections were imaged on an Olympus IX71 fluorescence microscope fitted with the appropriate filters. The images were processed using the analysis LifeScience® software package in the Oncology Research Laboratory, Department of Internal Medicine. A composite red-green-blue image was produced by capturing the images using red, green and blue filters fitted to the microscope. The deep partial thickness wounds were imaged at 20x magnification to incorporate the epidermis and underlying granulation tissue. The regions of interest (ROI's) were created as 200 pixels wide and 300 pixels high immediately below the epidermis (Figure 2.5). This measure was repeated three times across the entire length of the captured image. The ROI's were analysed as described below. The full thickness wounds were imaged in the middle of the wound site midway of the dermis. The entire image was considered as the region of interest and was analysed as described below.

The image analysis performed was based on the method of McMullen, *et al.* (121). Briefly, the image was analysed on the grey scale luminosity and the resulting image histogram. The image histogram quantifies the number of pixels per shade of 256 shades of grey. Each shade was referred to as a "bin" and from the image histogram the number of pixels per bin (shade of grey) was determined. In this case the images were desaturated using the GIMP software package (version 2.6.8). Following desaturation, each image was saved as a high quality JPEG and re-opened in IMAGE J (version 1.4.3.67) and the histogram generated. The pixel count for each bin was calculated by the software and the copied into Microsoft's Office 2013 EXCEL package.

The specimens that were analysed included control sections that were used to optimise the analysis of the histogram pixel distributions. Due to the nature of the histogram distributions being skewed the 1st, 2nd, and 3rd quartiles were calculated for each of the control sections. The positions of each of the quartiles within the series of 256 bins were determined and this served as the parameters around which the experimental sections could be analysed. From

the control section distributions, the average bin position for each of the quartiles provided a gate within which the total sum of the pixels was calculated. The following gates were used and further referred to as; Area 1 = Bin 0 – 1st Quartile Bin position, Area 2 = 1st Quartile Bin position – 2nd Quartile Bin position, Area 3 = 2nd Quartile Bin position – 3rd Quartile Bin position, Area 4 = 3rd Quartile Bin position – Bin 256.

From the control sections it was seen that the majority of the mature collagen occurred in Area 4. In the deep partial thickness wounds 81% and 72% of pixels occurred in the deep partial thickness and full thickness control sections respectively. As the majority of the pixels occurred in Area 4, only this area was considered for statistical analysis. A ratio was calculated for the experimental sections by taking the pixel count in area 4 of the experimental sections over the pixel count of area 4 of the control sections (as is seen in the equation below). The resultant collagen infiltrations were plotted against time (days post-operative).

$$\text{Collagen Content} = \frac{\text{Experimental Area 4 Pixel Count}}{\text{Control Area 4 Pixel Count}}$$

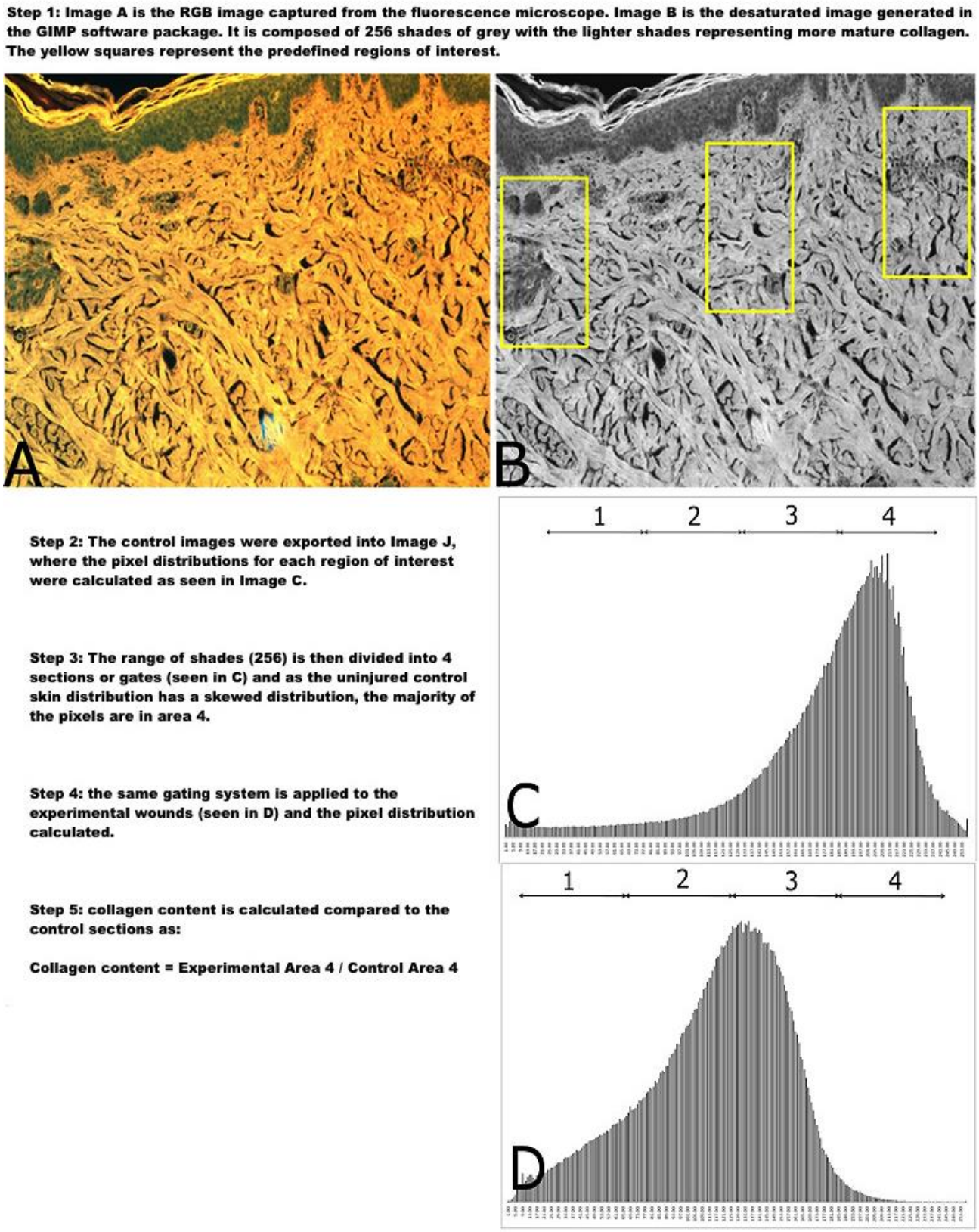


Figure 2.5. Picrosirius red analysis algorithm. The image A, represents the original PSR stained section imaged under fluorescence light as described above. Image B represents the desaturated image that is generated for further analysis. The yellow areas represent the ROI's that were considered for the analysis. The pixel distributions for each ROI were averaged and the gating system applied to describe the distributions.

2.3.10 Safety Analysis of Liver Hepato-toxicity

Jugular venous blood was collected on the sample collection days for liver function tests in 8.5ml yellow top SST gel tubes (BD Biosciences) and sent to Contract Lab Services (CLS) at the National Institute for Occupational Health (NIOH), Braamfontein for analysis. In addition to the experimental pigs that were exposed to the *Senecio* based therapy, blood was taken for comparison purposes from 3 other pigs involved in another similar study with the same wound model. These pigs were exposed to the same anaesthetic agents, wounding mechanism, diet and sample collection days.

A month post completion of the experiments, seven of the animals were euthanized and liver biopsies were taken from 2 lobes of the liver and placed in 10% buffered formalin. The samples were sent to Golden Vet Pathologists (Onderstepoort, Pretoria) for analysis of acute and chronic pyrrolizidine alkaloid poisoning.

2.3.11 Statistical Analysis

Statistical significance was determined using Statistica (Version 9). Analysis between the treatment groups was determined using the Kruskal-Wallis test, coupled with a *post-hoc* analysis. Significance was accepted at $p < 0.05$.

2.4 Results

2.4.1 Deep Partial Thickness Wound pH

Measured wound surface pH over the course of the experiment can be seen in Figure 2.6, with the corresponding data and statistical analysis was tabulated in Table 2.1. The pH of fresh wounds at day 0 post-operative, increased from between 7.93 and 7.97, then spiked to around 8.02 for the *Senecio* treated wounds, 8.37 for the activated carbon wound group (p = 0.001 compared to the plant treated group), and 8.41 for the negative control treated group (p = 0.013 compared to the plant treated group) on day 2 post-operatively.

From day 2 post-operatively, the pH in all treatment groups decreased to reach a similar end point by day 16 post-operatively. Additionally, throughout the observational period, the rates of decline differed. Day 5 post-operative marked a point where the initial rapid decrease changed to a more gradual decrease in all treatment groups. Thereafter, the rate of decline in pH reduced further and from day 12 post-operative onwards stabilised in the *Senecio* treated wounds. In contrast, the pH of the other two treatment groups continued to decline, without statistically significant differences compared to the *Senecio* treated wounds.

Table 2.1. Wound pH at specific post-operative days. Data are presented as mean ± SEM (n). Underlined p – values are significant at p < 0.05.

Days Post-operative	Negative Control	Activated Carbon	*Senecio*	Group wise *p* - value	*Senecio* vs. Negative Control *p* - value	*Senecio* vs. Activated Carbon *p* - value	Negative Control vs. Activated Carbon *p* - value
0	7.93 ± 0.07 (12)	7.97 ± 0.08 (12)	7.95 ± 0.08 (12)	0.928	0.596	0.259	0.895
2	8.39 ± 0.05 (11)	8.47 ± 0.04 (11)	8.02 ± 0.09 (9)	0.001	0.001	0.013	0.658
5	7.17 ± 0.08 (10)	7.29 ± 0.12 (10)	7.02 ± 0.06 (11)	0.107	0.480	0.064	0.724
7	6.62 ± 0.14 (6)	6.82 ± 0.16 (6)	6.87 ± 0.13 (8)	0.470	0.220	0.358	0.897
8	6.70 ± 0.08 (9)	6.75 ± 0.08 (6)	6.73 ± 0.09 (9)	0.932	0.665	0.508	0.149
9	6.67 ± 0.09 (7)	6.43 ± 0.09 (6)	6.56 ± 0.08 (7)	0.165	0.418	0.284	0.156
12	6.23 ± 0.12 (9)	6.24 ± 0.12 (7)	6.22 ± 0.12 (9)	0.996	0.962	0.916	0.563
16	5.75 ± 0.16 (6)	5.83 ± 0.14 (6)	6.20 ± 0.20 (6)	0.138	0.284	0.452	0.949

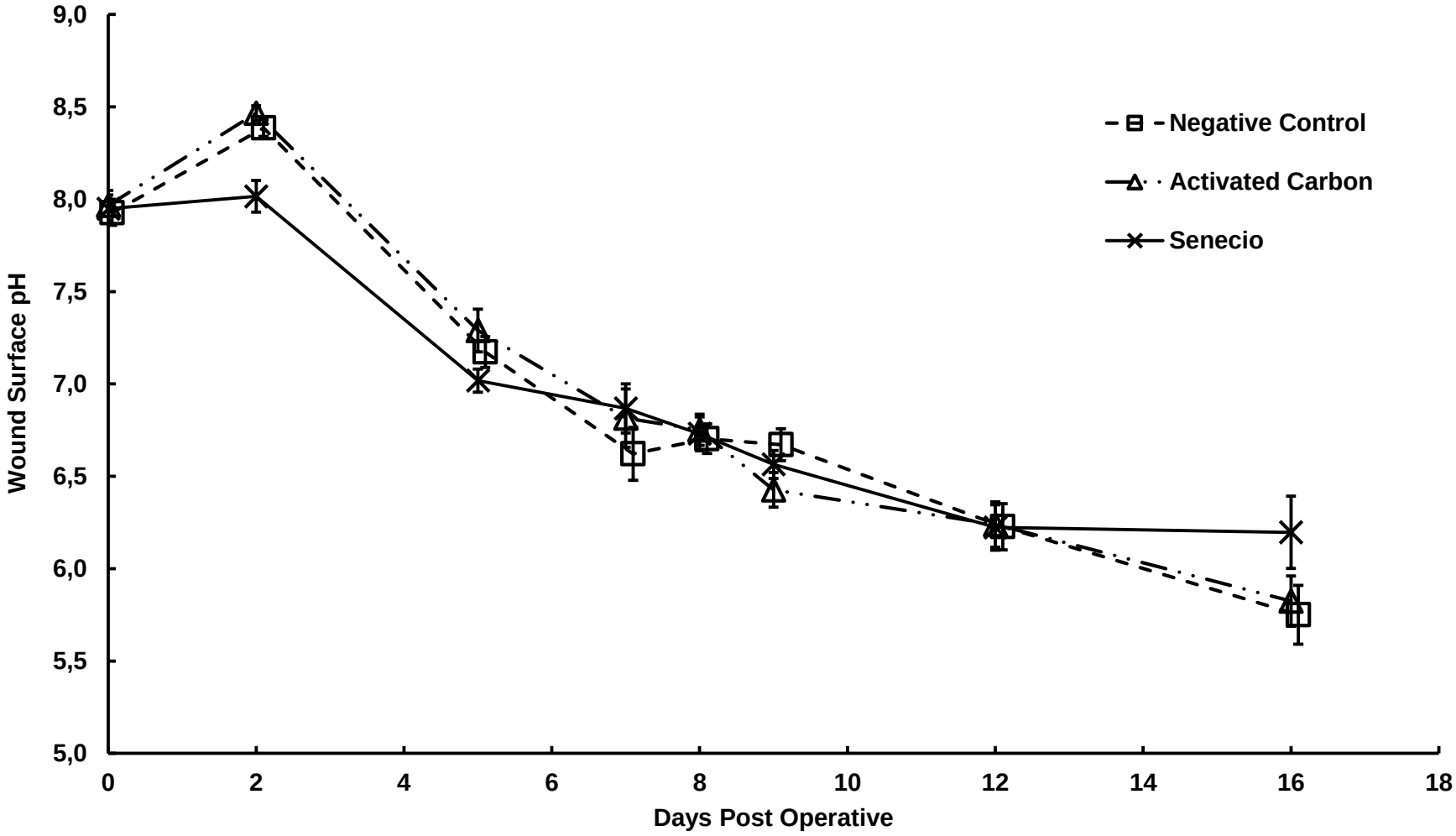


Figure 2.6. Wound pH plotted against time (Days post-operative). Error bars represent the SEM.

2.4.2 Deep Partial Thickness Wound Gross and Histological Analysis

Sequential photographs of the deep partial thickness wounds recorded the overall wound healing pattern. On day 2 post-operatively, all wounds appeared the same, with the fresh wound beds easily seen after the residual Senecio material and activated carbon was removed (Figure 2.7 - A, B and C). No epidermis was observed on histology in any of the treatment groups (Figure 2.7 - D, E and F). There also appear to be no differences between treatments as to whether debriding the residual material from the wound bed had affected the wounds.

At day 5 post-operatively, histological sections demonstrated a newly formed epidermis in all three treatment groups which appeared similar in thickness (Figure 2.8 - D, E and F) and at this point the wounds were regarded as being 're-epithelialised'. At day 7 post-operative, the epidermis in the Senecio treated wounds appeared thicker when compared to the controls (Figure 2.9 - D, E and F). On debriding, the integrity of the newly formed epidermis in the Senecio group and in the activated carbon treated wounds differed. The epidermis in the Senecio group appeared to be more resilient to debriding and less prone to rupture compared to the activated carbon treated wound where the epidermis was easily ruptured with associated haemorrhaging.

Figure 2.10, Figure 2.11 and Figure 2.12 were representive of the remainder of the observational days. The epidermis is seen to become thinner from days 7/9 post-operative where a similar thickness is seen in all three treatment groups at day 16 post-operative (Figures 2.9 to Figure 2.11 - D, E and F).

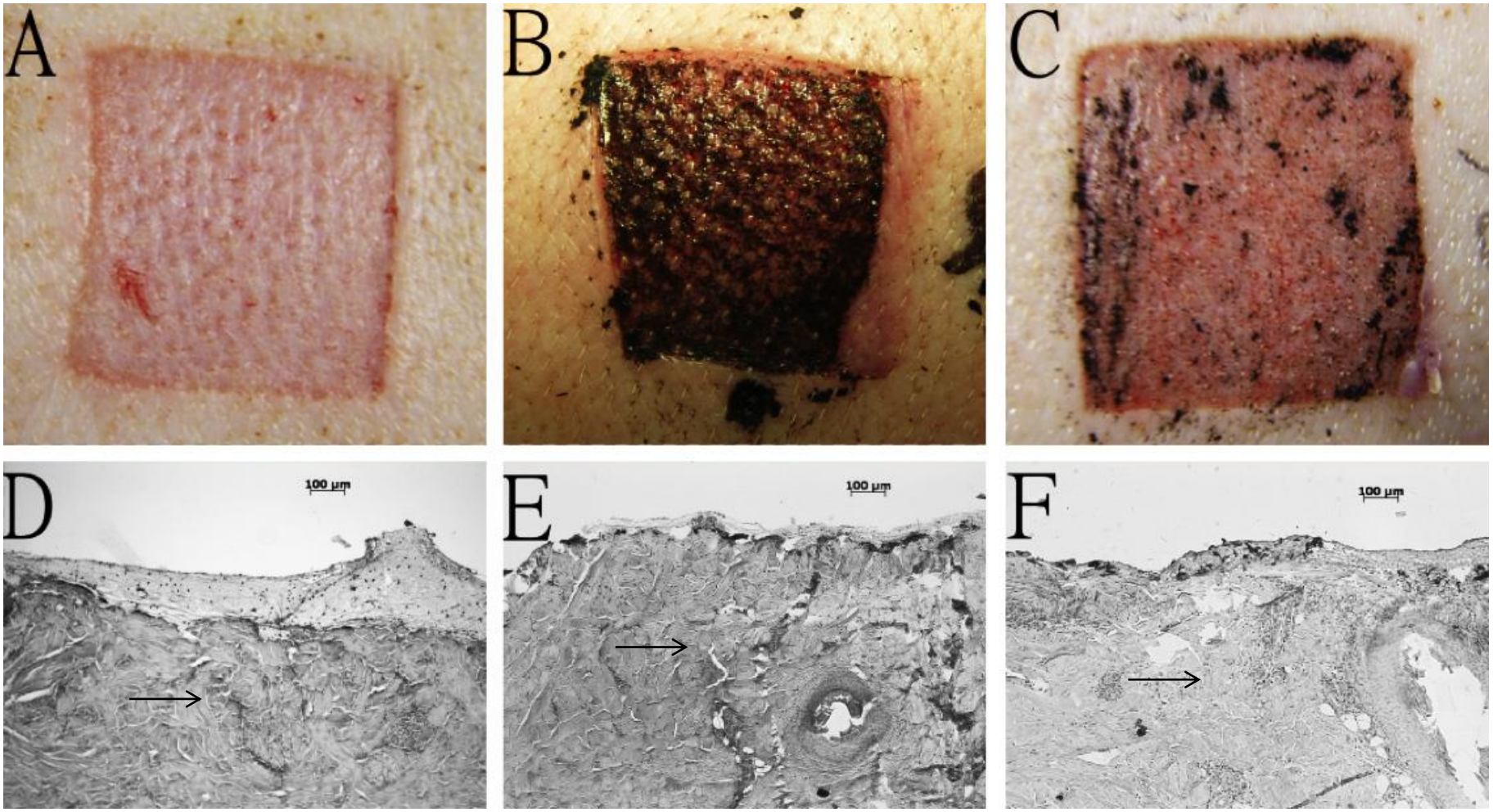


Figure 2.7. Wounds viewed on day 2 post-operative with the negative control (A), activated carbon (B), and Senecio (C). Corresponding histological sections are represented in D, E, and F being negative control (D), activated carbon (E), and Senecio (F). In the gross pictures (A, B and C) the initial wound edges are still evident with minimal contraction noted. The black arrows indicate the remaining dermis 2 days after the wounds were created. Histological sections were imaged at 100x magnification.

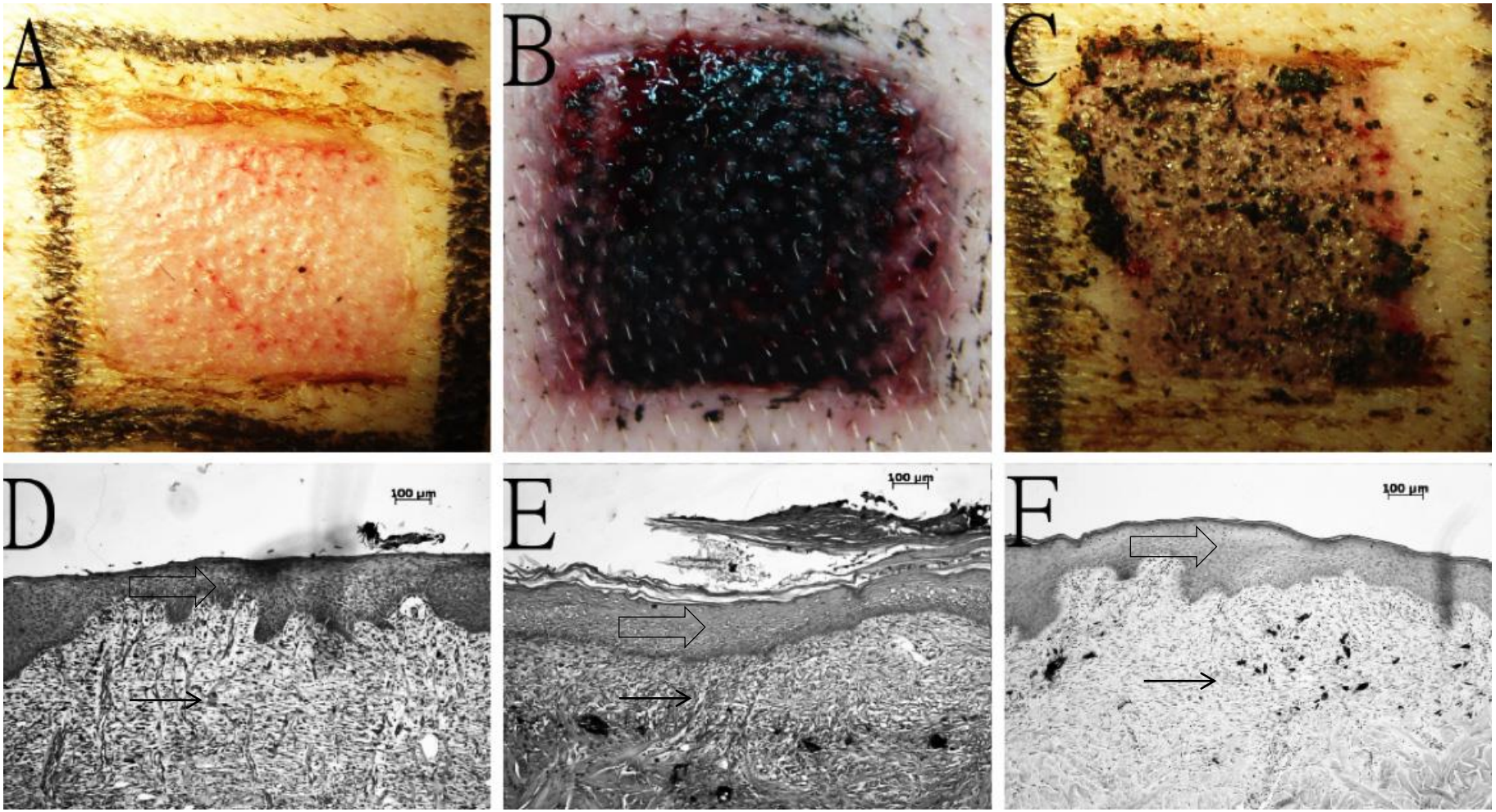


Figure 2.8. Wounds viewed on day 5 post-operative with the negative control (A), activated carbon (B), and Senecio (C). Corresponding histological sections are seen in D, E, and F being negative control (D), activated carbon (E), and Senecio (F). In the gross images (A, B and C) a prominent epithelial layer is present in the Senecio treated wounds, which was not evident in the control. In the histological sections, the arrows that are not filled indicate the regenerating epidermis, which was not evident in the corresponding gross images of the control wounds. The solid arrows indicate the granulation tissue deep to the epidermis. Histological sections were imaged at 100x magnification.

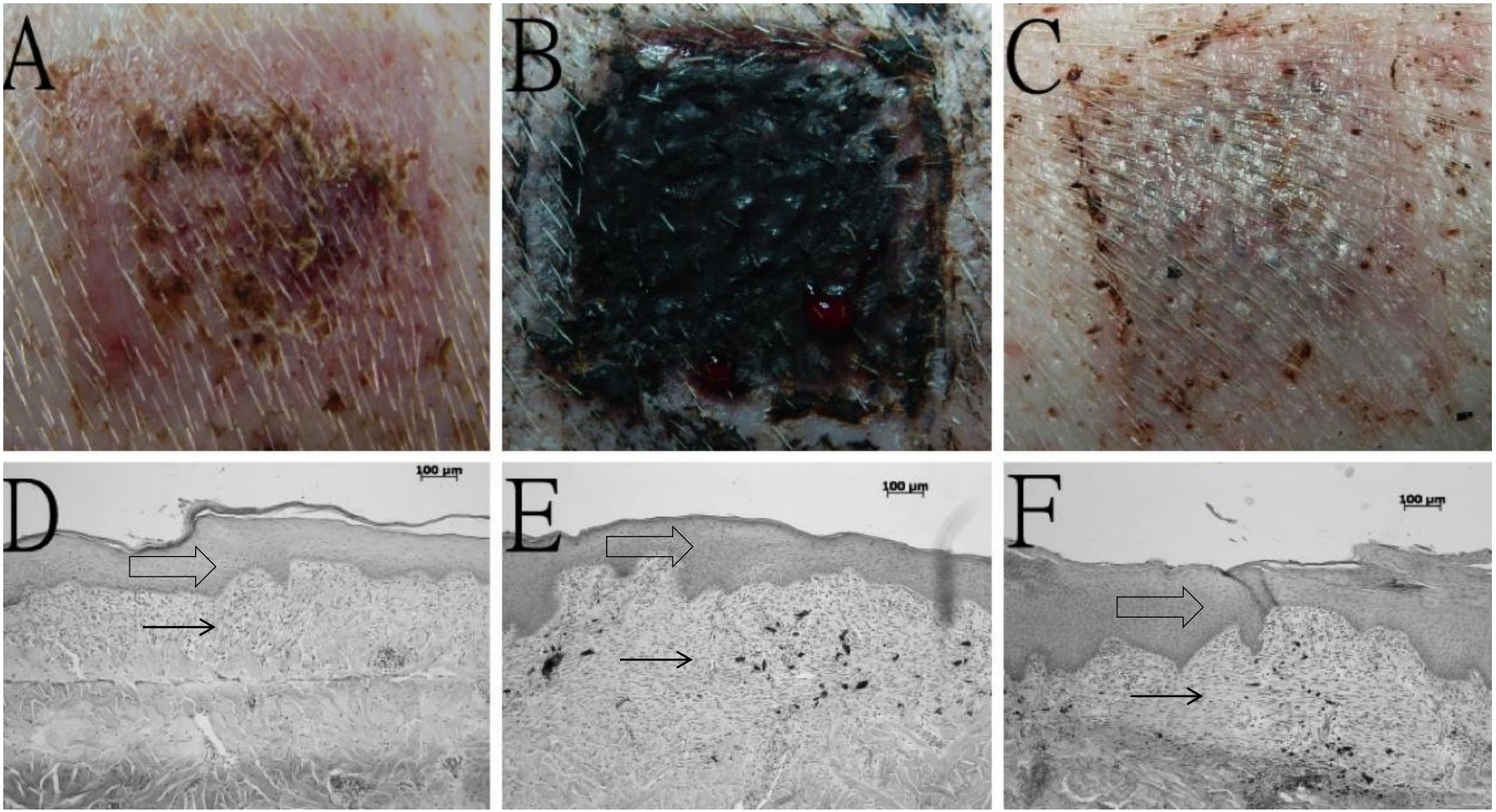


Figure 2.9. Wounds viewed on day 7 post-operative with the negative control (A), activated carbon (B), and Senecio (C). Corresponding histological sections are seen in D, E, and F being negative control (D), activated carbon (E), and Senecio (F). In the gross images (A, B and C) a prominent eschar was seen in the control wounds (A and B) but was not seen in the Senecio treated wounds. In the histological sections, the arrows that are not filled indicate the regenerating epidermis, which was thicker in the Senecio treated wounds. The solid arrows indicate the granulation tissue deep to the epidermis. Histological sections were imaged at 100x magnification.

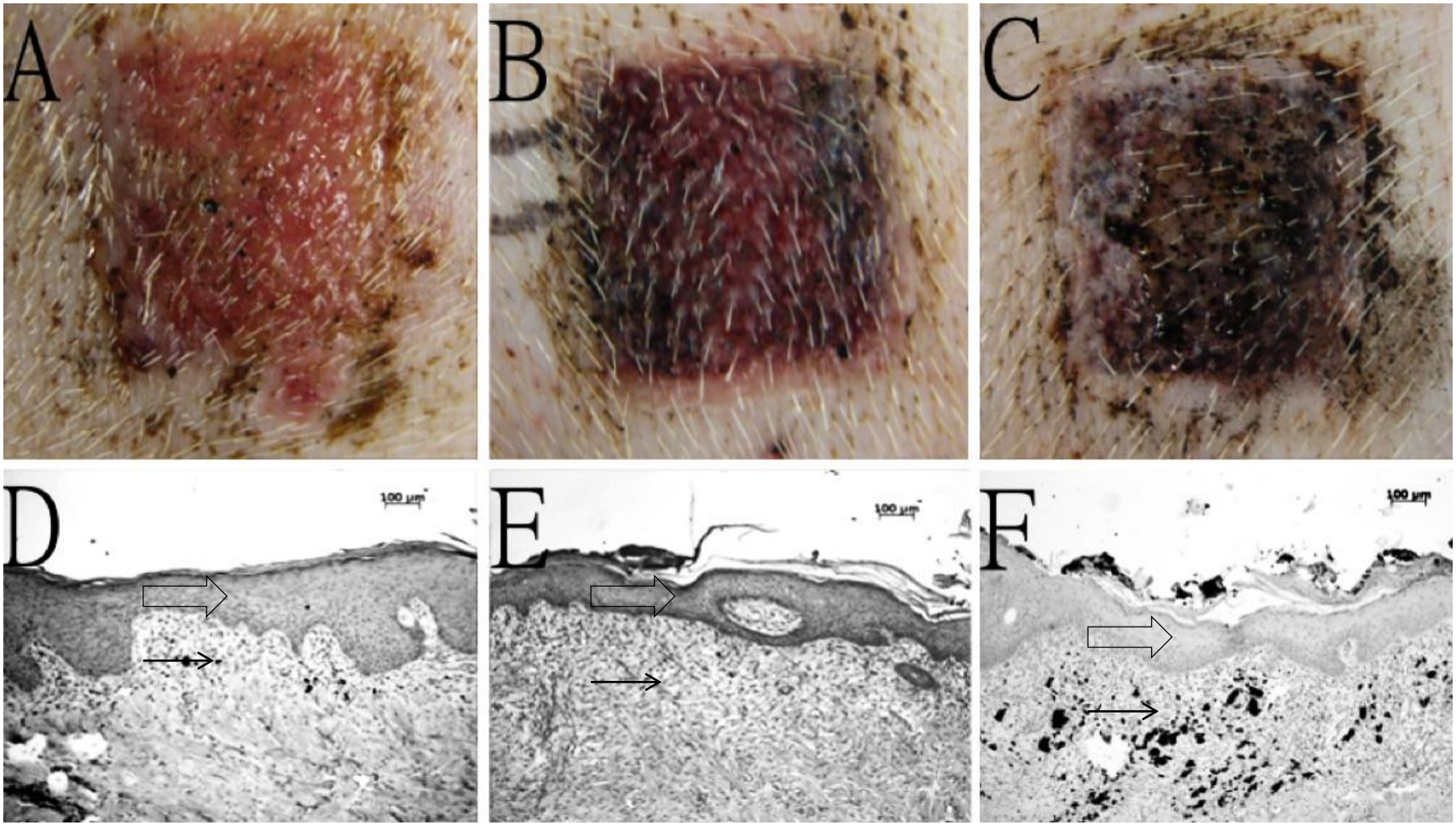


Figure 2.10. Wounds viewed on day 9 post-operative with the negative control (A), activated carbon (B), and Senecio (C). Corresponding histological sections are seen in D, E, and F being negative control (D), activated carbon (E), and Senecio (F). In the gross images (A, B and C) the Senecio treated wounds have a more prominent epithelial layer but the control also has a more established epithelial layer. In the histological sections, the arrows that are not filled indicate the regenerating epidermis, which was thicker in the control treated wounds. The solid arrows indicate the granulation tissue deep to the epidermis. Histological sections were imaged at 100x magnification.

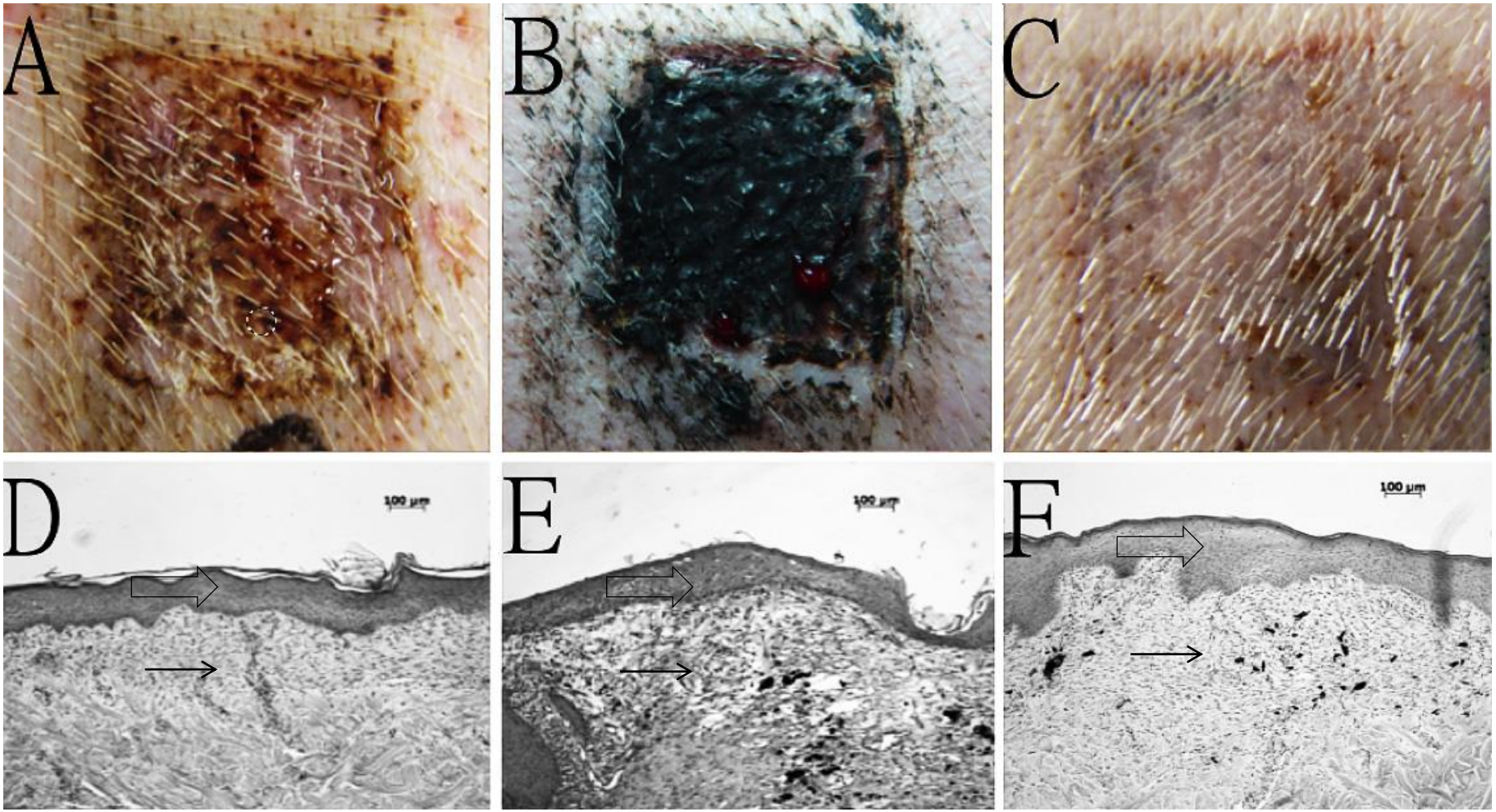


Figure 2.11. Wounds viewed on day 12 post-operative with the negative control (A), activated carbon (B), and Senecio (C). Corresponding histological sections are seen in D, E, and F being negative control (D), activated carbon (E), and Senecio (F). In the gross images (A, B and C) the eschar on the control treated wounds is still evident but is absent in the Senecio treated wounds. In the histological sections, the arrows that are not filled indicate the regenerating epidermis, which was equal in all treatment groups. The solid arrows indicate the granulation tissue deep to the epidermis. Histological sections were imaged at 100x magnification.

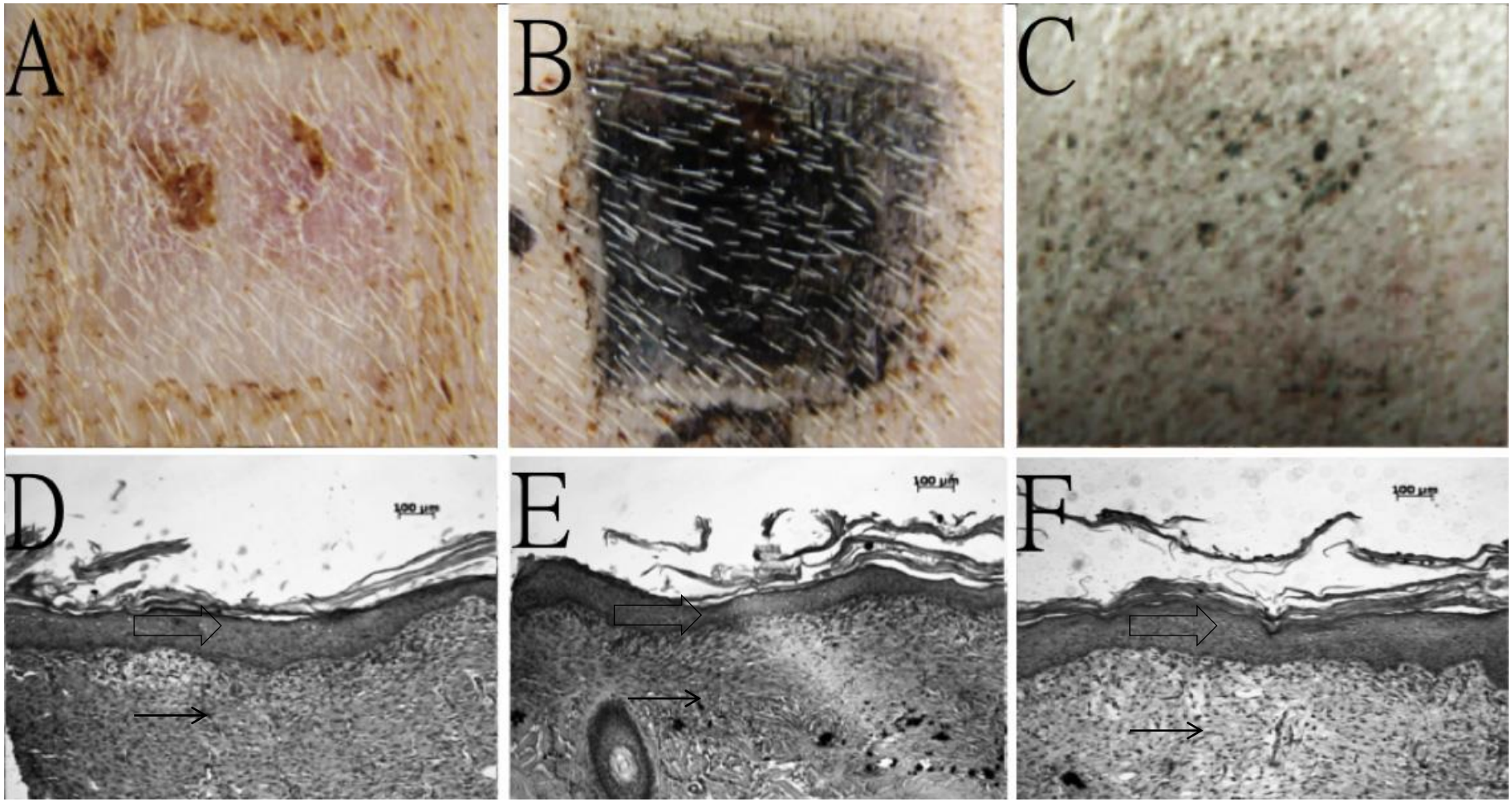


Figure 2.12. Wounds viewed on day 16 post-operative with the negative control (A), activated carbon (B), and Senecio (C). Corresponding histological sections are seen in D, E, and F being negative control (D), activated carbon (E), and Senecio (F). In the gross images (A, B and C) minimal eschar is present in all treatment groups. The original wound area is no longer present in the Senecio treated wounds but can still be seen in the controls. In the histological sections, the arrows that are not filled indicate the regenerating epidermis, which was equal in all treatment groups. The presence of desquamating keratinised epidermal layers is evident in all treatment groups. The solid arrows indicate the granulation tissue deep to the epidermis. Histological sections were imaged at 100x magnification.

2.4.3 Morphometric Analysis

Deep Partial Thickness Wound Morphometric Analysis

Epidermal Thickness

Significant differences in the thickness of the epidermis was seen at all days except at day 16 (Table 2.2). Compared to the negative control, the *Senecio* treated group had a significantly thicker epidermis at days 5 (p = 0.0001), 7 (p = 0.0002) and 9 (p = 0.031) but not at days 12 (p = 0.121) and 16 (p = 0.623). When comparing the *Senecio* treated group to the activated carbon treated group there was a significantly thicker epidermis in the Senecio group at days 5 (p = 0.017) and 7 (p = 0.002) but not at days 9 (p = 0.231), 12 (p = 0.241) and 16 (p = 0.212). The comparison between the vehicle and negative control shows that the vehicle had a significantly thicker epidermis at days 7 (p = 0.005), 9 (p = 0.009), and 12 (p = 0.011) but not at day 5 (p = 0.140) and 16 (p = 0.427).

These data above are represented graphically (Figure 2.13) and showed a rapid increase in the epidermal thickness to a maximum value followed by a progressive decline to similar values at day 16. Compared to the other groups, the initial thickness of the *Senecio* treated group was greater, with an earlier maximum thickness at day 7, followed by the decline (Figure 2.13). The other two treatments followed a similar pattern, with the maximum value later at day 9 with for the negative control and vehicle groups.

Epidermal Thickness Ratio

The epidermal thickness ratio of the *Senecio* treated group was significantly greater than the negative control (opsite only) at post-operative days 7 (p = 0.005) and 12 (p = 0.026) but not at other times (Table 2.3). The ratio of *Senecio* treated group was also significantly greater than the vehicle treated group (actvated carbon) at post-operative days 5 (p = 0.0002) and 7 (p = 0.004). Finally, compared to the vehicle, the negative control had a statistically significantly greater ratio at post-operative days 5 (p = 0.004), 9 (p = 0.009), whereas the ratio of the vehicle was only greater than the negative control at day 12 (p = 0.010). The graphical representation (Figure 2.14) of the ratio follows a similar pattern as before with the peak in the *Senecio* being 2 days before that of the controls.

Table 2.2. Epidermal thickness measurements (μm) at specific post-operative days. Data are presented as mean ± SEM (n). Underlined p – values are significant.

Days Post-operative	Negative Control	Activated Carbon	*Senecio*	Group wise *p* - value	*Senecio* vs. Negative Control *p* - value	*Senecio* vs. Activated Carbon *p* - value	Negative Control vs. Activated Carbon *p* - value
5	122.30 ± 2.30 (10)	125.74 ± 19.20 (10)	186.51 ± 9.81 (10)	0.001	0.000	0.017	0.141
7	116.14 ± 10.34 (10)	161.51 ± 13.54 (10)	263.30 ± 21.20 (10)	0.000	0.000	0.002	0.005
9	148.27 ± 14.58 (10)	247.76 ± 21.70 (10)	217.98 ± 20.83 (10)	0.012	0.031	0.241	0.009
12	116.59 ± 8.28 (10)	153.75 ± 10.38 (10)	137.68 ± 8.48 (10)	0.028	0.121	0.241	0.011
16	134.35 ± 9.00 (10)	147.99 ± 12.40 (10)	124.55 ± 3.95 (10)	0.412	0.623	0.212	0.427

Table 2.3. Epidermal thickness ratio at specific post-operative days. Data are presented as mean ± SEM (n). Underlined p – values are significant.

Days Post-operative	Negative Control	Activated Carbon	*Senecio*	Group wise *p* - value	*Senecio* vs. Negative Control *p* - value	*Senecio* vs. Activated Carbon *p* - value	Negative Control vs. Activated Carbon *p* - value
5	2.32 ± 0.15 (10)	1.80 ± 0.09 (10)	2.39 ± 0.07 (10)	0.000	0.325	0.000	0.005
7	2.02 ± 0.21 (10)	2.15 ± 0.15 (10)	3.54 ± 0.43 (10)	0.003	0.005	0.004	0.791
9	2.79 ± 0.26 (10)	3.21 ± 0.18 (10)	3.04 ± 0.25 (10)	0.328	0.121	0.650	0.473
12	1.70 ± 0.14 (10)	2.24 ± 0.08 (10)	2.36 ± 0.19 (10)	0.013	0.026	0.521	0.007
16	2.03 ± 0.14 (10)	2.33 ± 0.12 (10)	2.29 ± 0.11 (10)	0.157	0.141	0.880	0.082

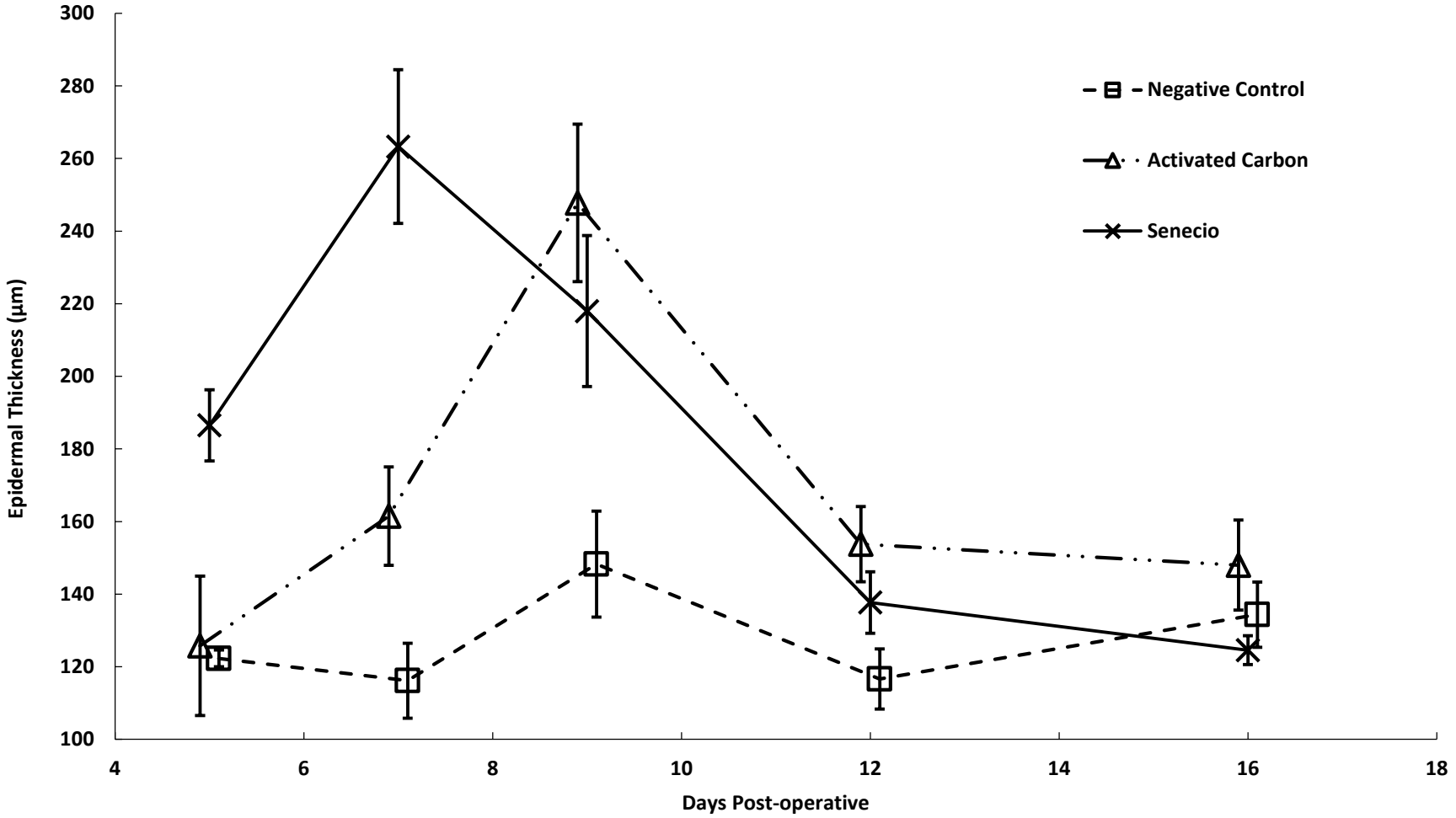


Figure 2.13. The mean epidermal thickness (µm) of the deep partial thickness wounds plotted against time (Days Post-operative). Error bars represent the SEM.

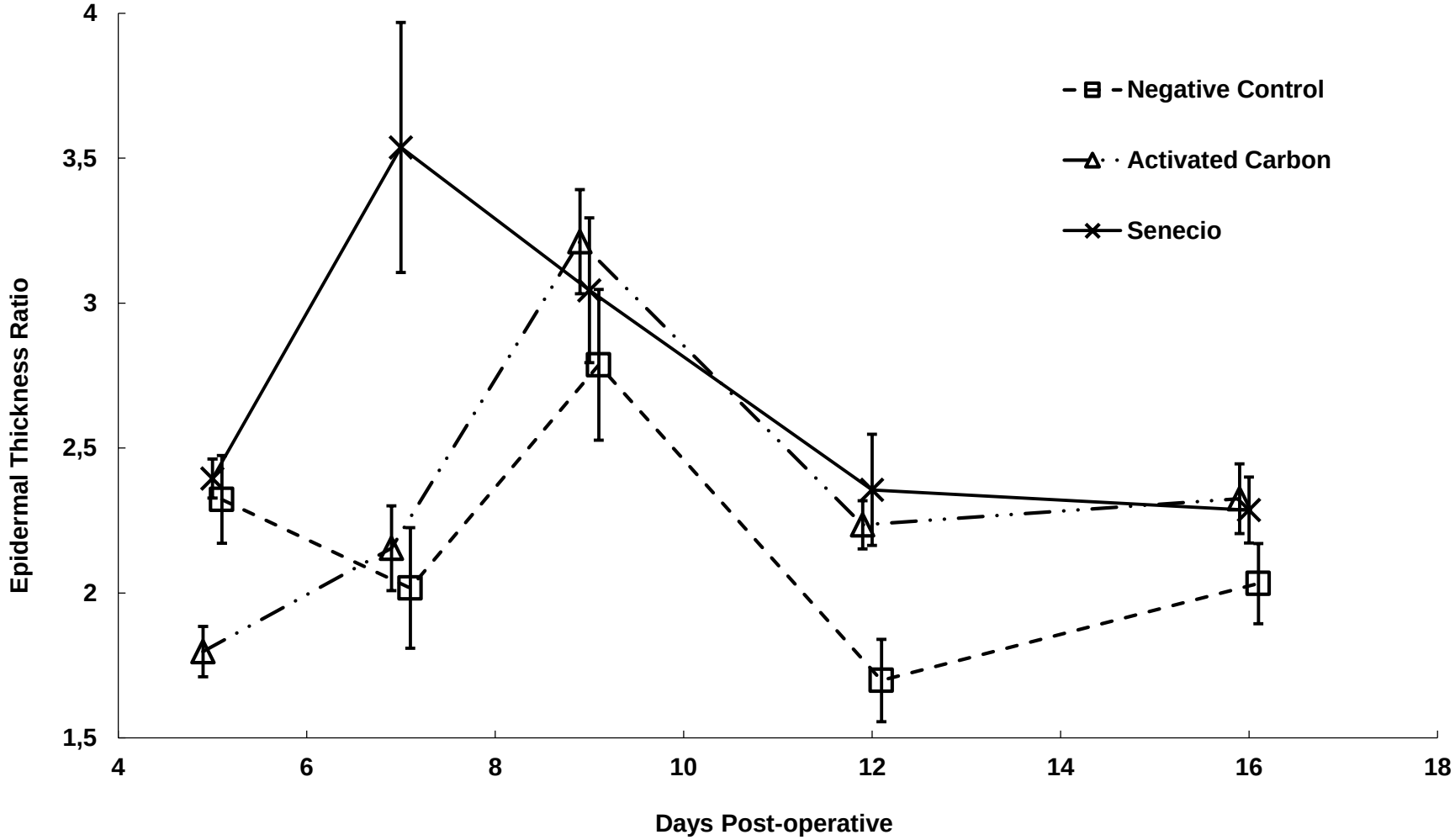


Figure 2.14. Epidermal thickness ratio (mean) of the deep partial thickness wounds plotted against time (Days Post-operative). Error bars represent the SEM.

Full Thickness Wound Morphometric Analysis

By day 8 post-operatively, 44% of the *Senecio* treated wounds had closed compared to the activated carbon treated wounds where only 33% of the wounds had closed. In the negative control treated wounds, 100% of wounds had closed by day 8 post-operatively. By day 16 all the wounds in all 3 treatment groups had closed.

The average tongue length at day 8 post-operative was not significantly different between the *Senecio* and activated carbon treatment groups (p = 0.566). No other comparisons could be drawn between the negative control group treated wounds and the other two treatment groups. By day 16 post-operative all the wounds had closed and it was not possible to measure the tongue lengths.

The mid-dermal deficit at day 8 and day 16 post-operative was not significantly different between any of the treatment groups.

The data represented graphically (Figure 2.15) shows a steep decline in the mid-dermal deficit in all treatment groups from day 0 to day 8 post-operatively. From day 8 to day 16 post-operative the decline is not as marked, however the decline in the *Senecio* treated wounds was greater compared to the negative control and activated carbon treated wound groups.

Table 2.4. Full thickness wound morphological analysis at specific post-operative days. Data are presented as mean ± SEM (n). Underlined p – values are significant.

Treatment	Days Post-Operative	Percentage Wounds Closed (%)
Negative Control	8	100
Activated Carbon	8	33
Senecio	8	44
Negative Control	16	100
Activated Carbon	16	100
Senecio	16	100

Treatment	Days Post-Operative	Average Tongue Length	Group wise *p* - value	Post-hoc Analysis	
Negative Control	8	Wound Closed	0.054	Senecio vs. Negative Control	NA
Activated Carbon	8	741.88 ± 190.38 (9)		Senecio vs. Activated Carbon	0.566
Senecio	8	558.39 ± 231.37 (9)		Negative Control vs. Activated Carbon	<u>NA</u>
Negative Control	16	Wound Closed			
Activated Carbon	16	Wound Closed	NA		
Senecio	16	Wound Closed			

Treatment	Days Post-Operative	Mid-Dermal Deficit	Group wise *p* - value	Post-hoc Analysis	
Negative Control	8	2159.33 ± 116.29 (9)	0.759	Senecio vs. Negative Control	0.810
Activated Carbon	8	2237.08 ± 82.68 (9)		Senecio vs. Activated Carbon	0.885
Senecio	8	2214.19 ± 435.51 (8)		Negative Control vs. Activated Carbon	0.427
Negative Control	16	1936.26 ± 256.02 (6)	0.365	Senecio vs. Negative Control	0.575
Activated Carbon	16	2251.18 ± 254.77 (6)		Senecio vs. Activated Carbon	0.230
Senecio	16	1726.27 ± 193.49 (6)		Negative Control vs. Activated Carbon	0.379

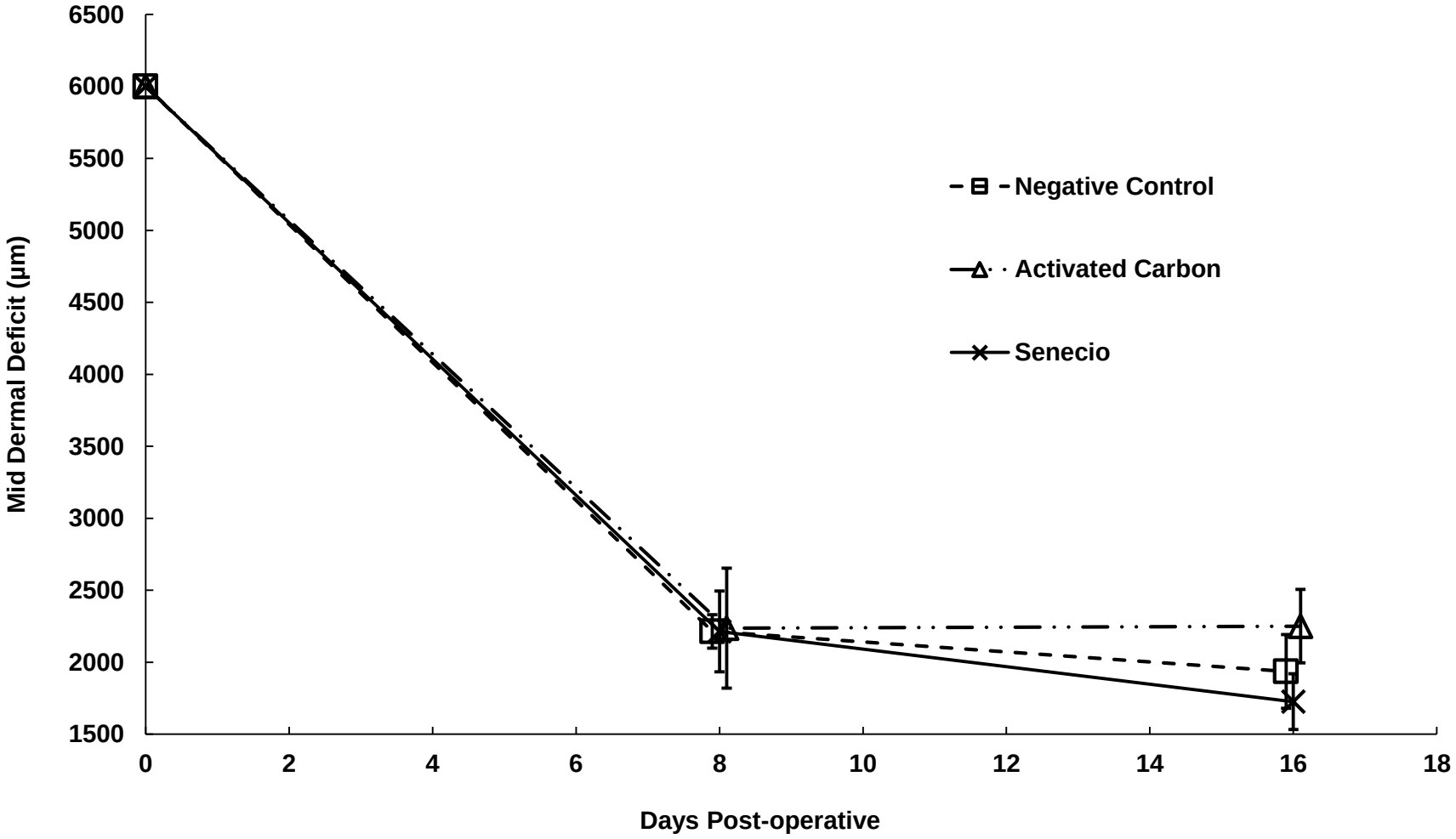


Figure 2.15. Mid-dermal deficit plotted against time (Days Post-operative). Error bars represent the SEM.

2.4.4 Collagen Analysis

Deep Partial Thickness Wound Collagen Analysis

Representative Picrosirius red stained sections of collagen deposition can be seen in Figure 2.16. For the analysis purposes, desaturated images that were generated have been shown immediately below each of the original stained sections. More mature collagen appears brighter in the desaturated images. This however is minimal at day 8 post-operative in all 3 treatment groups (Figure 2.16 - B, D, and F). At day 16, brighter collagen fibres can be seen in the *Senecio* and negative control treated wounds (Figure 2.16 - H and L) when compared to the activated carbon treated group (Figure 2.16 - J). The collagen fibres in the *Senecio* and negative control treated groups differ with the *Senecio* treated wounds showing a finer distribution of collagen fibres when compared to the negative control where fibres are generally thicker.

Table 2.5. Collagen content of the deep partial thickness wounds at specific post-operative days. Data are presented as mean ± SEM (n). Underlined p – values are significant at p < 0.05.

Days Post-operative	Negative Control	Activated Carbon	*Senecio*	Group wise *p* - value	*Senecio* vs. Negative Control *p* - value	*Senecio* vs. Activated Carbon *p* - value	Negative Control vs. Activated Carbon *p* - value
8	35.95 ± 2.42 (10)	67.60 ± 3.12 (10)	52.59 ± 2.78 (10)	<u>0.001</u>	<u>0.002</u>	<u>0.003</u>	<u>0.045</u>
16	79.82 ± 4.88 (10)	59.43 ± 8.88 (10)	77.99 ± 8.04 (10)	0.129	0.970	0.090	0.089

The analysis of the collagen content immediately deep to the epidermis of the DPT wounds (Table 2.5) shows a significant difference at day 8 only ($p = 0.001$). The *Senecio* and negative control treated groups, had a significantly lower collagen content compared to the activated carbon treated group ($p = 0.003$ and 0.045 respectively). The *Senecio* group had a significantly greater collagen content than the negative control treated group ($p = 0.002$). At day 16 there was no significant differences between any of the groups ($p = 0.129$).

The data represented graphically (Figure 2.17) shows that from wounding at day 0 to day 8 post-operatively, there is an increase in collagen content in all treatment groups. From day 8 to 16 there is a continued increase in the *Senecio* and negative control groups. The activated carbon treated wounds show a change in trend with a subsequent decrease in the collagen content from day 8 to day 16 post-operatively.

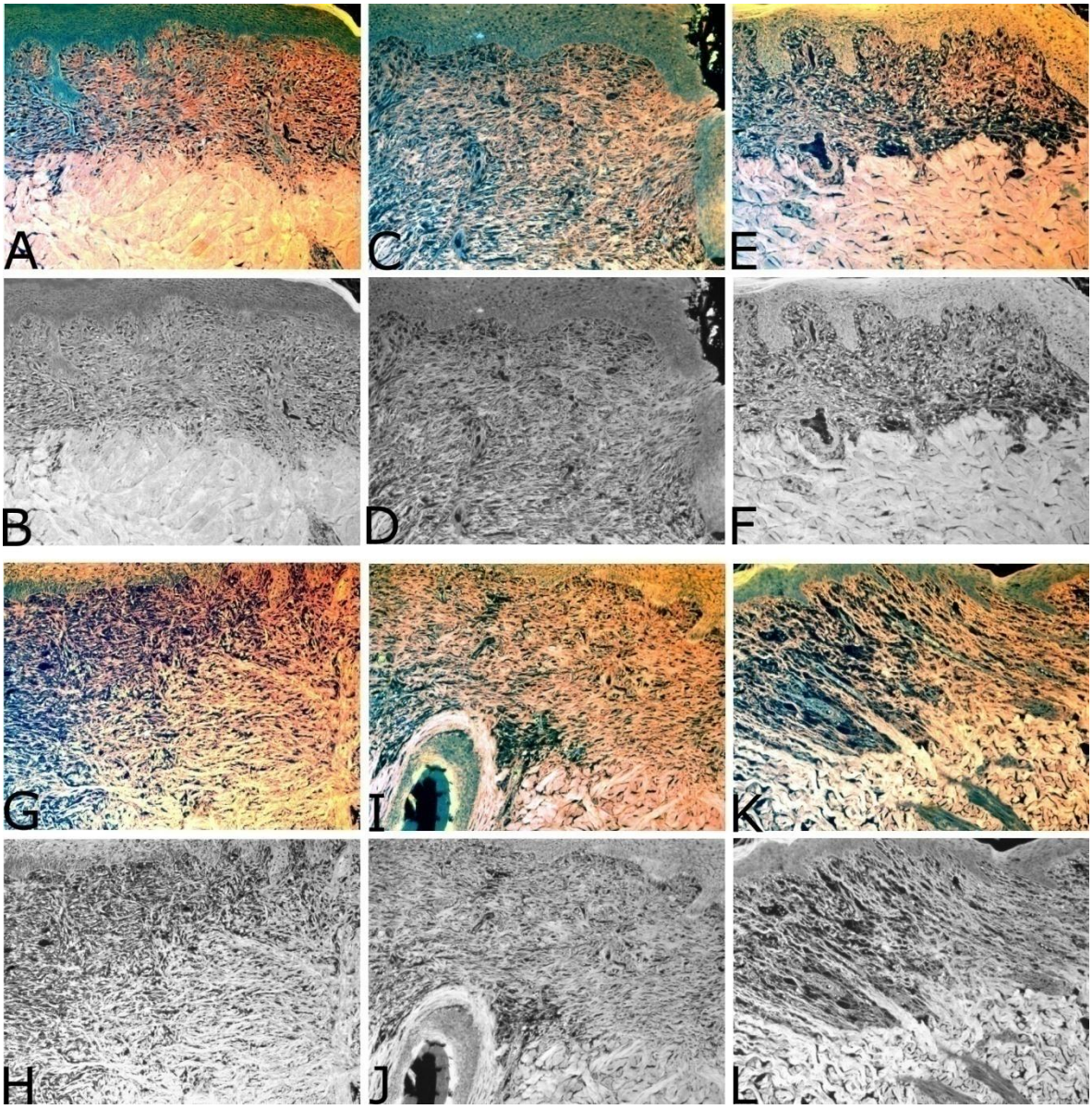


Figure 2.16. Deep partial thickness wounds post Picrosirius red staining. Images are shown as the original colour image with the later desaturation process shown immediately below as described in the materials and methods section. Senecio treated wounds are seen by A and B (Day 8) and G and H (day 16). The activated carbon treated wounds are seen in images C and D (day 8) and I and J (day 16). The negative control treated wounds are seen in images E and F (day 8) and K and L (day 16). At day 8 post-operative the collagen content in the Senecio and negative control treated wounds is less than that of the activated carbon treated wounds which is seen in the luminosity of the granulation tissue. From day 8 to day 16 post-operative it can be seen that collagen fibres are being laid down at an equal rate in all treatment groups.

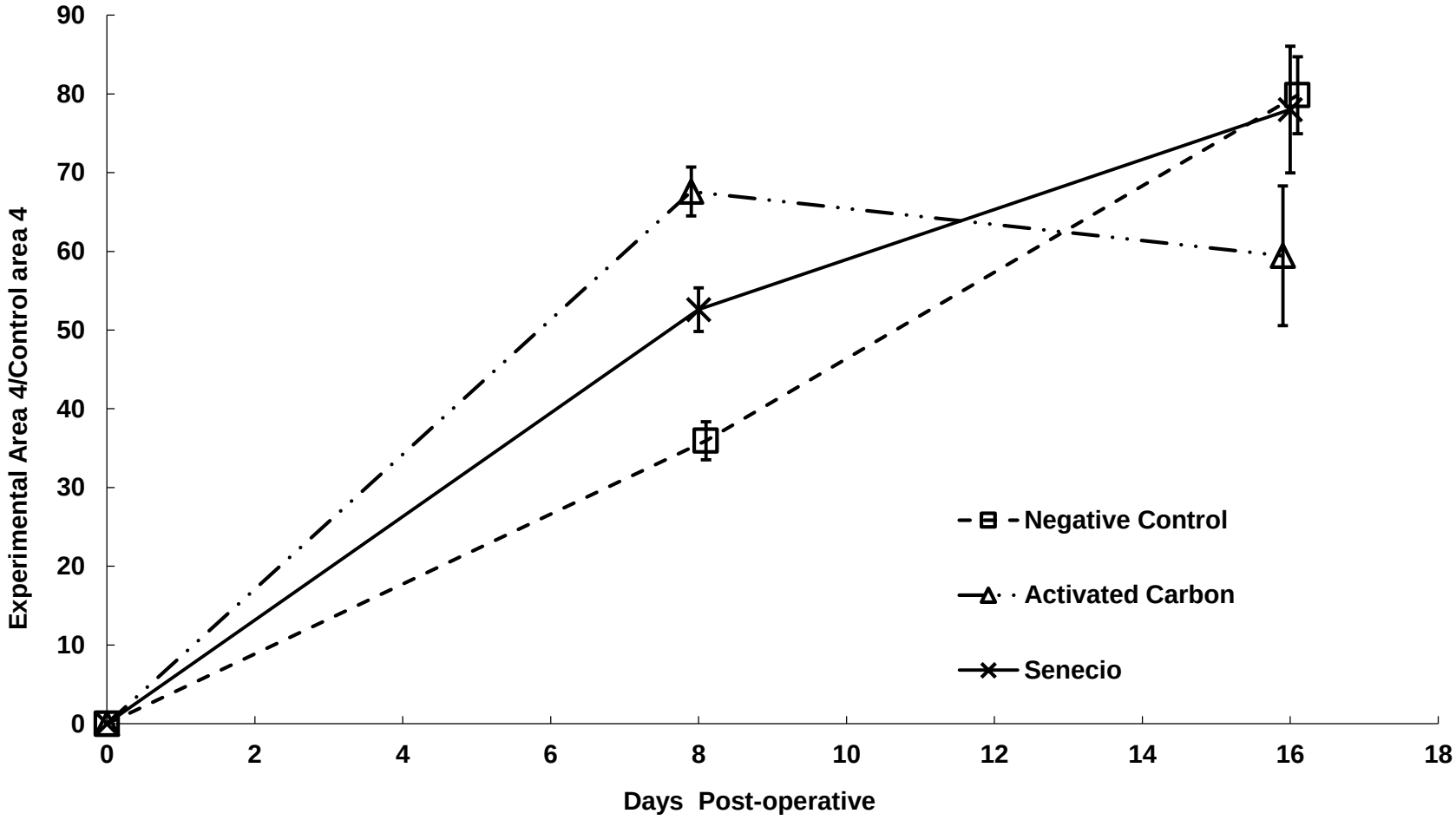


Figure 2.17. Collagen content of the deep partial thickness wounds plotted against time (Days Post-operative). Error bars represent the SEM.

Full Thickness Wound Collagen Analysis

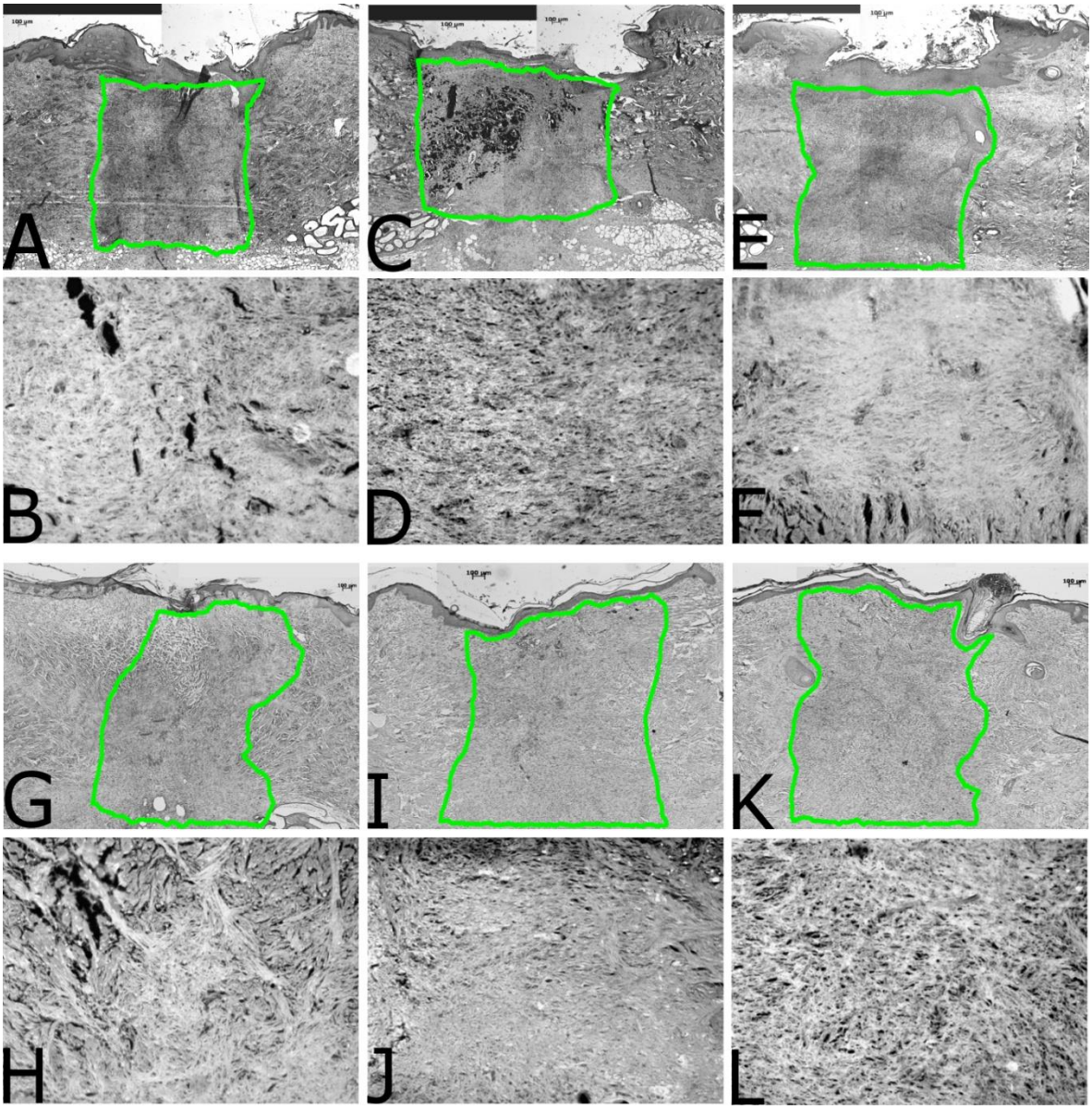


Figure 2.18. Full thickness wounds seen as the entire section above with the corresponding area analysed for collagen deposition below. The wound areas or dermal deficits are outlined in green in each of the sections. The same desaturation process and analysis was followed as described in the text before. The original stained images are not shown. Senecio treated wounds are seen by A and B (Day 8) and G and H (day 16). The activated carbon treated wounds are seen in images C and D (day 8) and I and J (day 16). The negative control treated wounds are seen in images E and F (day 8) and K and L (day 16). No difference in collagen content can be seen in any of the treatment groups at any of the observational days.

Table 2.6. Full thickness wound collagen analysis at specific post-operative days. Data are presented as mean ± SEM (n). Underlined p – values are significant.

Days Post-operative	Negative Control	Activated Carbon	*Senecio*	Group wise *p* - value	*Senecio* vs. Negative Control *p* - value	*Senecio* vs. Activated Carbon *p* - value	Negative Control vs. Activated Carbon *p* - value
8	85.48 ± 4.96 (7)	73.58 ± 9.00 (6)	77.44 ± 11.85 (7)	0.639	0.617	0.898	0.353
16	88.46 ± 6.01 (6)	96.17 ± 10.37 (6)	89.52 ± 6.08 (6)	0.796	0.936	0.575	0.689

Desaturated images show brighter collagen fibres in the *Senecio* (Figure 2.18 - B) and negative control (Figure 2.18 - F) treated wound groups at day 8 post-operative compared to the activated carbon treated wounds (Figure 2.18 - D). At day 16, brighter collagen fibres can be seen in the *Senecio* and negative control treated wounds (Figure 2.18 – H and L) when compared to the activated carbon treated group (Figure 2.18 - J).

There was no significant difference in collagen content on day 8 and 16 post-operative (Table 2.6) with $p = 0.639$ and 0.796 respectively. Graphical representation of the data (Figure 2.19) shows a marked increase from day 0 to 8 after which the rise in the collagen content of all 3 treatment groups decreases.

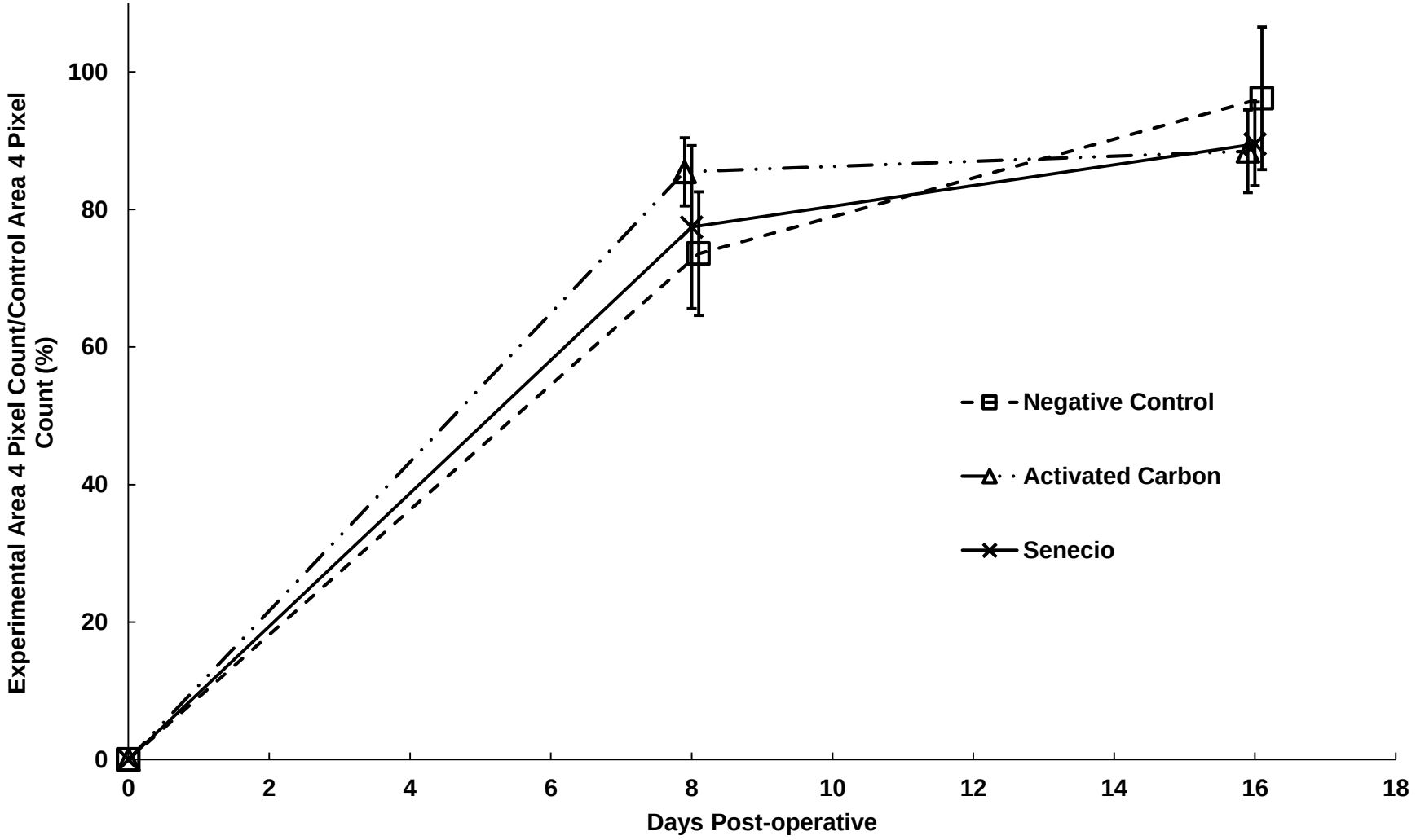


Figure 2.19. Full thickness wound collagen content plotted against time (Days Post-operative). Error bars represent the SEM.

2.4.5 Safety and Toxicity

With regards to the toxicity studies, LFTs were raised in all pigs with the majority of the elevations seen in the alanine aminotransferase (ALT) enzymes. There was no difference between the elevations seen in the pigs exposed to the plant and those that were not. Additionally, the liver samples that were sent to Golden Vet Pathologists for analysis, showed no signs of acute or chronic pyrrolizidine alkaloid poisoning.

Table 2.7. Screen for potential pyrrolizidine alkaloid toxicity.

Pig Identification	Raised LFT's	Acute Pyrrolizidine Alkaloid Poisoning	Chronic Pyrrolizidine Alkaloid Poisoning
Experimental Pig 1	**+**	**-**	**-**
Experimental Pig 2	**+**	**-**	**-**
Experimental Pig 3	**+**	**-**	**-**
Experimental Pig 4	**+**	**-**	**-**
Experimental Pig 5	**+**	**-**	**-**
Experimental Pig 6	**+**	**-**	**-**
Experimental Pig 7	**+**	**-**	**-**
Control Pig 1	**+**	**NA**	**NA**
Control Pig 2	**+**	**NA**	**NA**
Control Pig 3	**+**	**NA**	**NA**

LFT – liver function tests from jugular venous blood. Normal range as dictated by the Merck Veterinary guidelines, Reference Serum Biochemical Markers, Table 7 (http://www.merckvetmanual.com/mvm/htm/bc/tref7.htm).

2.5 Discussion

The majority of poisonings associated with the *Senecio* genus was due to consumption of the plants by livestock and humans in the various preparations (114). Despite the known toxicity, whether topical administration of the plant material causes toxicity has not been determined. This study evaluated the wound healing efficacy, morphological aspects of the healing process and carried out preliminary investigation of potential toxic effects of topically applied *Senecio serratuloides*.

2.5.1 Experimental Wound Model

To evaluate traditional wound healing remedies an appropriate animal model was required. Many studies have used readily available, easy to handle, affordable and versatile rodent models. Wounds created on rodents have been full thickness incisional or excisional wounds. Inert porous substrates (dead space models) can be embedded within these wounds to absorb fluids for determining important biochemical molecules within the wound space that may affect the healing process (Table 1.1 of Chapter 1). However, rodent skin has been regarded as a poor proxy for human skin as the panniculus carnosus contracts and closes the wounds rapidly, which does not allow the re-epithelialisation of the wound to be monitored (122).

In contrast, pig skin is similar to human skin (13) and a porcine model has previously been established in the Central Animal Unit at the University of the Witwatersrand (9, 10). Furthermore, according to Van Wyk, *et al*. (112) and Hutchings (111), the indications for the use of *Senecio* are abrasions and burns which are partial thickness wounds and therefore rodent models which can mostly accommodate full thickness wounds would not be appropriate. Furthermore for deep partial thickness wounds, rodent skin is not appplicable. Therefore a porcine deep partial thickness wound model was initially selected for these experiments.

Due to the erratic nature of wounds that can present it was important to include a full thickness wound model in this investigation. Full thickness wound models allow for the rate of wound contraction to be assessed from morphometric analysis of histological sections of the wound. The extent and rate of epithelialisation, dermal remodelling, fibroblast proliferation, inflammatory infiltrates, neovascularisation and collagen deposition can additionally be determined (Table 1.1 of Chapter 1). However, many such measures are often reported on subjective scoring scales. This has additional implications and is discussed further below.

2.5.2 Wound pH

With other investigations into the use of plant based therapies for wound healing 'broad' variables can be used whose outcome depicts multiple processes that are ongoing within the wound. As a commonly encountered example of a "broad" variable the measurement of wound tensile strength is seen in many of the studies listed in Table 1.1. Tensile strength has been measured in determining the effects of *Hypericum patulum* (29), *Achillea biebersteinii Afan*. (68), and in herbal formulations containing extracts of *Terminalia arjuna* (69). As previously stated in Chapter 1, the strength of a wound in the initial period is not nearly that of a wound that has remodelled over months or even when compared to normal uninjured skin. What is seen is that other factors in the wound environment such as the epithelial layers add to the tensile strength (123). With deep partial thickness wound models, measuring the tensile strength variable would not be suitable as a certain amount of the uninjured dermis could potentially interfere with overall results. Measuring tensile strength of a wound is therefore suited mostly to full thickness wounds.

In this case the alternative broad variable chosen was the pH of the wounds. Intact skin produces and maintains an acidic environment and is important for the barrier function ascribed to skin (124). What is also known is that a gradient exists from the neutral deeper skin layers to the more acidic mantle of the stratum corneum but the mechanism by which the epidermis is acidified is currently hypothetical (125). What is seen is that for the skin to produce a normal pH it needs to be intact and so makes an excellent "broad" variable to describe the overall integrity of the newly formed skin and specific to this investigation where deep partial thickness wounds were assessed.

From the investigations seen here, the pH on day 2 post-operative was lower for the *Senecio* treated wounds after which no other differences were detected statistically. The pH decreased at a similar rate in all treatment groups with a change in the rate around day 5 post-operative. This change could be associated with development of the newly formed epidermis which was documented histologically here. With the presence of the newly formed epidermis, a modulatory effect on the pH may be developing. Moreover, at day 5 post-operative, the pH would reflect the state of the newly formed epidermis and not the state of the acute wound environment. On this premise there appears to be no difference from a functional perspective in that all rates of pH changes for the treatment groups were similar. But from a wound environment perspective, metabolic activity could be affected due to the differing pH in the *Senecio* treated wounds group on day 2 post-operatively where no epidermis is present.

2.5.3 Deep Partial Thickness Wound Morphometric Analysis

Histological analyses of the wounds is mostly employed which includes the variables epithelialisation, dermal remodelling, fibroblast proliferation, inflammatory infiltrates, neovascularisation and collagen deposition. These variables are mostly assessed in full thickness wound models and an additional drawback of this approach is that in many instances these results were based on subjective scoring systems. In this investigation it was important to develop an objective parameter that could be easily reproducible with minimal *intra* and *inter* observer error. The major variable for assessment identified here was the epidermal thickness. Quantification of the thickness of the epidermis may identify a variable that could be used for *in-vitro* assays at a later stage.

Previous studies measuring epidermal thickness examined only the actual epidermal thickness at one time point only (126, 127) and without expressing the thickness as a ratio relative to normal skin. Here the epidermal thickness was monitored over an extended period where it was apparent that the epidermis thickens substantially for a certain period of time after which it thins to resemble the thickness of normal skin. The process by which the epidermis thickens in these investigations is unknown at this point but multiple processes may be at play namely, epidermal proliferation, epidermal hypertrophy or migration from outer uninjured skin.

With the documentation of the increase and subsequent decrease in epidermal thickness, there is no indication as to whether the skin is actually normal from a thickness perspective at the end of the observational period. In this event the use of an epidermal thickness ratio would indicate at which point the newly formed skin's thickness is indeed that of un-injured skin. The premise can therefore be made that when the epidermal thickness ratio reaches 1, it may serve as an end-point at which epidermal layers have completed a process of thickening and then subsequent thickening.

The skin thickness and thickness ratio increased and then decreased and we postulate that the ratio followed sequential phases of proliferation/hypertrophy/migration followed by maturation. The peak in the epidermal ratio for the *Senecio* treated wounds was 2 days earlier than that of the other treatment groups with all 3 three treatment groups having a similar epidermal ratio on day 16. This may suggest that the *Senecio* plant accelerated the proliferation/hypertrophy/ migration of the epidermal layer which was then followed by an earlier maturation phase. However, the epidermal thickness and epidermal thickness ratio measurements are limited when determining treatment efficacy as they do not describe the functional state of the epidermis and therefore further analysis may be required to fully evaluate efficacy.

2.5.4 Full Thickness Wound Morphometric Analysis

In previous studies the rate of contraction was measured macroscopically by visualizing the wound area and determining the change in the size of the wound over successive days. In this study, histological sections were examined and the change in mid-dermal deficit represented the contraction of the wound. The change in the dermal deficit size in this case is a product of the contraction due to myofibroblasts but this only accounts for roughly 40% of the decrease in wound size (63, 64), therefore the collagen content is responsible for the rest of the dermal regeneration.

With the collagen content being a major component of wound contraction it is also vital for the migration of keratinocytes into wounds. In the case of the activated carbon treated wounds, the epidermis was seen to be delicate during debriding on sample collection days which may be accounted for by the lower collagen concentrations even though they were not significant. This point was also noted by Abercrombie, *et al*. (128).

2.5.5 Collagen Deposition

Investigations into collagen deposition in the wound are an important variables in the healing wound. Assessment of the collagen deposition is commonly achieved by tensiometry experiments or biochemical colorimetric assays to determine the concentration of hydroxyproline, a surrogate marker of collagen turnover (102). Tensile strength was shown to correlate with collagen content of wounds and became an early measured variable in wound healing investigations (129). It has also been measured in multiple studies regarding plant based therapies as was listed above. Colorimetric estimation of collagen has been used in studies on *Catharanthus roseus* (130)*, Calotropis procera* (131), *Terminalia chebula* (132)*,* and *Mimosa pudica* (133).

A qualitative technique that has shown to be particularly useful is the Picrosirius red staining method of histological sections. Although, the highly specific Picrosirius red stain for thin and thick collagen fibres has an advantage over other more commonly used modalities but the use of this technique is limited to qualitative studies (134). This validated staining technique (135) has been used for formalin fixed, paraffin embedded tissue samples (136) and coupled with fluorescence microscopy, this approach allows for greater image resolution (137). More commonly, polarised light has been used to view and image collagen subtypes (134). However in this case the fluorescent imaging allowed for the best resolution. It is therefore proposed that the image can be subjected to image analysis techniques to quantify the collagen content.

In this Chapter, an algorithm was developed to analyse and quantify collagen deposition in deep partial thickness and full thickness wounds. With the image analysis approach here, the change in luminosity from darker to lighter distributions is expected as more collagen is deposited within the wound. Additionally with the shift in luminosity it was clear that with the gating system proposed here, direct quantification of the more mature collagen could be performed and ultimately compared between treatment groups.

In the deep partial thickness wounds at day 8 post-operative, using this technique, the *Senecio* group had more collagen than the negative control treated wounds but not as much as the activated carbon treatment wounds. Subsequently, the collagen content in the *Senecio* and negative control treated wounds continue to increase, whereas the activated carbon treated wounds decreased, and at the end of experiment the groups were similar.

Importantly the described technique may allow quantification of collagen directly as compared to colorimetric techniques. The limitation of collagen colorimetric assays was (138) the requirement for accurate collection of wound samples, free of unwounded skin collagen which would be difficult to obtain. Furthermore, the method was based on the measurement of hydroxyproline which is not incorporated directly into the newly formed collagen but is rather a by-product of the synthetic process and its measurement may be more suited to collagen turnover (138). This technique may therefore be more suited to the deep partial thickness wounds as it represents an "*in vitro*" measurement where residual collagen from unwounded tissue could be excluded.

In the full thickness wound model, a similar pattern was seen with collagen concentrations similar in the *Senecio* and negative control treated wounds, which were not significantly less than the activated carbon treated wounds. At day 16 there was a significant difference between the activated carbon treated wounds and both the *Senecio* and negative control treated wounds.

2.5.6 Plant Toxicity

Toxicity associated with plants within the genus *Senecio*, and specifically with *Senecio serratuloides*, has been demonstrated by Elgorashi, *et al.* (118) using the AMES and VITOTOX® assays. These assays are based on bacterial cultures that are susceptible to various toxins. Importantly the majority of poisonings associated with the *Senecio* genus are due to consumption of the plant and are so subjected to the acids and conditions in the gastrointestinal tract (114). In human subjects, and commonly in the paediatric patients, the oral administration of traditional

medicines containing species from the *Senecio* genus leads to hepatic veno-occlusive disease (139) and has also been associated with hepatic malignancies (140). This was demonstrated by Zuckerman, *et al.* (141) where traditional preparations containing *Senecio latifolius* lead to the rapid decompensation of a three year old infant. Additionally they isolated pyrrolizidine alkaloids from the traditional preparations and their demonstrated their toxic potential in an *in-vitro* assay.

At present, little is known about the chemical composition of pyrrolizidine alkaloids and the relevant concentrations used in this and other studies. *Senecio* is classified as poisonous according to the South African National Biodiversity Institute (SANBI), with pyrrolizidine alkaloids existing as either the hepatotoxic free base form or the less toxic N-oxide form. However when the plants are ingested, the *N*-oxides are converted to the free base form in the gastro-intestinal tract resulting in the reported hepatotoxicity (142).

The topical administration of application may result in direct action of any active substances, including toxic compounds directly within the wound site where they may or may not be absorbed systemically. In this study, to determine possible toxicity, liver function tests were performed, and livers of the test animals were biopsied one month after completion of the experiments. Here no toxicity was detected in liver samples sent to accredited pathologists.

A possibility for the lack of toxicity may be due to observations made by Brauchli, *et al.* (143), who showed that the conversion to the toxic free base format was not as pronounced when administered percutaneously and could therefore explain why no toxicity was detected. In this model, the extent of the experimental wounds exposed to the potential toxic compounds was less than would be seen when ingested or in a clinical wound setting, especially in extensive burn injuries. Therefore the toxicity, if any, cannot be completely ruled out. In addition, the lack of knowledge with regards to the chemical composition of the plant investigated here is limited and more detailed investigations are warranted.

2.6 Conclusion

The results suggest that the *Senecio* based therapy prepared according to traditional healer's instructions and applied topically:

a) Decreased the initial wound pH;
b) Lead to an earlier increase and decrease of the thickness of the epidermis suggesting effects on cell proliferation or maturation;
c) Did not appear to alter collagen content in the wounds;
d) Preliminary data suggested signs of pyrrolizidine alkaloid toxicity were not present when the plant was applied topically.

Further isolation and identification of the possible active compounds would need to be done in order develop the application of the *Senecio* based therapy and to further validate the safety of these preparations.

Chapter 3 – Mechanistic Investigation of Senecio serratuloides: Cytokine, Tyrosine Phosphorylation and Proliferating Cell Nuclear Antigen Quantification

3.1 Introduction

The importance of cellular signalling needs to be investigated as a possible mechanism by which the plant acts. The basis of this is due to a study by Toma, *et al.* (144) where extracts of the plant *Senecio brasilliensis* (known to contain pyrrolizidine alkaloids) was used to treat acute and chronic gastric ulcers in a shorter time period when compared to proton pump inhibitors and 0,9% saline. This mechanim by which this occurred was through the upregulation of epidermal growth factor (EGF). With minimal evidence available on the plant in question together with the complexity of the wound healing process, this provides a starting point for the investigation into the potential mechanism by which the plant acts.

To further complicate the scenario proposed here, multiple additional factors are known to play important roles in wound healing. An extensive review by Werner and Grose, (80) focussed on the regulation of wound healing by growth factors and cytokines which have been shown to be key regulators in the wound healing process. Even though the effects and applications of these factors are well documented with extensive work gone into their application in wound healing, their success could be measured based on their routine application in the clinical setting. To date only recombinant PDGF (becaplermin, marketed as Regranex by OMJ Pharmaceuticals) has been registered with the United States Food and Drug Administration as a biological agent (a term used for cytokine/growth factor derived interventions) used for wound healing (145).

More recent information from a search for wound healing products on the DrugBank website (http://www.drugbank.ca) shows that the only other product that has been investigated and approved is Oprelvekin (an active ingredient of Neumega, Genetic Institute Inc.), a recombinant IL-11 used for intestinal wound healing. With only two products approved for clinical use, it is clear that the application of growth factors has not been a success. A link between in-vitro discovery and clinical application has been missed, Robson and Mustoe, (146) postulate that this may possibly be due to the mode of delivery of these factors and synergistic effects seen between various factors. Quite possibly an additional cost related factor or legislation may come into play.

Another possible reason for the lack of marketable products is the concept of synergism with many of the factors (146). Multiple authors demonstrate this concept as can be seen in the application of platelet gels (containing a cocktail of factors namely TGF-α and β, PDGF, EGF, and VEGF) (77) or different combinations of growth factors (namely EGF, TGF-α and β, FGF, IGF-1

and PDGF) (127) with the observation that the individual components are not as effective compared to the combinations.

It is therefore clear that analysing a couple of factors that are potentially applicable to wound healing may not be extensive enough in identifying a mechanism by which a plant based therapy may act. In light of this another approach may be to assay a common feature of these factors. The available literature describes phosphorylation of the receptor linked tyrosine residues as a potential target for analysis.

3.1.2 The Role of Tyrosine Phosphorylation

In the review by Werner and Grose (80), a significant proportion of factors bind to receptors that act via tyrosine residue phosphorylation thereby transmiting their signals down various cascades and are therefore known as the receptor linked tyrosine kinase (RLTK) receptors. It has been shown that while activation of the RTLK via their ligands does lead to improved wound healing, due to the complexity of the process and the known synergistic effects of the ligands, analysing single or at most two ligands has the potential to miss possible actions of wound care modalities (147). In the present study, it was therefore a logical assumption to focus on a common link between most of the ligands and their receptors, this being the phosphorylation of the tyrosine residues on the membrane bound receptors as well as the cytoplasmic response messenger proteins. Table 3.1 lists the recognised factors with the associated receptor phosphorylation.

Table 3.1. Tabulation of the recognised growth factors and associated receptor activity known to be beneficial in the wound healing process.

Ligand	Receptor Phosphorylation	Reference
Epidermal growth factor (EGF)	Tyrosine	148, 149, 150
Basic fibroblast growth factor (bFGF)	Tyrosine	151, 152, 153, 154, 155
Insulin-like growth factor (IGF)	Tyrosine	156, 157
Keratinocyte growth factor-1 (KGF-1), platelet derived growth factor (PDGF)	Tyrosine	158, 159, 160
Transforming growth factor (TGF) - α	Tyrosine	161, 162
Interleukins 1β, 6, 8, 10, and TNF-α	Tyrosine	95, 163, 164, 165, 166

Cell membrane receptors that function through tyrosine phosphorylation contain 20 subfamilies, and these subfamilies are based on the ligands that bind to and activate them (167). The activation of these receptors is known to control cell survival, proliferation and differentiation, all of which are important to wound healing (168). The generic receptor format includes a glycosylated extra-cellular ligand binding domain, linked to the intra-cellular domains via a single transmembrane helix (169). It is the intracellular domain that contains the tyrosine residues that are phosphorylated resulting in the downstream activation of cytoplasmic messenger molecules that transduce signals to the cell nucleus, thus influencing gene transcription (170).

Once the receptor has been activated, further signalling pathways are activated through the recruitment of regulatory proteins known as the adaptor and scaffolding proteins. On these adaptor and scaffolding proteins various amino acid domains are present that activate the respective pathways, importantly the Src homology 2 (SH2) and Phosphotyrosine-binding (PTB) domains are known act via tyrosine phosphorylation (171). Pathways that are generally activated by receptor tyrosine phosphorylation include the phosphoinositide 3-kinase (PI3k) pathway, the extracellular signal-related kinase (ERK) or mitogen-activated protein kinase (MAPK) pathway, the phospholipase C-γ (PLC- γ) pathway and the Janus kinase / signal transducer and activator

of transcription (Jak/STAT) pathway (172). Although these pathways have predominant actions via their associated signalling cascades, there exists a significant overlap between many of these pathways. This point is highlighted in review articles by Morrison (173) and by Bennasrourne, *et al.* (171). However, the scope and complexity of these pathways is beyond this investigation.

Thus in this investigation, there is a broad focus on tyrosine phosphorylation without making a distinction between any one of the signalling pathways. The addition of an outcome response (and in this case, cellular proliferation) is important as it has been proposed that the amount of tyrosine phosphorylation does not necessarily correlate with the amount of response (174).

3.1.3 Proliferating Cell Nuclear Antigen

Proliferating cell nuclear antigen (PCNA) is a protein that is highly conserved from an evolutionary perspective and is up-regulated in the G_1 and S phases of cellular proliferation and so correlates with the proliferative state seen in most eukaryotic cells (175). The information available on PCNA within the cutaneous wound healing context is few. Examination of the available literature concerning wound healing shows that PCNA is mostly used as a marker of proliferation with little consideration for the activity or function of the molecule.

The importance of PCNA is as an outcome measure of cellular proliferation secondary to tyrosine phosphorylation, but a close relationship between these targets is also recognised. The PCNA molecule has been shown to be phosphorylated on the 211 tyrosine residue in response to activation of EGFR (176) additionally the phosphorylation of this residue is important to maintain the function of PCNA in proliferating cells (177) by protecting the PCNA molecule from ubiquitylation-mediated degradation but this is only of the chromatin bound moiety and not the free form (178). Furthermore proliferating cell nuclear antigen is expressed in migrating cells (179).

3.1.4 Inflammatory Cytokines

Even with extensive work on the role of the above mentioned growth factors, there is a clear failure in their clinical application. The role of inflammatory cytokines however, has been largely ignored when plant based therapies are concerned. However, it is of particular interest that select inflammatory cytokines also act through tyrosine phosphorylation. Table 3.1 tabulates the cytokines linked to tyrosine phosphorylation which includes the pro-inflammatory cytokines, interleukins-1β, 6, 8, TNF-α and the anti-inflammatory cytokine interleukin-10.

Interleukin - 1β (IL-1β): IL-1β is known to be an important mediator of inflammation in the wound milieu and has various synergistic effects with other mediators active in the wound healing process. IL-1β is however site and injury specific with regards to expression and activity (180). IL-1β has a role in the induction of keratinocyte migration and proliferation together with the induction of fibroblast proliferation and synthetic functions (being mostly collagen synthesis) (181).

Furthermore the activity of IL-1 is not only limited to the proliferative response of various cell populations but also important in their distribution within tissues which was demonstrated by Wilson, *et al.* (182) in a corneal tissue wound model. The authors found that keratinocytes and fibroblasts were redistributed and underwent apoptosis in response to IL-1 which was either a normal or pathological response to mechanical injury. Although these results were obtained in corneal tissues, the fundamental response of fibroblasts and keratinocytes is universal in the wound healing process.

Interleukin – 12p70 (IL-12p70): Little is known regarding to the role of IL-12p70 in wound healing. However, IL-12p70 is a major contributor in the development of T-helper cells to mature into either TH1 (inflammatory) or TH2 (anti-inflammatory) mediators, with high IL-12p70 concentrations favouring the TH1 response (183). The various TH responses manipulate the functionality of macrophages and may determine wound healing outcomes (184). IL-12p70 induces Inducible Nitric Oxide Synthase (iNOS) due to the activation of the pro-inflammatory functionalities (185). The authors demonstrated this relationship in an allograft rat model, where the rate of rejection was decreased with an increase in iNOS when treated with IL-12p70.

Interleukin – 6 (IL-6): IL-6 has a modulatory effect as it has roles in producing inflammatory responses and in the differentiation of lymphocyte populations (186). The IL-6 ligand is able to bind directly to the IL-6 receptor on cell surfaces and induce dimerization of the gp-130 molecule, however a soluble form (not membrane bound) of the receptor is expressed which bind the ligand thereafter activating the gp-130 molecule (187). This allows IL-6 to interact with cells that do not express the receptor and so increases the scope of the activity.

The extent of IL-6's role in inflammation has been demonstrated in inflammatory conditions such as Sjögren's syndrome (188) and uveitis (189). These conditions are clearly more related to the eye, but in a study by Mc Farland-Mancini, *et al.* (186) the role of IL-6 was demonstrated in a

cutaneous wound model. Detrimental effects were shown in mice lacking a combination of IL-6 and its receptor where a reduction in macrophage infiltration, fibrin clearance and wound contraction was seen. Interestingly this study showed that the effects were mediated through the phosphorylation of the tyrosine residues on the gp130 intracellular receptor domains.

Interleukin – 8 (IL-8): IL-8 has a major role in chemotaxis of polymorphonuclear cells whose main function is to debride the wound of cellular debris and foreign materials (190). Although this is an important component of wound healing additional interest in IL-8 lies in its ability to modulate keratinocyte proliferation in a time dependent manner (191). Kleinbeck, *et al.* (191) describe an important concept in that the cytokines seem to operate to a satisfactory level at a narrow concentration range.

Tumour Necrosis Factor – α (TNF-α): As an integral component of the inflammatory process during wound healing, excessive concentrations are associated with the formation of chronic wounds (192). Although it is known to be mostly derived from monocyte/macrophage populations (97) evidence has shown that it may also be produced by neutrophils (98). As the evidence suggests that TNF-α may be associated with chronic non-healing wounds, there is also a role for the cytokine in normal wounds, as it important for mitogenic and angiogenic events (99). Steenfos, *et al.* (99) showed that TNF-α has the potential to inhibit key growth factors specifically TGF-β, but in these rat studies the effect of this inhibition was not detrimental to the wound healing process. Similar to IL-1, TNF-α is able to induce cellular proliferation through the activation of fibroblastic growth factors but when acting alone the unwanted result of chronic wound formation predominates (193).

Interleukin-10 (IL-10): As a prominent anti-inflammatory cytokine active in the skin, Berg, *et al.* (94) demonstrated the role of IL-10 in Croton oil irritated skin in a mouse model where the effects of IL-10 were assessed based on its potential to reduce the inflammatory induced necrosis of skin tissue. Results showed that IL10 was active in decreasing the expression of TNF-α which is a prominent pro-inflammatory cytokine, an observation also made by Sato, *et al.* (95). In addition to this observation other cytokines were also shown to be decreased namely IL-1β and IL-6. In addition to the suppression of inflammatory cytokine expression, Sato, *et al.* (95) also demonstrated the inhibition of chemotaxis of neutrophils and macrophages to the affected site.

However evidence presented by Eming, *et al.* (72) shows that depression of IL-10 accelerates the closure of wounds in a mouse model. In the IL-10 knockout mice, they observed accelerated epithelialisation and wound contraction. This suggests that the role of other cytokines inhibited by the actions of IL-10 may have a positive contribution to the wound healing process and not only active as pro-inflammatory agents.

3.2 Aims

The aims of this Chapter where to:

a) Quantify the relative concentrations of IL-10, IL-12, IL-1β, IL-6, IL-8 and TNF-α;
b) Quantify the extent of tyrosine phosphorylation in the epidermis;
c) Quantify the outcome response of cellular proliferation by assessing the concentration of proliferating cell nuclear antigen.

3.3 Materials and Methods

3.3.1 Animal Model and Test Groups

The wound model, surgery, treatment groups, dressings, the timing of and taking of skin biopsies was as described in Chapter 2. The occlusive dressings contained an absorptive pad to trap the wound exudate for this part of the study.

3.3.2 Wound Exudate Collection and Analysis

On day 5 post-operative, the absorptive pads of the occlusive dressings were cut free and placed in sample collection tubes and placed immediately on ice. Once in the laboratory the absorptive pads were placed in syringe barrels and inserted into collection tubes. The dressings were spun down at 2000 rpm; the supernatant/exudate was collected, aliquoted into 500 µl Eppendorf tubes and frozen at -70 ^{o}C. The wound fluid from the treated and control wounds were analysed to quantify the concentrations of the inflammatory cytokines namely IL-10, IL-12, IL-1β, IL-6, IL-8, TNF-α.

3.3.3 Cytokine Analysis

The concentrations of the inflammatory cytokines in the wound exudates were analysed using the Multiplexed Human Inflammatory Cytokine Bead Array kit (BD Biosciences, Cat. No: 551811). The manufacturer's instructions were followed with some modifications during the initial sample processing. EDTA was added due to the associated proteolytic activity associated with wounded tissue.

Twelve standard concentrations for each interleukin were prepared by serial dilution ranging from 0 pg/ml to 5000 pg/ml. Eighteen samples were analysed in duplicate therefore 36 samples with twelve standards resulted in 48 preparations all together. According to manufacturer's instruction, 25 µl per sample of each cytokine capture bead was combined to produce a stock solution amounting to 6 different cytokines x 48 samples x 25 µl capture beads = 7 200 µl combined capture beads. The combined reconstituted capture beads were centrifuged at 2000 rpm and the supernatant discarded. The capture beads were suspended in 7 200 µl serum enhancement buffer, vortexed and incubated at room temperature for 30 minutes. During this incubation period, 150 µl of each wound fluid sample was placed separately in EDTA Vacutainers (BD Vacutainer) and incubated for 20 minutes.

Standard samples were reconstituted in 2 ml assay diluents and allowed to equilibrate for 15 minutes. They were then mixed by pipette and a serial dilution prepared from 5000 pg/ml of protein to 0 pg/ml of protein. Standards were prepared in 15 ml BD Falcon tubes (Cat. No. 352008).

Standards and experimental samples (100 µl) were placed into separate Eppendorf tubes and incubated for 2 hours with 25 µl of combined capture beads. All samples were centrifuged in 500 µl wash buffer, supernatant discarded, 25 µl PE detection reagent added and incubated for a further 2 hours at room temperature. Samples were centrifuged with 500 µl wash buffer, reconstituted in a further 100µl wash buffer and transferred to a 96 well plate. The labelled beads were be analysed on a FACSArray Flow Cytometer (BD biosciences). Instrument settings can be seen in Table 3.2 below. Final cytokine concentrations were determined using the software supplied with the instrument.

Table 3.2. Flow Cytometer Parameters as run on the FACSArray Flow Cytometer.

Physical Properties	Voltage (mV)
Forward Scatter	249
Side Scatter	270
Laser Properties	
Far Red	578
Yellow	480
NIR	500
Red	395

3.3.4 Immunofluorescence Staining and Analysis

Solutions and buffers used were made up in the Department of Surgery and all staining was performed in the Oncology Research Laboratory, Department of Internal Medicine. On the days of incubation sections were dewaxed in two changes of Xylene and then rehydrated through a graded series of alcohols and then rinsed in distilled, de-ionised water. Following this, sections

were placed in a microwavable slide rack, immersed in tris-ethylenediamine tetra-acetic acid (Tris-EDTA) buffer (pH 9.0) and microwaved at medium heat for 5 minutes and then allowed to cool for 20 minutes on the bench top. Next, sections were placed in phosphate buffered saline (PBS) for 5 minutes, after which they were permeabilised in 0.1% Triton-X100 in 0.1% Bovine Serum Albumin (BSA)/PBS for 10 minutes. Once permiabelised, sections were washed in 3 changes of 0.1% BSA/PBS, then aspirated and marked with a DAKO pen around each section.

Primary antibodies include Mouse anti-Proliferating Cell Nuclear Antigen (PCNA), clone 10, isotype IgG2a (Invitrogen, Cat. No. 13-3900) and anti-Phosphotyrosine (4G10), mouse monoclonal IgG2bk (Millipore, Cat. No. 05-321). The PCNA anti-body was detected when conjugated to the Alexa Fluor® 488 secondary antibody (Molecular Probes®, Cat. No. A 21131) that specifically targets the IgG2a isotype and fluoresces on a green fluorescent channel. The anti-phosphotyrosine antibody was detected when conjugated to the Alexa Fluor® 568 secondary antibody, (Molecular Probes®, Cat. No. A 21124) specifically targeted to the IgG2bk isotype that fluoresces on a red fluorescent channel. Both positive and negative controls were included in the immunofluorescence staining runs. The positive control used was paraffin embedded sections of rat kidney and the negative control was skin sections obtained from this study wherein the primary antibody mixture was omitted and substituted with an equivalent volume of 0.1 % BSA/PBS.

For dual immunofluorescence labelling of the sections, dilutions were determined prior to complete analysis on separate sections at a dilution of 1:150 for each of the primary antibodies. For dual labelling purposes the dilutions were maintained at 1:150 diluted in 0.1% BSA/PBS. Sections were incubated overnight with 25 µl of the primary antibody mixture at 4 ^{o}C in an airtight container lined with moistened blotting paper.

The slides were washed in three changes of 0.1% BSA/PBS for 5 minutes at each wash. The secondary antibodies used were prepared with a dilution ratio of 1:200 diluted in 0.1% BSA/PBS. Sections were incubated with 25 µl of the secondary antibody mixture for an hour at room temperature in the dark. After incubation with the secondary antibodies, sections were washed in 3 changes of PBS after which they were mounted with 100 µl of Fluoro-mount (Sigma, RSA).

3.3.5 Section Imaging and Image Analysis

Sections were imaged on an Olympus IX71 fluorescent microscope and processed using the analysis LifeScience® software package in the Oncology Research Laboratory, Department of Internal Medicine. Images were captured at a 40x magnification and exposure time of 1000

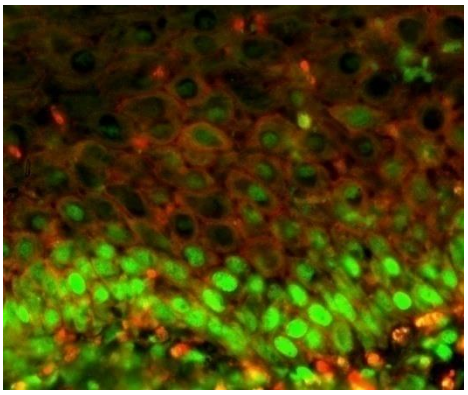
milliseconds (ms). At this magnification, three images were taken for analysis, laterally at either side of the section and in the midline to supply an evenly distributed representation of the sections. The images generated were a RGB composite which were then decomposed into the separate channels for further analysis (Figure 3.1). The blue channel was omitted as no signal was expected there and only the red (denoting tyrosine phosphorylation positivity) and green (denoting proliferating cell nuclear antigen) channels were analysed.

Each channel was further analysed by importing the image into the planimetric software package IMAGE J (version 1.4.3.67) where the regions of interest were isolated and the mean fluorescence intensity (MFI) calculated. This was done in all the images on each of the sampling days. An average MFI of each treatment on each day was calculated and represented graphically.

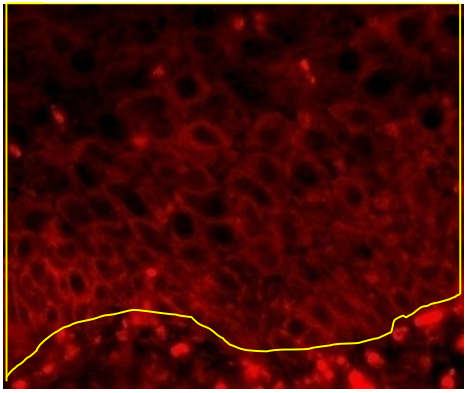
3.3.6 Statistical Analysis

Statistical Analysis was done using the software package Statistica (ver. 9). All data was tested for normality using the Shapiro-Wilk Normality test accepting non-parametric data at $p < 0.05$. Data was found to be non-parametric; therefore the Kruskal-Wallis test was used for significance testing.

Initial Fluorescence Image with the ROI
indicated by the yellow outline.



Initial fluorescence Image decomposed into the green (PCNA) and red (4G10) Channels. At this point the mean intensity of the ROI is calculated which is denoted by the yellow lines.



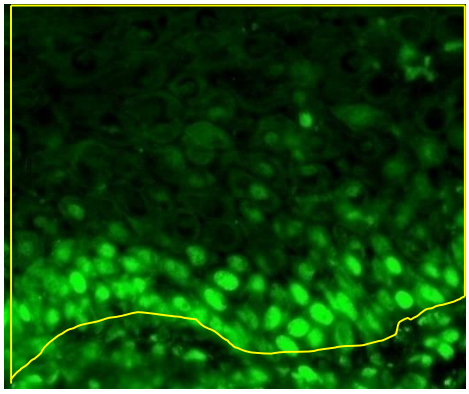


Figure 3.1. Immunofluorescence analysis algorithm.

3.4 Results

3.4.1 Cytokine Analysis

The results from the cytokine analysis at day 5 post-operative are shown in Table 3.3. The *Senecio* treatment group had a significantly greater IL - 1β when compared to the negative control ($p = 0.017$) but not when compared to the activated carbon treated wounds ($p = 0.566$). The activated carbon treated wounds had a significantly greater concentrations of IL - 1β than the negative control ($p = 0.005$). There were no significant differences in the other cytokines analysed.

Table 3.3. Cytokine concentrations (pg. protein/ml wound fluid) at day 5 post-operative. Data are presented as mean ± SEM (n). Underlined p – values are significant.

Cytokine	Negative Control	Activated Carbon	*Senecio*	Group wise *p* - value	*Senecio* vs. Negative Control *p* - value	*Senecio* vs. Activated Carbon *p* - value	Negative Control vs. Activated Carbon *p* - value
IL - 8	13.50 ± 2.78 (9)	20.50 ± 2.69 (9)	20.30 ± 4.84 (9)	0.325	0.158	0.724	0.331
IL - 1β	8.02 ± 1.05 (9)	17.91 ± 2.66 (9)	25.52 ± 5.79 (9)	0.009	0.005	0.566	0.017
IL - 6	8.93 ± 2.19 (9)	13.03 ± 2.29 (9)	15.43 ± 3.80 (9)	0.163	0.112	0.930	0.112
IL - 10	9.09 ± 2.23 (9)	16.87 ± 3.39 (9)	11.93 ± 3.21 (9)	0.095	0.058	0.133	0.377
TNF - α	18.09 ± 3.56 (9)	19.86 ± 3.14 (9)	18.63 ± 4.19 (9)	0.797	0.627	0.566	0.965
IL - 12p70	18.40 ± 2.62 (9)	22.88 ± 2.93 (9)	25.32 ± 8.11 (9)	0.505	0.270	0.427	0.724

3.4.2 Tyrosine Phosphorylation and Cellular Proliferation

Results for the tyrosine phosphorylation of the healing epidermis are shown in Table 3.4. Tyrosine phosphorylation in the healing epidermis for the *Senecio* and negative control treated wounds were similar throughout the duration of the experiment with no difference detected statistically throughout the observation period.

The *Senecio* treated wounds had significantly greater tyrosine phosphorylation than the activated carbon treated wounds on days 9 ($p = 0.042$) and day 12 ($p = 0.034$) post-operative but was significantly lower at day 16 ($p = 0.017$). The negative control treated wounds were only significantly greater than the activated carbon treated wounds ($p = 0.015$) on day 7 post-operative.

Table 3.4. Epidermal tyrosine phosphorylation (4G10 MFI) at specific post-operative days. Data are presented as mean ± SEM (n). Underlined p – values are significant.

Days Post-operative	Negative Control	Activated Carbon	*Senecio*	Group wise *p* - value	*Senecio* vs. Negative Control *p* - value	*Senecio* vs. Activated Carbon *p* - value	Negative Control vs. Activated Carbon *p* - value
5	107.10 ± 2.13 (9)	98.06 ± 10.57 (9)	99.59 ± 6.53 (9)	0.377	0.537	0.4799	0.185
7	113.67 ± 3.19 (9)	100.89 ± 5.77 (9)	120.84 ± 6.46 (9)	0.038	0.251	0.077	0.015
9	116.25 ± 11.62 (9)	99.54 ± 6.78 (9)	119.55 ± 3.04 (9)	0.180	0.659	0.042	0.289
12	114.91 ± 9.17 (9)	100.76 ± 9.54 (9)	126.43 ± 4.74 (9)	0.107	0.427	0.034	0.289
16	118.40 ± 6.61 (9)	131.92 ± 5.55 (9)	113.01 ± 4.08 (9)	0.075	0.659	0.017	0.216

Shown graphically the levels of tyrosine phosphorylation (Figure 3.2) increased rapidly for the *Senecio* treated wounds from day 5 to day 7, and remained elevated to day 12 post-operative and decreased after day 12. The negative control treated wounds showed a moderate elevation in tyrosine phosphorylation from day 5 to day 9 post-operative, after which it remained constant until day 16 post-operative. The activated carbon treated wounds remained constant at lower levels compared to the other treatments until day 12 when it increased to day 16 post-operative.

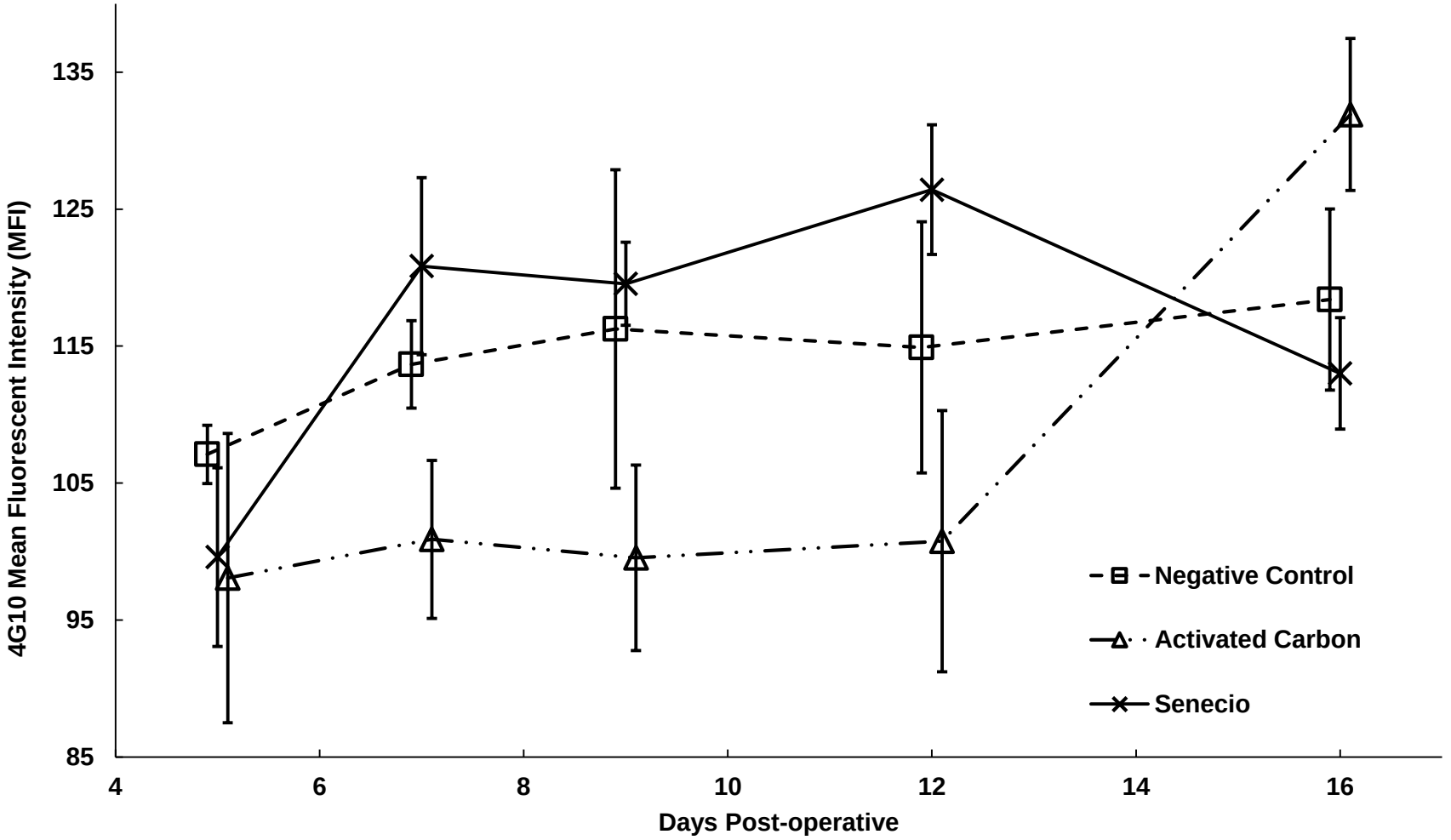


Figure 3.2. Epidermal tyrosine phosphorylation (4G10 MFI) plotted against time (Days Post-operative). Error bars represent the SEM.

Results for epidermal proliferation seen in the healing epidermis are shown in Table 3.5. The *Senecio* treated wounds had significantly less proliferation at day 5 post-operative when compared to both the negative control negative control treated wounds (p = 0.001) and activated carbon treated wounds (p = 0.003). From day 7 to day 16 post-operative, no other differences were noted when the *Senecio* treated wounds were compared to the negative control treated wounds. The *Senecio* treated wounds had significantly greater levels of proliferation than the activated carbon treated wounds at days 9 (p = 0.013) and 12 (p = 0.017). At day 16, the activated carbon treated wounds had significantly more proliferation than the negative control treated wounds (p = 0.042).

Table 3.5. Epidermal proliferation (PCNA MFI) at specific post-operative days. Data are presented as mean ± SEM (n). Underlined p – values are significant.

Days Post-operative	Negative Control	Activated Carbon	*Senecio*	Group wise *p* - value	*Senecio* vs. Negative Control *p* - value	*Senecio* vs. Activated Carbon *p* - value	Negative Control vs. Activated Carbon *p* - value
5	86.91 ± 3.51 (9)	84.03 ± 3.87 (9)	66.71 ± 2.47 (9)	0.001	0.001	0.003	0.595
7	69.47 ± 6.05 (9)	75.21 ± 6.27 (9)	70.49 ± 5.58 (9)	0.783	0.930	0.427	0.957
9	53.87 ± 4.53 (9)	49.92 ± 4.46 (9)	71.17 ± 7.29 (9)	0.052	0.157	0.013	0.596
12	83.77 ± 9.56 (9)	66.23 ± 8.85 (9)	95.78 ± 7.06 (9)	0.030	0.185	0.017	0.112
16	70.88 ± 6.61 (9)	84.87 ± 4.30 (9)	73.68 ± 7.83 (9)	0.080	0.589	0.093	0.042

Shown graphically in Figure 3.3, the level of proliferation in the *Senecio* treated wounds was maintained from day 5 to day 9 post-operative, whereas the level of proliferation in the negative control and activated carbon treated wounds decrease in the same time period. From day 9 to day 12 post-operative, all treatments show an increase in levels of proliferation. At day 12 post-operative, the *Senecio* and negative control treated wounds show a decline in levels of proliferation to day 16 post-operative, whereas the activated carbon treated wounds continue to increase.

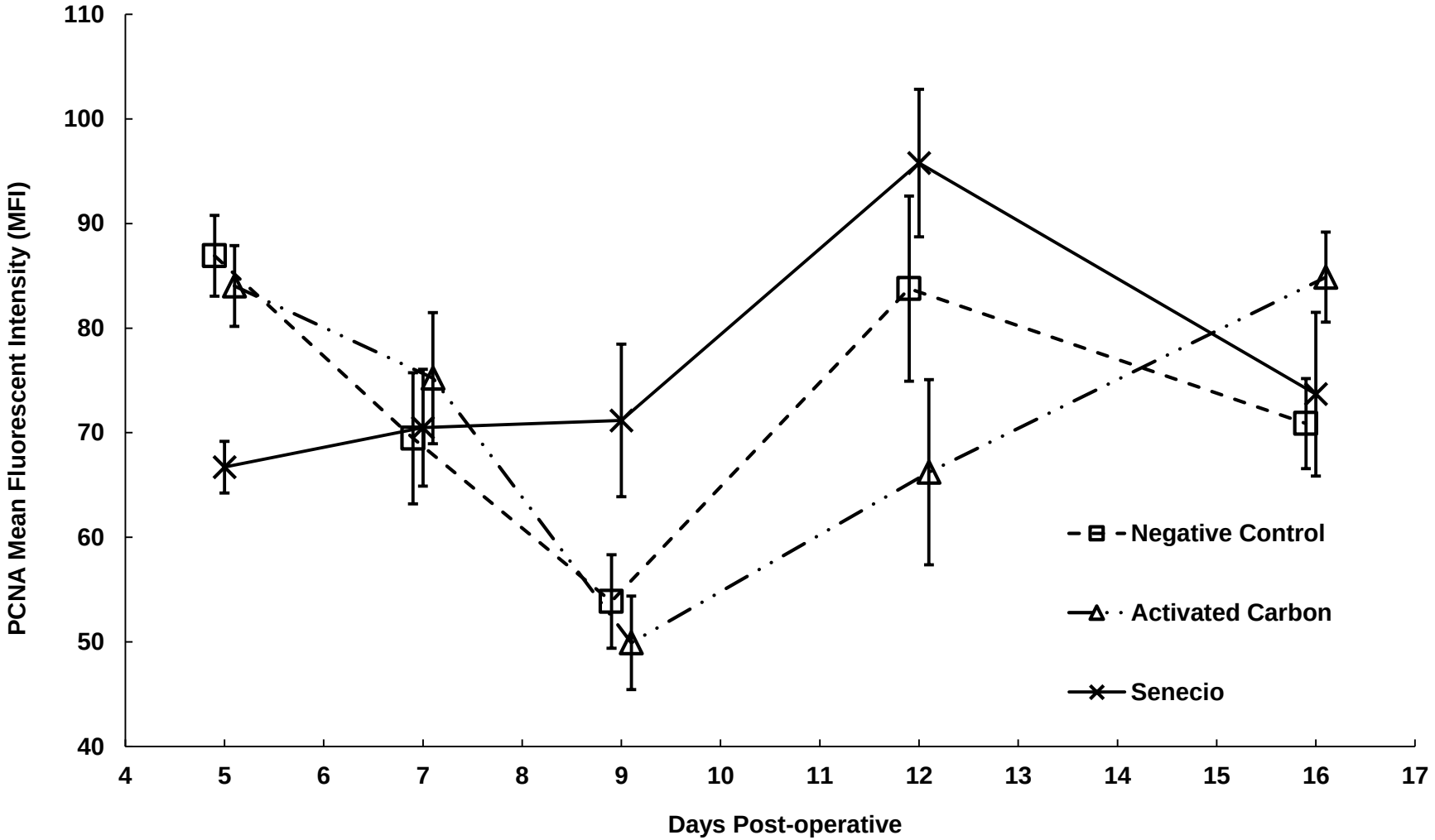


Figure 3.3. Epidermal Proliferation (PCNA MFI) plotted against time (Days Post-operative). Error bars represent the SEM.

3.5 Discussion

The main finding from the cytokine assays shows that on day 5 post-operative, the IL-1β concentration was significantly higher in the *Senecio* and activated carbon treated wounds. At the same time point, although the *Senecio* treated wounds had a significantly lower level of proliferation, the level of tyrosine phosphorylation was the same for all treatment groups. From day 5 post-operative, the level of proliferation in the *Senecio* treated wounds is maintained at a steady state. This was not seen in the activated carbon or negative control treated wounds where a rapid decline is seen at the same point in time which recovers later. From day 5 post-operative there is an increase in tyrosine phosphorylation in the *Senecio* treated wounds which was not evident in the controls.

The specific mechanisms by which a wound is re-epithelialized is proliferation and migration of keratinocytes from the wound edges and remaining hair follicles. It is quite possible that the cells in all treatment groups are migrating into the wound which would account for the thickening of the epidermal layers. In addition to the migratory input in the *Senecio* treated wounds, there was an added proliferative response (from days 5 to 9 post-operative) as was shown by the sustained levels of the proliferating cell nuclear antigen which may also account for the epidermal thickness.

Reasons for why the proliferative response was sustained in the *Senecio* treated wounds may be related to the tyrosine phosphorylation. Tyrosine phosphorylation has a role in cellular signalling mechanisms which are important in cell migration, proliferation and differentiation (168). Although, significant at day 7 post-operative the *Senecio* treated wounds maintained greater and sustained levels of tyrosine phosphorylation. These findings were similar to those of Murphy and Blenis (194) where the sustained and elevated levels of cellular signalling may be account for the differences observed in outcomes such as cellular proliferation and not neccesarily the actual amount of signal or tyrosine phosphorylation.

The cell signalling pathways that are activated by tyrosine phosphorylation, although distinct are seen to overlap, and multiple ligands may bind to the same receptor linked pathway but with different effects. For example, MAPK pathways can be triggered by growth factors as well as inflammatory cytokines (194). Murphy and Blenis (194) reviewed the hypothesis that the same pathway could be manipulated to produce specific effects via different control mechanisms. Signal transduction could be manipulated by the density of membrane receptors and the duration of the tyrosine phosphorylation or the half-life of the specific phosphorylated protein.

The idea that ligand concentration is not the only factor driving cell responses and may be reason for the previously noted complexity of cell responses to stimulation. This contributing factor in the differential results of various growth factors brings into question the biochemical properties and kinetics of tyrosine phosphoryation, a topic that is highly complex and not yet fully elucidated.

Responses to tyrosine phosphorylation is also determined by cell type and locality. The concept of signal transduction as a regulatory factor was initially proposed by Marshall (172) due to Fibroblast Growth Factor induces proliferation in fibroblasts but in PC12 cells the same growth factor induces differentiation. Signalling pathways in keratinocytes and fibroblasts (key cell populations in wound healing), a “proliferative” signal in keratinocytes has the opposite effect on fibroblasts where a “differentiation” signal is expected (195). An important pathway that is linked to keratinocyte differentiation is the activation of protein kinase C (intially activated by PLC- γ) with the concurrent influx of calcium, a potent mediator of this process (196). In keeping with the observation of Miteva (195) where the converse occures in fibroblasts who proliferate when the protein kinase C pathway is activated.

PCNA is both a marker for cellular proliferation and has a key role in maintaining the proliferative response. Specifically PCNA assists with the tethering of DNA polymerase epsilon, a key enzyme involved in DNA synthesis and repair, to its DNA targets (197). Once bound to chromatin, its function is dependent on the tyrosine kinase activity of the EGF receptor (EGFR) within the nucleus (198) which leads to the phosphorylation of Tyrosine 211 residue of chromatin bound PCNA molecule to stabilize it. Furthermore, consistently raised PCNA Tyrosine 211 residue phosphorylation is correlated with pronounced cell proliferation (198). Thus the sustained expression of PCNA, possibly due to elevated or sustained levels of tyrosine phosphorylation, may have contributed to the significantly thicker epidermis measured on day 7 post-operative, as described in the previous Chapter.

As simple as this explanation might be, prior to the increase in the epidermal thickness there are lower levels of PCNA in all treatment groups which requires explanation. In the negative control and activated carbon treated wounds the lowest concentrations of PCNA are noted at day 9 post-operative coinciding with the point at which the epidermal thickness is maximal for these treatment groups. In the *Senecio* treated wounds the lowest concentrations of PCNA are seen around day 5 and 7 post-operative, again coinciding with the time point at which the epidermal thickness is maximal. At day 5 post-operative where the *Senecio* treated group had significantly

lower concentration of PCNA compared to the controls, it had a significantly thicker epidermis than both the controls but, with the sustained levels of PCNA the epidermis continued to thicken until day 7 post-operative.

In summary, the *Senecio* treated group's initial low levels of PCNA coincide with a significantly thicker epidermis and sustained levels of PCNA coincided with an earlier maximum in epidermal thickness. In the control groups, a lower level of PCNA also coincided with an increase in epidermal thickness. These data may suggest that the role of PCNA was to maintain a proliferative response and, with greater sustained levels of tyrosine phosphorylation may have resulted in the greater epidermal thickness between days 5 to 7 after creating the wounds. Of note within the *Senecio* treated wounds, data was absent prior to day 5 post-operative and the trend of PCNA expression before the thickening of the epidermis could not be determined.

Importantly in this study, IL – 1β was the only cytokine which was shown to be significantly higher in the *Senecio* group and only on day 5 post-operative. With the related functions being keratinocyte migration, keratinocyte and fibroblast proliferation and fibroblast synthetic function (181) the responses observed in the *Senecio* treated wounds may well be linked to the raised levels of this cytokine.

Even though there were no observed differences in the other cytokines their roles are vital in wound healing and even though a significant elevation of IL – 1β was detected it would be naïve to consider this the important distinguishing feature because not all the potentially implicated ligands were measured here. The reason for this is that it was not financially possible to do so and again the importance of measuring the tyrosine phosphorylation is emphasised as it is a common link between many of the ligands (80).

Although significant differences between the groups were determined, the specific proteins that were phosphorylated were not analysed. It is thus not currently known whether different signalling cascades were activated by diffferent ligands which was a limitation of this study. Furthermore as overlap between the signalling cascades (173) would further complicate determining the specific pathways involved, the approach of measuring overall tyrosine phosphoryation and proliferation was probably correct.

3.6 Conclusion

Tyrosine phosphorylation and PCNA was elevated in *Senecio* treated wounds. The sustained elevated levels of tyrosine phosphorylation seen in these wounds may maintain and stabilise the function of PCNA, a factor known to be important in DNA synthesis and cellular proliferation. It is feasible that the raised levels of tyrosine phosphorylation in the *Senecio* treated wounds more than the controls was associated with the significantly greater concentrations of IL-1β. This cytokine is known to be important in keratinocyte proliferation and is also associated with receptor linked tyrosine kinases. Given the morphometric analysis showing that the epidermal thickness and cellular proliferation were significantly increased when the wounds were treated with the *Senecio* preparation, suggests that an assay determining keratinocyte proliferation could be used to measure accelerated wound healing by *Senecio serratuloides* var. Such an *in-vitro* assay could be used in a high throughput assay to identify possible lead compounds from plant extractions and isolates.

4.1 Introduction

In Chapters 2 and 3 it was shown that treating deep partial thickness wounds in a porcine model with *Senecio* preparations lead to the formation of a significantly thicker epidermis associated with increased tyrosine phosphorylation and sustained proliferation of the epidermal layers. The data therefore suggests that active compounds in the plant increase cellular proliferation in the epidermal layers.

In the epidermal layer, 95% of the cell population are keratinocytes (199). *In-vitro* keratinocyte cultures can be used in a cell proliferation assay to screen for active fractions of the plant to isolate and characterise lead molecules. These molecules and their derivatives could potentially be patented to protect the indigenous knowledge and possibly secure an income for the owners of such knowledge.

To identify lead compounds, active fractions needed to be assayed for wound healing activity. This requires the simultaneous extraction and fractionation of the plant together with the development of a simple and rapid screening *in-vitro* assay. Furthermore the development of the *in-vitro* assay needs to be compatible with the high-throughput assay format, for reasons that will be discussed further.

4.1.2 Previous Plant Based Studies

Studies focussing on plants described with wound healing activity have been reviewed in Chapter 1 and highlighted again in Table 4.1. Colorimetric tests were used to identify the chemical class of active components in *Semecarpus anacardium* (24)*, Zantboxylum chalybeum* and *Warbugiaugandensis* (18)*, Ranunculus pedatus* (45)*, Euphorbia caducifolia* (26)*, Trichosanthes dioica Roxb* (27)*, Glycosmis arborea* (28)*, Hypericum patulum* (29)*, Terminalia arjuna* (35)*, Dendrophthoe falcata* (L.f) Ettingsh (36). Such approaches identified tannins, saponins, steroids, flavonoids, phenols, glycosides and alkaloids all of which react to specific staining agents that can visualised under normal light, UV light or spectrophotometrically. Following these phytochemical screens, the “whole” extracts were tested on various wound models to prove efficacy but few studies continued to isolate and identify active components. An example was the study of the *Michauxia species* (46) that specifically determined polyphenols spectrophotometrically (200). These were then tested on rodent incisional

and excisional wound models and demonstrated efficacy but no further attempt was made to separate or identify specific phenolic compounds.

In contrast, studies on *Murraya koenigii* (31)*, Croton zehntneri* (54)*, Holoptelea integrifolia* (37) and *Cichorium intybus L.* (47) used HPLC/MS. This approached identified carbazole alkaloids (important pro-apoptotic agents in leukaemia's, lymphomas, and prostatic malignancies) and sesquiterpine phenolic compounds from essential oils from *Murraya koenigii* (31). Several alkaloids fractions and the essential oils as a whole, showed significantly enhanced epithelialisation at the midpoint of the observational period in rodent wound model experiments but not at the end of the experiment, an observation also made in this study (please see Chapters 2 and 3). Furthermore the activities of the separated alkaloids were compared and identified as previously described compounds.

Suntar, *et al.* (201) investigated and characterised the active fractions from *Cichorium intybus L.* using a rodent model, solvent extractions, thin layer chromatography (TLC) and spectrophotometric techniques (mass spectrometry, UV spectrometry, ^{1}H-^{13}C and nuclear magnetic resonance) and determined β-sitosterol as the active compound.

Table 4.1. Selected studies where plants used for wound healing have been assessed for potential active compounds.

Plant Name	Extraction Solvent	Further Evaluation	Compounds	Reference
Jatyadi Taila	100% Methanol	HPTLC	Flavonoids, Essential oils, Tannins, Glycosides, Alkaloids, Resins, Steroids	(22)
Cichorium intybus L	85% Methanol and sub fractionation	Nil	Phenolics	(201)
Semecarpus anacardium	100% Methanol	Nil	Flavonoids, Phenolics, Glycosides, Tannins	(24)
Zanthoxylum chalybeum **and** ***Warbugia ugandensis***	Ethanol	Nil	Polyurinides, Reducing Compounds, Saponins, Tannins, Alkaloids, Glycosides, Anthracenisides, Coumarin Derivatives, Flavonoids	(18)
Murraya koenigii	Ethanol	GCMS	Alkaloids, Essential oils	(31)
Ranunculus pedatus **and** ***Ranunculus constantipolitanus***	Diethyl ether, n-hexane, Ethyl acetate, Methanol, Water	Nil	Steroids, Triterpenes, Alkaloids, Saponins, Tannin, Anthraquinones, Flavonoids, Flavonoids, Sugars, Starch, Coumarins, Starch	(45)
Michauxia L'Herit	Methanol	Nil	Polyphenols	(46)
Pinus species	Water - Hydro distillation	Nil	Essential oils	(47)
Euphorbia caducifolia	Latex resin	Nil	Carbohydrates, Amino acids, Phytosterols, Saponins, Glycosides, Fatty acids	(26)
Croton zehntneri	Steam distillation	GCMS	Essential oils	(54)
Trichosanthes dioca Roxb	Methanol	Nil	Alkaloids, Flavonoids	(27)
Glycomis arborea	50 % Ethanol	Nil	Flavonoids, Triterpinoids, Alkaloids, Phenols	(28)
Hypericum patulum	Methanol	Nil	Steroids, Flavonoids	(29)
Plagiochasma appendiculatum Lehm. Et Lind	Petroleum Ether, acetone, chloroform, ethanol, water, hydro alcoholic acid	Nil	Alkaloids, Anthraquinones, Saponins, Flavonoids, Sesquiterpenes, Terpines	(32)
Sesamum indicum	No active extraction	Nil	Constituent Sesamol used	(33)
Terminalia arjuna	50% Ethanol	Nil	Tannins, Saponins, Reducing Sugars	(35)
Dendrophthoe falcata	Ethanol	Nil	Alkaloids, Saponins, Flavonoids, Terpines, Steroids, Glycosides, Tannins	(36)
Holoptelea integrifolia	Methanol	HPTLC	Alkaloids, Saponins, Flavonoids, Terpines, Steroids, Glycosides, Tannins, Anthraquinolones	(37)
Anredera diffusa	90% Ethanol	NMR, HPLC	Oleonolic Acid	(59)

When determining and identifying active components, experimental controls are critical and should be based on previously established treatments with proven efficacy and market related success. For example, Reddy, *et al.* (37) investigated the chemical constituents in *Holoptelea integrifolia* using high performance thin layer chromatography (HPTLC) and assessed both wound healing efficacy and anti-microbial effects of the extract. Comparison was made between the plant and Nitrofurazone, a common topical anti-microbial. In contrast, Malveira Cavalcanti, *et al*. (54) separated and identified essential oils from *Croton zehntneri* by gas chromatography and mass spectrometry (GC/MS) and tested these tested for wound healing effect. The most abundant essential oil was *trans*-anethole. To determine whether *trans*-anethole was the compound of interest, its efficacy was compared to the whole essential oil extract, with corticosteroids and fibrinolysin controls in a rodent model. Such controls are not commonly used in clinical practice and therefore may not be appropriate.

4.1.3 Approach to Identifying Potential Compounds of Interest

A number of protocols have been used to isolate active substances in plants. Neutral, acidic or basic water or solvent extracts of plant material provide a convenient means of extracting active substances from large amounts of plant material in sufficient quantities to undertake further isolation, assay and analysis of the active substances. The initial extract will indicate whether the substances are polar or non-polar and simple screening by thin layer chromatography (TLC) with colorimetric spray reagents can indicate the class of potential substances with activity. Further separation including high performance liquid chromatography (HPLC) and gas chromatography (GC), coupled with mass spectrometry (MS) allows for elucidation of chemical structures. Scale-up and fractionation from nano- or microgram scale to the gram scale may involve large and expensive preparative columns. Once purified, the isolated compound's structure can be confirmed using techniques including infra-red spectroscopy, nuclear magnetic resonance and X-ray crystallography.

4.1.4 Alkaloid Detection and Characterisation – Gas Chromatography and Mass Spectrometry

Available literature suggests a potential compound class of interest in wound healing are the pyrrolizidine alkaloids with their role in gastric ulcer healing (144) and furthermore, many useful drugs in use today are alkaloid based.

The alkaloid group of plant compounds is generally described as being nitrogen containing cyclic compounds often synthesized from an amino acid precursor. The class of alkaloids is known to contain many compounds and with more sophisticated investigations being routinely employed, the isolation and characterization of these compounds has accelerated. Currently known alkaloids have been classified (110). Four classification criteria are used:

a) Chemical Classification – the most widely used classification based on the chemical nucleus.
b) Biosynthetic Classification – based on the amino acid precursor being tryptophan, lysine, ornithine, tyrosine and histidine.
c) Pharmacological Classification – based on the therapeutic outcome which is a broad classification and somewhat simplistic for novel agent identification.
d) Taxonomic Classification – based on the plant taxonomy, again being an extremely broad classification.

Chemical classification has an additional sub-classification based on the cyclic nucleus common to those alkaloids (Figure 4.1) and are either non-heterocyclic (one element – usually carbon) or heterocyclic with more than one element in the nucleus (carbon and nitrogen). In alkaloids with non-heterocyclic nuclei nitrogen resides within the side chains or functional groups. Additionally a distinction can be made on the number of rings present within each of these nuclei. Our investigation used GC/MS and mass spectra data from the nuclei is readily available from the National Institute of Standards and Technology (NIST) (202). If possible once a potential nucleus was identified further investigation of functional groups was made.

Alkaloids are derived from amino acid precursors such as ornithine, lysine, tyrosine and tryptophan derived classes, and similar fragmentation patterns are observable within each of the amino acid sub-groups. Pyrrolizidine and tropane type alkaloids have base ions of 80-82 *m/z* for the pyrrolizidine alkaloids and the ion at 82 *m/z* as the base ion with a second peak 20% of the base ion at 83 *m/z* is commonly seen in the tropane alkaloids (203). Distinguishing ions for these 2 compounds are based on triplet fragments of 93-95, 119-121 and 136-138 *m/z* for the pyrrolizidine alkaloids (204) and an additional fragment at 94 *m/z* is common for the tropane alkaloids (203).

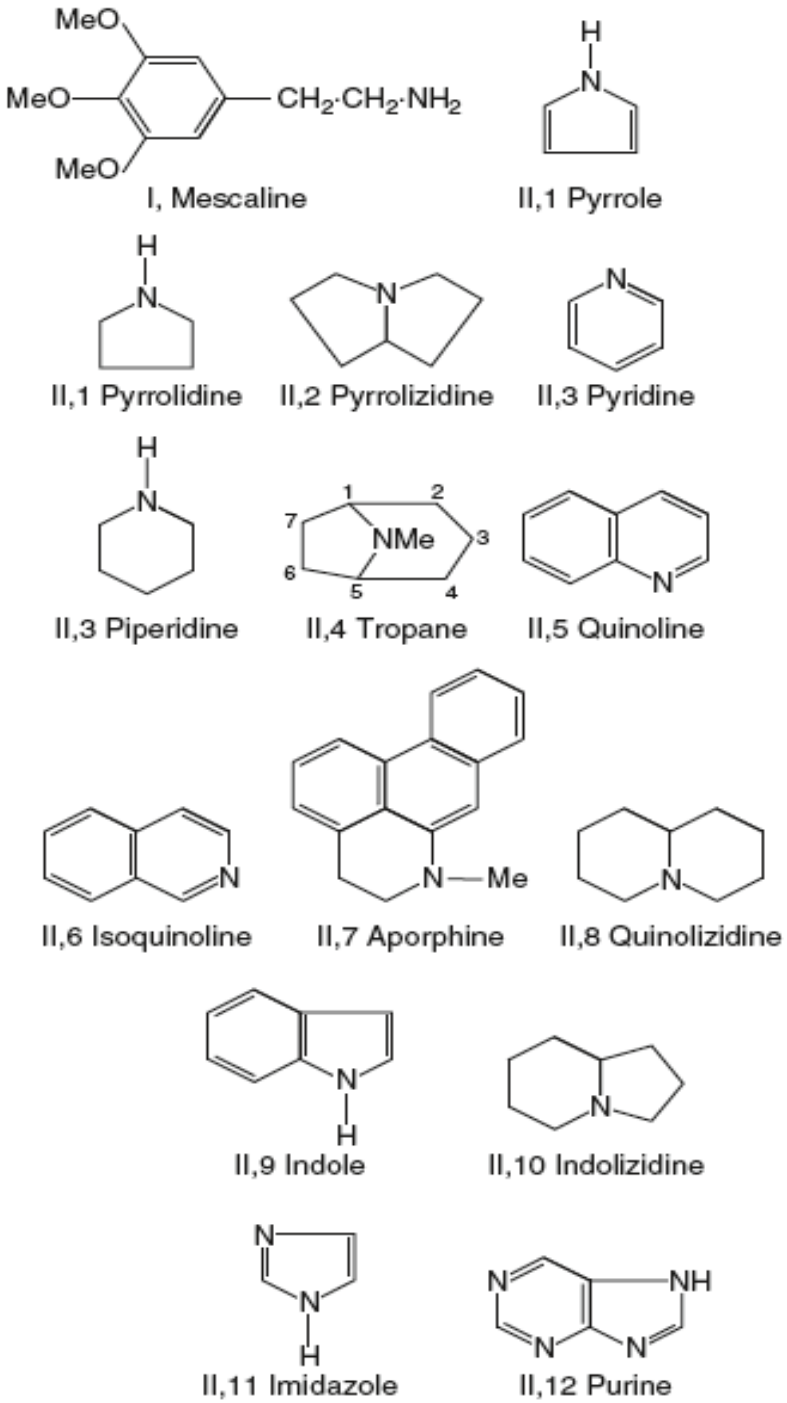


*Figure 4.1. Common alkaloid nuclei making up a major classification system. Taken from Trease and Evans Pharmacognosy **(110)**.*

4.1.5 Approach to Identifying Potential Compounds

Mass spectral fragmentation patterns allow for the identification of the common alkaloid nuclei which are represented in Figure 4.1 and with the corresponding fragmentation patterns seen in Table 4.2. Such data provides a starting point for identification of the possible class of compounds of interest. In general the fragments less than 100 *m/z* are fairly non-specific and are present in most cases. However, fragments around 40 *m/z* (± 5 *m/z*), specifically less than 40 *m/z*, are seen in the glycine, tyrosine, tryptophan, and pyridine type alkaloids. Those more than 40 *m/z* are common in the ornithine, lysine and histidine type alkaloids. Additional fragments greater than 55 *m/z* but less than 60 *m/z* are common in the ornithine and lysine type alkaloids and less than 55 *m/z* are common in the tyrosine, tryptophan and pyridine type alkaloids. Fragments greater than 60 *m/z* but less than 65 *m/z* are more common in the tyrosine and tryptophan classes. Identification of the alkaloid nuclei in the smaller fragments can lead to identification of the functional groups that are attached to the alkaloid nuclei and would be represented in the larger fragments.

These ions and the fragmentation pattern are matched to similar fragmentation patterns in databases and in most cases this is an automated process and multiple computational algorithms have been developed for this purpose. When comparing unknown molecules, comparisons to spectral libraries will lead to non- or miss identifications and therefore additional algorithms have been developed to analyse the generated spectra of unknown compounds (205). These include 1) searching for similar spectra in a database and generating a percentage similarity, 2) rule based spectrum prediction using fragmentation principles, 3) combinational fragmentation using fragments to describe the compounds structure, 4) fragmentation trees and 5) mass spectral classifiers (205).

Fragmentation patterns generated by electron impact ionization have been useful for identification of alkaloids using the mass spectral classifiers approach. Electron impact ionization gives rise to abundant molecular or parent masses, and complex fragmentation patterns to provide mass spectral classifiers (206).

Table 4.2. GCMS data for the relevant alkaloid bases. Data is presented as compounds occurring within an amino acid group with examples included. The formula and mass ion are shown with the mass ion represented as a range with the most common ion bolded. The fragmentation pattern depicted here is based on those from the NIST database with the prominent ions represented as a range and most common ion being bolded and in brackets. Key or base ions of each compound are underlined.

Amino Acid Precursor	Alkaloid Base	Important Example	Formula	M m/z (range of M)	Fragmentation Pattern (m/z)
Glycine	Pyrrole	Basic Building Block	C4H5N	**67.01** (66-68)	50-53 (**52**) , 36-42 (**39**) , 25-28 (**28**)
Ornithine	Pyrrolidine	Nicotine	C4H9N	**71.12** (68-71)	37-44 (**43**) , 26-30 (**28**)
	Pyrrolizidine	Senecionine/Retrosine	C7H13N	**111.18** (109-112)	93-98 , 80-85 (**83**) , 67-70 , 52-58 (**55**) , 39-44 (**42**) , 27-30 (**28**)
	Tropane	Cocaine	C8H15N	**125.21** (122-126)	112-113 (**113**) , 91-98 (**96**) , 77-84 (**82**) , 66-71 (**67**) , 51-58 (**57**) , 39-44 (**42**) , 27-31 (**27**)
Lysine	Piperidine	Basic Building Block	C5H11N	**85.15** (84-86)	67-70 (**70**) , 51-58 (**56/57**) , 39-44 (**44**) , 26-30 (**29**)
	Quinolizidine	Sparteine	C7H17N	**139.24** (138-140)	110 , 96-97 (**96**) , 81-83 (82) , 67-68 , 53-55 , 39-41
	Indolizidine	Swanisionine	C8H15N	**125.21** (120-126)	108-110 (**110**) , 93-98 (**97**) , 81-84 (**83**) , 67-71 (**69**) , 52-57 (**55**) , 39-43(**41**), 26-30 (**27**)
Tyrosine	Isoquinoline	Morphine	C9H7N	**129.16** (128-130)	100-103 (**102**) , 74-78 (**76)** , 61-64 (**63**) , 50-52 (**51**) , 38-39
	Mescaline	Mescaline	C11H17NO3	**211.26** (209-211)	179-183 (**182**) , 165-168 (**166**) , 151-152 , 133-139 (**136**) , 120-124 (**121**) , 105-109 (**105**) , 89-95 (**91**) , 77-81 (**80**) , 63-67 (**65**) , 50-54 (**52**) , 38-45 (**39**), 29-31 (**30**)
Tryptophan	Indole	Ergotamine	C8H7N	**117.15** (116-118)	89-91 (**90**) , 61-64 (**63**) , 50-52 (**51**) , 37-39 (**39**)
	Quinoline	Quinine	C9H7N	**129.16** (128-130)	100-103 (**102**) , 74-78 (**76)** , 61-64 (**63**) , 50-52 (**51**) , 38-39
Histidine	Imidazole	Pilocarpine	C3H4N2	**68.08** (67-69)	38-42 (**41**) , 26-28 (**28**)
Pyridine	Pyridine	Basic Building Block	C5H5N	**79.10** (75-80)	49-53 (**52**) , 37-40 (39) , 26-27

4.1.6 In-vitro Wound Healing Assays

Scratch assays are widely used cell culture based bioassays where a cell monolayer is grown on a coverslip and the monolayer is “scratched” to create a wound or disruption. The cells can be treated with the substance being assessed and the migration of the cells back into the wounded area can be quantified (207).

Previous Chapters demonstrated that in the *in-vivo* porcine wound model, cell migration was not significantly affected when comparing the various treatment modalities. In the deep partial thickness wounds, all wounds, regardless of treatment, were re-epithelialised to some degree by day 5 post-operative and in the full thickness wounds there was no difference in the extent of the migrating epidermal tongues. Although the process of wound healing requires cell migration into the wound space, this was not seen to be affected by the treatment modalities. From the immunofluorescence investigations, it was evident that cellular proliferation was the key variable and simple and inexpensive assays were required to assess this parameter when determining potential active constituents that affect wounds in the *Senecio* plant preparation.

Cellular proliferation assays using tetrazolium salt and bromodeoxyuridine (BrdU) have been widely used to assess the potential of novel compounds for therapeutic use. However, despite their widespread use the tetrazolium salts are known to be toxic as the formazin dye that is produced has been shown to be carcinogenic. Furthermore these assays require the lysis of the cells to release and quantify the dye to determine cell proliferation. These assays cannot be used in on-going real time assays and would be difficult to adapt to high-throughput assays.

An alternative to the tetrazolium salt and BrdU based assays is the use of resazurin based detection reagents. The resazurin based dyes have been used in cell proliferation assays for over 50 years and may offer significant advantages over the tetrazolium and BrdU approaches (208). Firstly the resultant fluorescent resorufin and is non-toxic to the cells and operator, making it a safer option (209). Secondly and importantly for our purposes, the cells do not need to be lysed to release the fluorescent metabolite for spectrophotometric quatification and therefore allow for a real time assessment of cellular proliferation.

With the known complexity of the wound healing process single time point assays have the potential to miss important prior or subsequent events or effects. *In-vivo* monitoring and sampling of the wounds at multiple time points as opposed to a single time point has led to the detection of when the plant based therapy differs from controls and when it exerts specific effects. The development of a real time assay would be particularly useful to gain further insight into the wound healing effects.

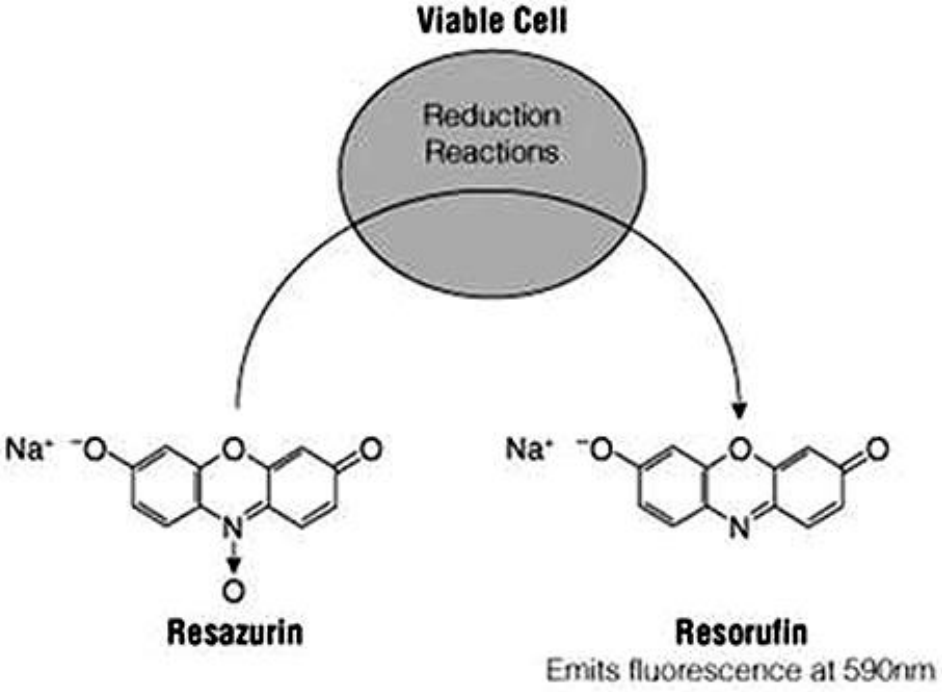


Figure 4.2. Reduction of the Resazurin dye (accessed from www.pharmacelsus.de.).

Past studies where resazurin assays have been employed in traditional or plant based therapies focus on the anti-proliferative aspects of potential lead compounds and so were mostly utilised in oncological investigations. The study of the antiproliferative properties of citrus flavonoids by Kawaii, *et al.* (210), using human lung carcinoma, mouse melanoma, human T-cell leukaemia and human gastric cancer cells emphasises this point. Studies on plant based therapeutics (Table 1.1) for wound healing made use of the tetrazolium salt and BrdU based assays and include *Bulbine natalensis* and *Bulbine frutescens* (9), the *Astragalus* genus (211) and multiple Brazilian derived plants (56). A PubMed search for the use of resazurin based assays in wound healing was unable to detect any previous publications in this regard and therefore makes our approach here a novel one.

4.1.7 High-Throughput Assay Platform

After identifying an *in-vitro* assay which could be used to identify potential lead compounds, the development of a high-throughput assay platform was explored. Such platforms have become the current pharmaceutical gold standard (212) and allow the screening of numerous compounds obtained from databases and in our case plant based therapies for a particular

desired response. These assays have often been automated to reduce the investigators input required to identify and develop therapeutic agents. Furthermore high throughput assays allow for screening of known compounds in established databases and identification of compound classes from preliminary investigations when testing synthetic molecules. Furthermore such assays avoid expensive and time-consuming *in-vivo* models. However unlike *in-vivo* models, in vitro assays do not fully account for the complexity of the healing wound.

Scratch assays have been the standard protocol for many investigations into wound healing and lead molecule identification, but it does not lend itself entirely to the high-throughput assay platform as its application to automated systems using multiwell plates is complex. Attempts have been made to adapt cell migration assays to high-throughput screening modalities (213). These authors were able to apply scratch based assays to multiwell plates (96 and 384) which were monitored using time lapse microscopy and then further quantified. Although this format fulfils the requirements for a high throughput assay, factors pertinent to wound healing appear to have been neglected and for our purposes would not suffice. Importantly cell proliferation could not be taken into account unless further staining techniques were employed thereby reducing the potential to automate the assay. As cellular proliferation was shown to be key to the present investigations, scratch assays would be difficult to adapt to high through assays for determining cellular proliferation.

In development of the high throughput assays, a suitable target needs to be identified that responds in such a way that a therapeutic effect can be measured and compared (214). Suitable targets are mostly in the format of membrane receptors, enzymatic activity, ion channels and DNA responses (215). Additional general cellular responses could be measured but would require additional cell culture steps with longer preparation and assay times. The goal in the present experiments was to rapidly measure cellular proliferation. The format of these assays could be in 96 up to 384 multi-well plates.

4.2 Aims

The aims of this study are therefore to:

a) Develop an easily reproducible plant extraction protocol that can be adapted to scaling up isolation of lead fractions;
b) Develop an *in-vitro* assay, which has high throughput assay applications, to identify possible lead fractions;
c) Determine the constituents of the possible lead fractions.

4.3 Materials and Methods

4.3.1 Plant Extraction and Analysis

Whole Plant Extract

The plant material was prepared as previously described in Chapter 2. A whole plant extract was prepared by extracting 5 g of previously prepared plant material in 100ml of deionised water. The extraction was continued for 24 hours after which it was sonicated for 90 minutes in a 200ml flat bottomed flask. The extract was filtered through a Number 1 Whattman filter paper and then filtered through a 0.22 µm syringe filter (Millex, Millipore). The extract was aliquoted into 5ml aliquots and stored at -70^{o}C until use. Prior to experimentation the whole extract was prepared by serial dilution ranging from a 1:40 dilution to a 1:10 240 dilution.

Plant Fractionation

A water based solvent was used with the aim of extracting basic, neutral and acidic compounds. Therefore 5g of previously prepared plant material was extracted in either pure de-ionised water, 0.05M sulphuric acid in deionised water or 5% (v/v) ammonia in deionised water. The extraction volumes were each at 100 ml and the extraction continued for 24 hours. The extracts were sonicated for 90 minutes in 200 ml flat bottomed flasks. Following sonication, the extracts were filtered through no, 1 Whattman filter papers and then through a 0.22 µm syringe filter (Millex, Millipore).

For further extraction, 3 preconditioned 35cc/6g hydrophobic lipophilic (HLB) solid phase extraction cartridges (Oasis, Waters) were used. The solvents that were used were allowed to pass through the columns by gravitational force and each extraction took place over 6 hours. As per the manufacturers protocol, the cartridges were pre-conditioned with 100% methanol and equilibrated with deionised water. The sample was loaded and the resultant effluent was retained after which the cartridges were washed with 5% methanol in deionised water (wash 1).

For elution of the acidic compounds the acidic extract was subjected to a 2nd wash of 2% formic acid in methanol after which the cartridge was eluted firstly with 5% ammonia and secondly in 0.05M sulphuric acid in deionised water. The procedure for the neutral and basic compounds was the same up to the first wash after which the second wash was 5% ammonia in methanol; and eluted firstly with 2% formic acid in methanol, followed by the second elution of 0.05 M sulphuric acid.

Once all the extracts had been passed through the cartridges, the presence of alkaloids in each of the various fractions was detected by spotting the fractions on thin layer chromatography plates, and spraying the plates with Dragendorff's reagent followed by heating the plates in an oven set to 150ºC for 20 minutes. The first wash and the subsequent elutions were retained for the cell culture based assays with a resultant twelve fractions in total being tested. Prior to the *in-vitro* proliferation assay, the various fractions were evaporated to dryness after which they were reconstituted in phosphate buffered saline (PBS) at a concentration of 1:40 of the original extraction volume. The fractions were sterile filtered using a 0.22 µm syringe filter (Millex, Millipore) and then serial dilutions were prepared for use for the proliferation assays. All serial dilutions were stored at -70 ºC until use.

Table 4.3. Description of the various extractions and resultant fractions.

Solvent Step	Acidic Extract	Neutral Extract	Basic Extract
Water Extract	Whole plant Extract		
5% MeOH	Acidic Extract Wash 1	Neutral Extract Wash 1	Basic Extract Wash 1
2% formic acid / 5% ammonia	Acidic Extract Wash 2	Neutral Extract Wash 2	Basic Extract Wash 2
2% formic acid / 5% ammonia	Acidic Extract Elution 1	Neutral Extract Elution 1	Basic Extract Elution 1
0,05 M sulphuric acid	Acidic Extract Elution 2	Neutral Extract Elution 2	Basic Extract Elution 2

4.3.2 Proliferation Assays

Cell Culture Conditions

Based on the animal work described above, keratinocytes were identified as cells which are potentially the target of the active fractions of *Senecio*. Immortalised keratinocytes (HaCat) were obtained from Dr Nalini Pather from the School of Anatomy, University of the Witwatersrand. The protocol for *in-vitro* analysis was based on work by Hsu, *et al.* (216). Cells for the analysis were grown in Dulbecco's Modified Eagle's Medium (DMEM) (Highveld Biological, South Africa, P02) supplemented with 5% Foetal Bovine Serum (FBS) (Gibco – Invitrogen, South Africa, 41F5180F). The cells were grown in 25 cm^3 Corning culture flasks

(Sigma, South Africa) with 5 ml of cultured media. Subculture of the cells was done when the flasks were 80-90% confluent. The used media was discarded and the cells were washed with phosphate buffered saline (PBS) after which the flasks were trypsinised with 2 ml Trypsin-EDTA for 5 minutes after which it was neutralised with a further 2 ml of culture media. Once detached the cells were centrifuged at 1500 rpm in 15ml culture tubes for 2 minutes. The supernatant was discarded and the pellet re-suspended in 10 ml of culture media. Once re-suspended, the final volume was split into two flasks each containing 5ml of culture media and cells. The flasks were incubated in 5% carbon dioxide at 37 ^{o}C.

Resazurin Based Proliferation Assay

In order to conduct the proliferation assays, the cells were harvested from the culture flasks and counted using a haemocytometer. Cells for analysis were seeded into 96-well plates at a concentration of 0.5 X 10^4 cells/ml. Plates where further incubated for a further 24 hours after which they were treated with either the extracts as described above or the controls.

Proliferation Assay Optimisation

To assess the validity of the resazurin based assay multiple controls were employed. To negate any possible effects of the plant fractions as possible reducing agents, wells were left unseeded with cells and then treated with concentrated fractions (1:80). To negate any possible effects of the media, wells were seeded with cells, and left un-treated and the resazurin dye was omitted from these wells.

Control and Resazurin Dye Preparation

Controls included the vehicle (PBS only) acting as a negative control and epidermal growth factor (EGF) as the positive control. Lyophilised murine submandibular EGF (Sigma, South Africa) was reconstituted in 1% FBS in PBS to produce a stock solution of 340 ng/ml. From this stock solution, aliquots were prepared to adjust the concentration of EGF to 6.5 ng/20µl.

For the quantification of proliferation, resazurin sodium salt (Sigma, South Africa) was made up to a standard 10% solution in DMEM and sterile filtered through a 0.22 µm syringe filter (Millex, Millipore) prior to use.

Whole Plant Extract and Plant Fraction Proliferation Assays

After the intial 24 hour incubation period and with the cells nearing confluence, they were treated with the various plant extract fractions and controls. A volume of 20 µl of either plant

fraction or control was added to the wells. Thereafter 10 µl of the Resazurin solution per 100 µl culture media was added to each of the wells at the time of treatment.

All treatments can therefore be summarised as:

a) Negative control – 20 µl PBS
b) EGF – 6.5 ng/20µl
c) Whole plant extract – 20 µl of each serial dilution ranging from 1:40 to 1:5120
d) Acidic extract fractions – 20 µl of each serial dilution ranging from 1:80 to 1:10240
e) Neutral extract fractions – 20 µl of each serial dilution ranging from 1:80 to 1:10240
f) Basic extract fractions – 20 µl of each serial dilution ranging from 1:80 to 1:10240

After 4 hours of incubation of the cells the plates were read on a Biotek PowerWave HT *UV* – vis microplate spectrophotometer at a wavelength of 570 nm and 600 nm. All treatment modalities and controls were run in quadruplicate. According to Al-Nasiry, *et al.* (208) the percentage reduction can be extrapolated from the absorbance measurements using the following equation:

$$\%\ \text{Resozurin reduction} = \frac{(\varepsilon_{ox}\lambda_2)(A\,\lambda_1) - (\varepsilon_{ox}\lambda_1)(A\,\lambda_2)}{(\varepsilon_{red}\lambda_1)(Ą\lambda_2) - (\varepsilon_{red}\lambda_2)(Ą\lambda_1)} \text{ x } 100$$

Key: $\varepsilon_{ox}\,\mathbf{x_1}$ = extinction co-efficient of Resazurin at 570 nm wavelength in the oxidised state, $\varepsilon_{ox}\,\mathbf{x_2}$ = extinction co-efficient of Resazurin at 600 nm wavelength in the oxidised state, $\varepsilon_{red}\,\lambda_1$ = extinction co-efficient of Resazurin at 570 nm wavelength in the reduced state, $\varepsilon_{red}\,\lambda_2$ = extinction co-efficient of Resazurin at 630 nm wavelength in the reduced state, $Ą\boldsymbol{\lambda_1}$ = Absorbance of negative control wells at 540 nm wavelength , $Ą\boldsymbol{\lambda_2}$ = Absorbance of negative control wells at 630 nm wavelength, $\boldsymbol{A\lambda_1}$ = Absorbance of the test wells at 540 nm wavelength, $\boldsymbol{A\lambda_2}$ = Absorbance of the test wells at 630 nm wavelength.

Real Time Proliferation Assays

To produce a real time assay the fractions at that specific dilution showing the best activity were repeated and monitored over 12 hours. The rate of proliferation was determined by generating linear equations for the first 4 hours of the experiments where the wells were treated with the identified fractions. Once the formulae's were generated the gradient was determined for all test wells and the fractions and was compared to each of the controls. The

rate of proliferation for each fraction was expressed as a percentage of the controls, namely the negative control and EGF controls.

4.3.3 Statistical Analysis

All results were presented as percentage (%) reduction of resazurin dye. Statistical Analysis was done using the software package Statistica (ver. 9). The one-way ANOVA test with the Tukey *post-hoc* analysis was used and significance was accepted at $p < 0.05$.

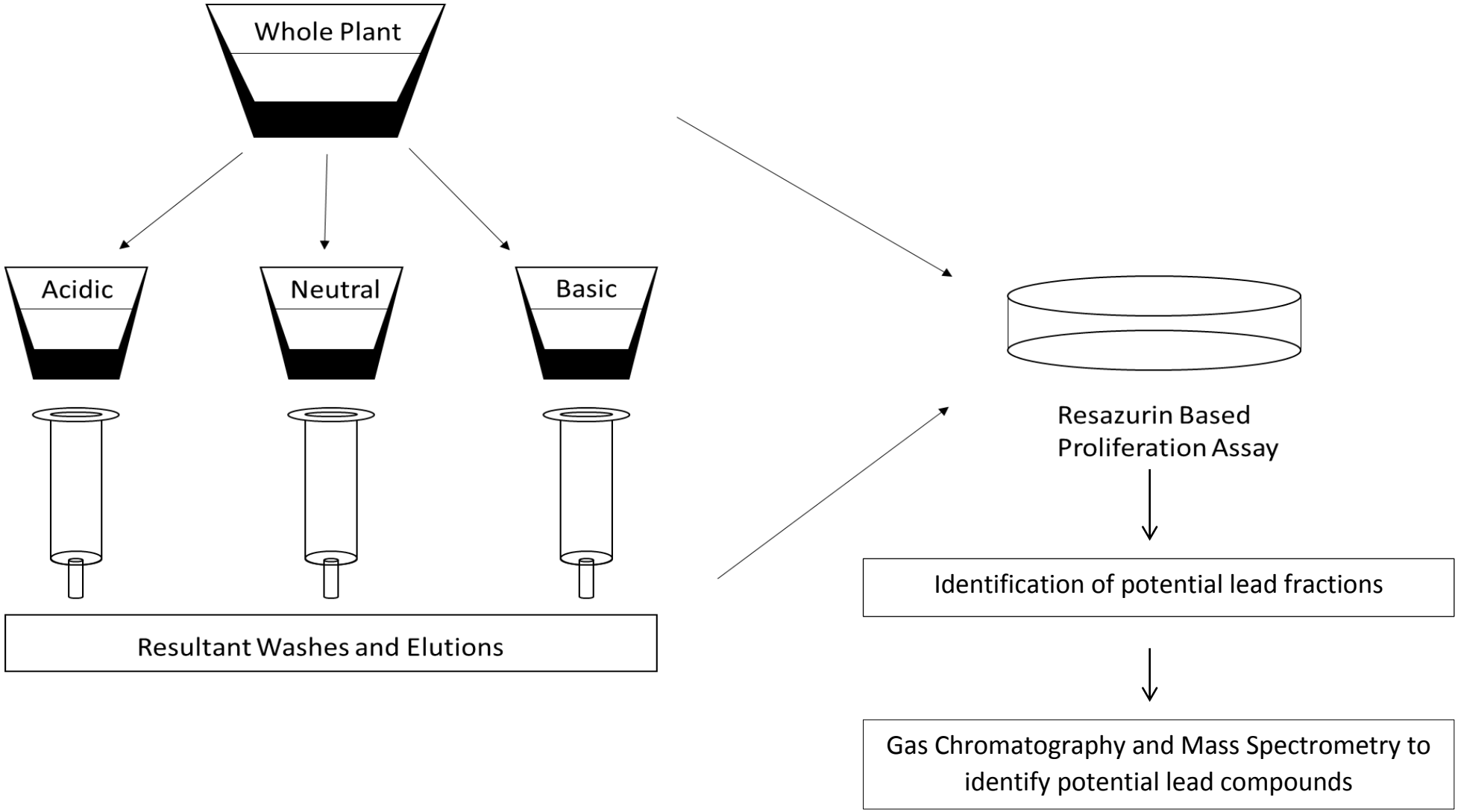


Figure 4.3. Schematic representation of the fractionation of the plant and subsequent steps thereafter.

4.3.4 Extract Analysis

The fractions that showed significant activity were further analysed using gas chromatography coupled with electron ionisation mass spectrometry namely a 7890A GC system coupled with a 5975C inert XL EI/CI MSD triple axis detector (Agilent Technologies) fitted with a DB5 gas chromatography column (30m x 250 µm x 25 µm) (Agilent Technologies). The instrument used was based in the Department of Chemical Pathology, School of Pathology, University of the Witwatersrand.

Samples for analysis were evaporated and reconstituted in 5 ml of HPLC grade methanol. The operation conditions for the analysis were as follows: samples were injected at a volume of 2 µl with an initial starting temperature of 100 ^{o}C for 5 minutes thereafter an incremental increase of 5 ^{o}C to 310 ^{o}C which was maintained for a further 15 minutes. The entire run time was 62 minutes. Nitrogen was used as the inert carrier gas with a pressure of 184.22 kPa at a flow rate of 1.0034 ml/min with an average velocity of 32.447 cm/sec.

The resultant chromatograms were further analysed for significant peaks. In each chromatogram the peaks were noted and the retention times, molecular ion (M), base ion and absolute abundance and fragmentation pattern recorded. To account for potential background noise, pure methanol was run in between the sample runs and background peaks identified here were subtracted from the plant fraction spectra to obtain an accurate mass spectrum. To compare the two fractions, the retention times for the major peaks previously recorded were analysed for similarities in the two fractions i.e., retention time A in the neutral extract was identified in the basic extract and the data recorded as before. Mass spectra obtained were also compared to common fragmentation patterns for alkaloid bases obtained from the NIST database.

4.4 Results

4.4.1 Cell Culture and Proliferation Assay

Assay optimisation

The results for the optimisation experiments are seen in Table 4.4. When the cells were not treated with either control or plant fraction, no resazurin reduction is seen until 2 hours after which they follow an incremental increase. The wells containing Cells + Resazurin dye and the wells without cells but with resazurin dye + 1:80 plant fraction show no reduction of the dye.

Results were represented graphically in Figure 4.3. The wells that were seeded with cells showed minimal resazurin dye reduction up to 2 hours after which an incremental reduction of the resazurin dye is seen up to 12 hours. The wells containing no cells (Cell–less) but with either the resazurin dye only and with the resazurin dye + 1:80 plant fraction showed no reduction of the resazurin dye throughout the observational period as is seen as flat lines in the graphical representation of the optimisation experiments.

Table 4.4. Percentage reductions of the optimisation of the resazurin based assays. Data are presented as mean ± SD (n).

Time (hours)	Negative Control	Cell-less + Resazurin + 1:80	Cells – Resazurin
0	29.22 ± 4.74 (6)	22.39 ± 4.55 (9)	24.24 ± 5.18 (9)
2	31.69 ± 2.11 (6)	22.43 ± 4.52 (9)	24.02 ± 4.82 (8)
4	43.42 ± 7.20 (6)	22.35 ± 4.50 (9)	23.81 ± 4.77 (9)
8	63.96 ± 13.84 (6)	21.71 ± 5.44 (6)	22.59 ± 5.39 (6)
12	89.70 ± 10.46 (6)	22.28 ± 4.54 (6)	23.52 ± 4.67 (6)

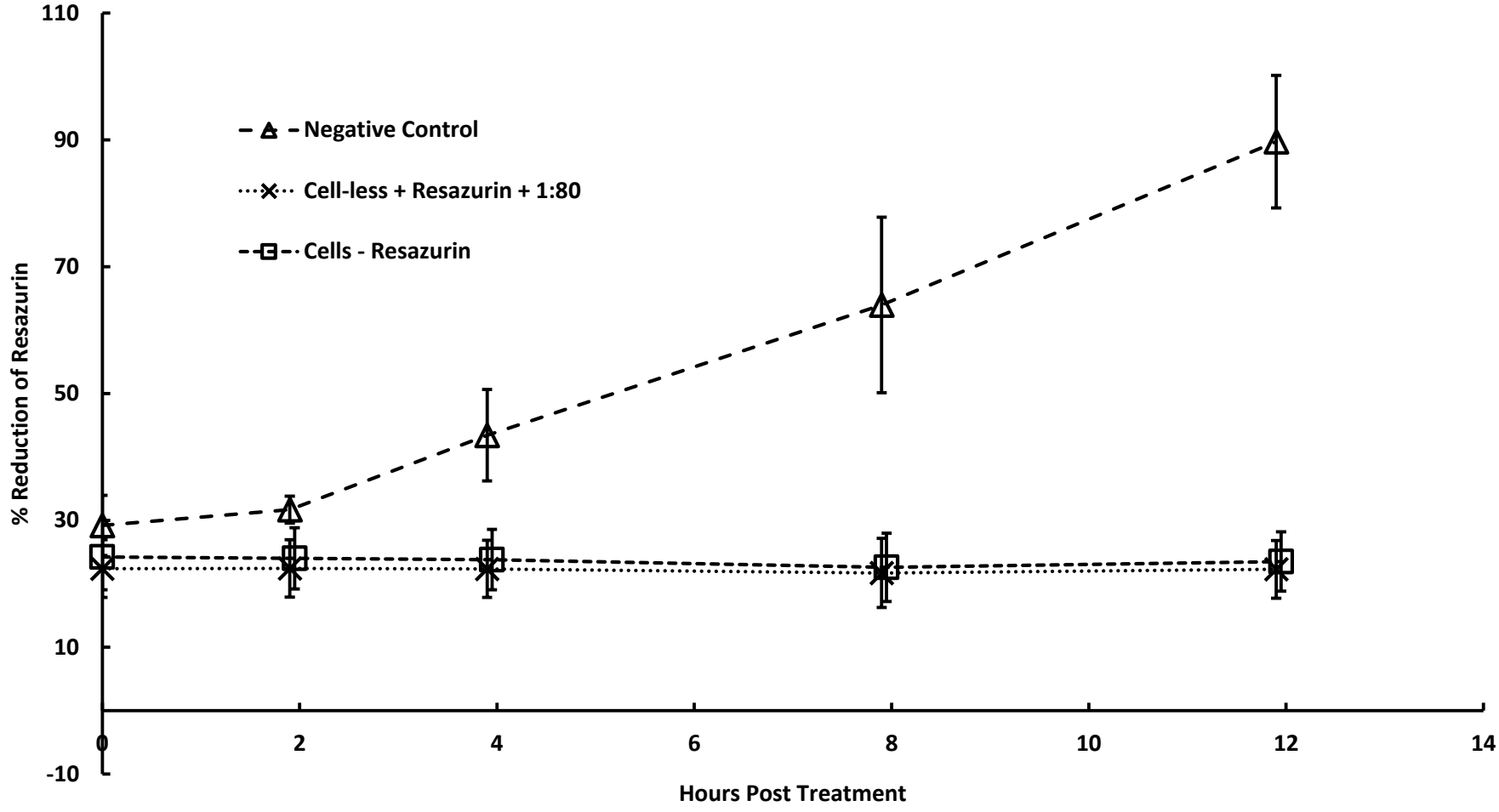


Figure 4.3 Graphical representation of the optimisation experiments plotted against time (hours). Each marker represents mean % reduction and the error bars represent the SD.

4.4.2 Whole Plant Extract Proliferation Assay

Results for the whole plant proliferation assay were shown in Table 4.5. At a dilution of 1:160 the whole plant extract had a significantly greater percentage reduction of the resazurin dye when compared to the negative control (p = 0.022) and EGF control (p = 0.008). No other significant differences were detected. The data is represented graphically in Figure 4.5. The whole plant extract shows increases in percentage reduction of the resazurin dye from a dilution of 1:160 to 1:1280 but was only significantly greater at the lower dilution.

Table 4.5. Percentage reductions of the whole plant extract. Data are presented as mean ± SEM (n). Corresponding comparisons between the negative control and EGF control were shown with p –values. Underlined p – values are significant.

Dilution	% Reduction	Negative Control Comparison *p* - value	Epidermal Growth Factor Comparison *p* - value
Negative Control	43.42 ± 7.09 (48)		
Epidermal Growth Factor	41.01 ± 6.52 (48)		
1:40	38.57 ± 1.24 (3)	0.485	0.825
1:80	41.60 ± 3.81 (3)	0.903	0.989
1:160	55.54 ± 3.74 (3)	<u>0.022</u>	<u>0.008</u>
1:320	53.39 ± 9.40 (3)	0.139	0.060
1:640	53.33 ± 9.39 (3)	0.142	0.061
1:1280	49.12 ± 2.34 (3)	0.383	0.165
1:2560	40.08 ± 5.67 (3)	0.732	0.976
1:5120	40.38 ± 5.60 (3)	0.770	0.989

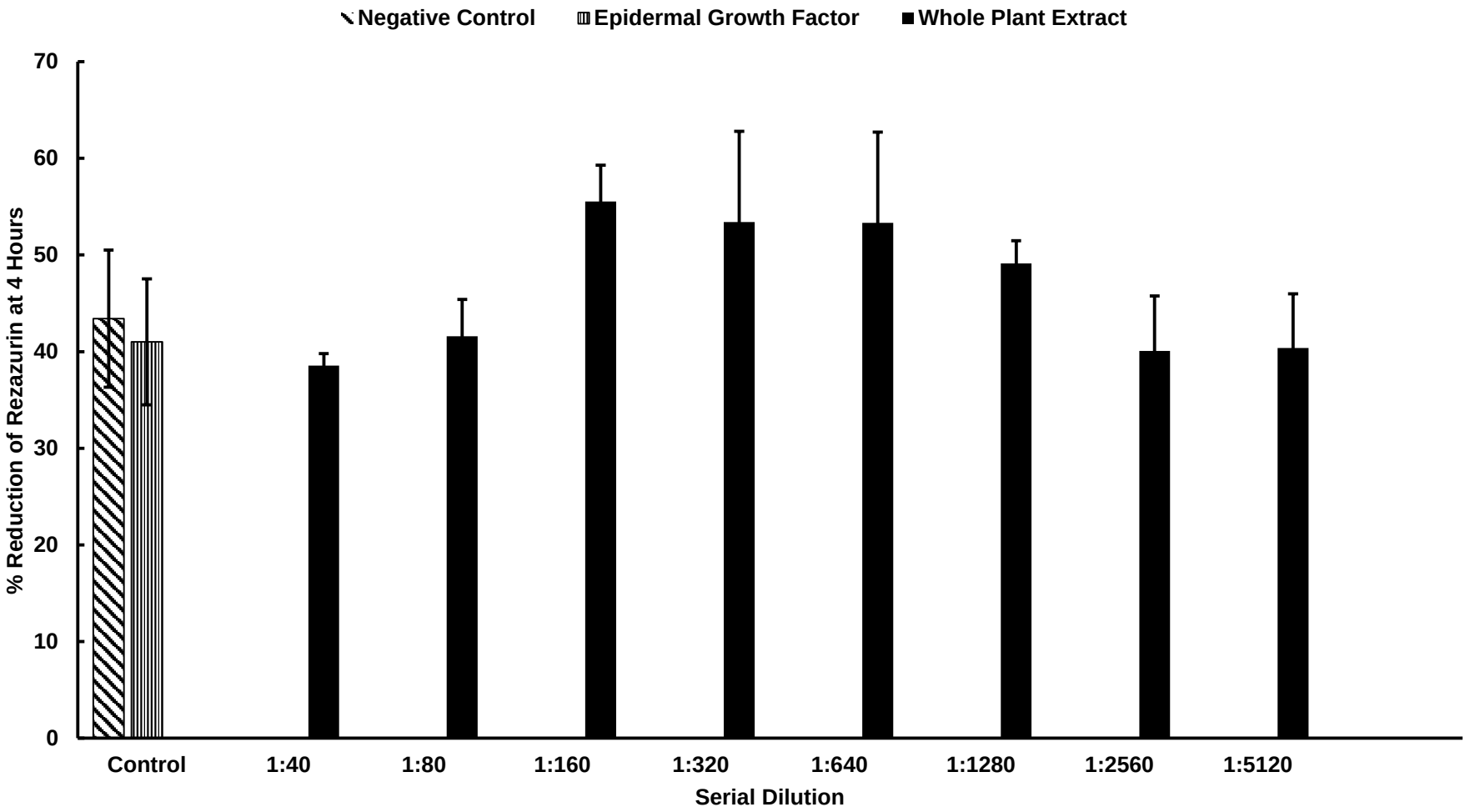


Figure 4.4. Graphical representation of the percentage reduction of the whole plant extract at 4 hours post treatment. Each bar represents mean % reduction and the error bars represent the SD. Significant differences were seen at the 1:160 dilution.

4.4.3 Plant Fraction Proliferation Assay

The generalised approach in this chapter is summarised in Figure 4.3. The results from the fraction's proliferation assays were shown in Tables 4.7 to 4.10. There was no significant increases in the first three collected fractions, being Wash 1 (Table 4.7), Wash 2 (Table 4.8) and the Elution 1 fraction (Table 4.9). There were significant increases in proliferation relative to the controls in the Elution 2 fraction (Table 4.10). The differences seen were in the basic and neutral extraction at the dilutions of 1:160 to 1:640.

At a dilution of 1:160, the basic extract had a significantly greater percentage reduction than the EGF control ($p = 0.029$) but not the negative control ($p = 0.136$). The neutral extract had a significantly greater percentage reduction than the EGF control ($p = 0.000$) and the negative control ($p = 0.000$).

At the dilution of 1:320 the neutral extract had a significantly greater percentage reduction than the EGF control treatment ($p = 0.001$) and the negative control ($p = 0.000$). At the 1:640 dilution the neutral extract had a significantly greater percentage reduction than the EGF control ($p = 0.042$) but not the negative control ($p = 0.160$).

Graphical representation can be seen in Figures 4.6 to 4.9. The majority of the proliferative activity were seen in Figure 4.9, the Elution 2 fraction. The percentage reduction for this fraction show levels elevated above that of the controls but the significant differences were seen in the 1:160 to 1:640 concentrations as stated previously.

Table 4.6. Percentage reduction of Wash 1 fraction of the acidic, neutral and basic extracts. Data are presented as mean ± SD (n). Corresponding comparisons between the negative control and EGF control were shown with p –values.

Extraction	Dilution	% Reduction	Negative Control Comparison *p* - value	Epidermal Growth Factor Comparison *p* - value
Controls	Negative Control	43.42 ± 7.09 (48)		
	Epidermal Growth Factor	41.01 ± 6.52 (48)		
Acidic Extract	1:80	33.87 ± 6.52 (4)	0.654	0.916
	1:160	33.70 ± 2.87 (4)	0.496	0.874
	1:320	32.04 ± 7.91 (4)	0.543	0.889
	1:640	34.49 ± 7.79 (4)	0.675	0.945
	1:1280	33.13 ± 7.52 (4)	0.358	0.747
	1:2560	34.98 ± 5.70 (4)	0.757	0.976
	1:5120	35.70 ± 0.46 (4)	0.999	1.000
	1:10240	34.63 ± 3.49 (4)	0.974	1.000
Neutral Extract	1:80	33.45 ± 3.82 (4)	0.703	0.939
	1:160	34.77 ± 5.50 (4)	0.450	0.842
	1:320	35.37 ± 2.41 (4)	0.657	0.944
	1:640	34.29 ± 2.58 (4)	0.437	0.803
	1:1280	34.21 ± 10.27 (4)	0.486	0.856
	1:2560	35.78 ± 6.83 (4)	0.560	0.902
	1:5120	37.81 ± 9.92 (4)	1.000	1.000
	1:10240	36.18 ± 5.73 (4)	0.922	0.998
Basic Extract	1:80	35.43 ± 4.72 (4)	0.970	0.999
	1:160	32.38 ± 4.13 (4)	0.114	0.382
	1:320	34.20 ± 8.31 (4)	0.178	0.491
	1:640	33.44 ± 5.31 (4)	0.424	0.792
	1:1280	33.83 ± 6.74 (4)	0.491	0.859
	1:2560	35.54 ± 9.27 (4)	0.449	0.829
	1:5120	36.41 ± 10.38 (4)	0.994	1.000
	1:10240	35.30 ± 7.93 (4)	0.951	0.999

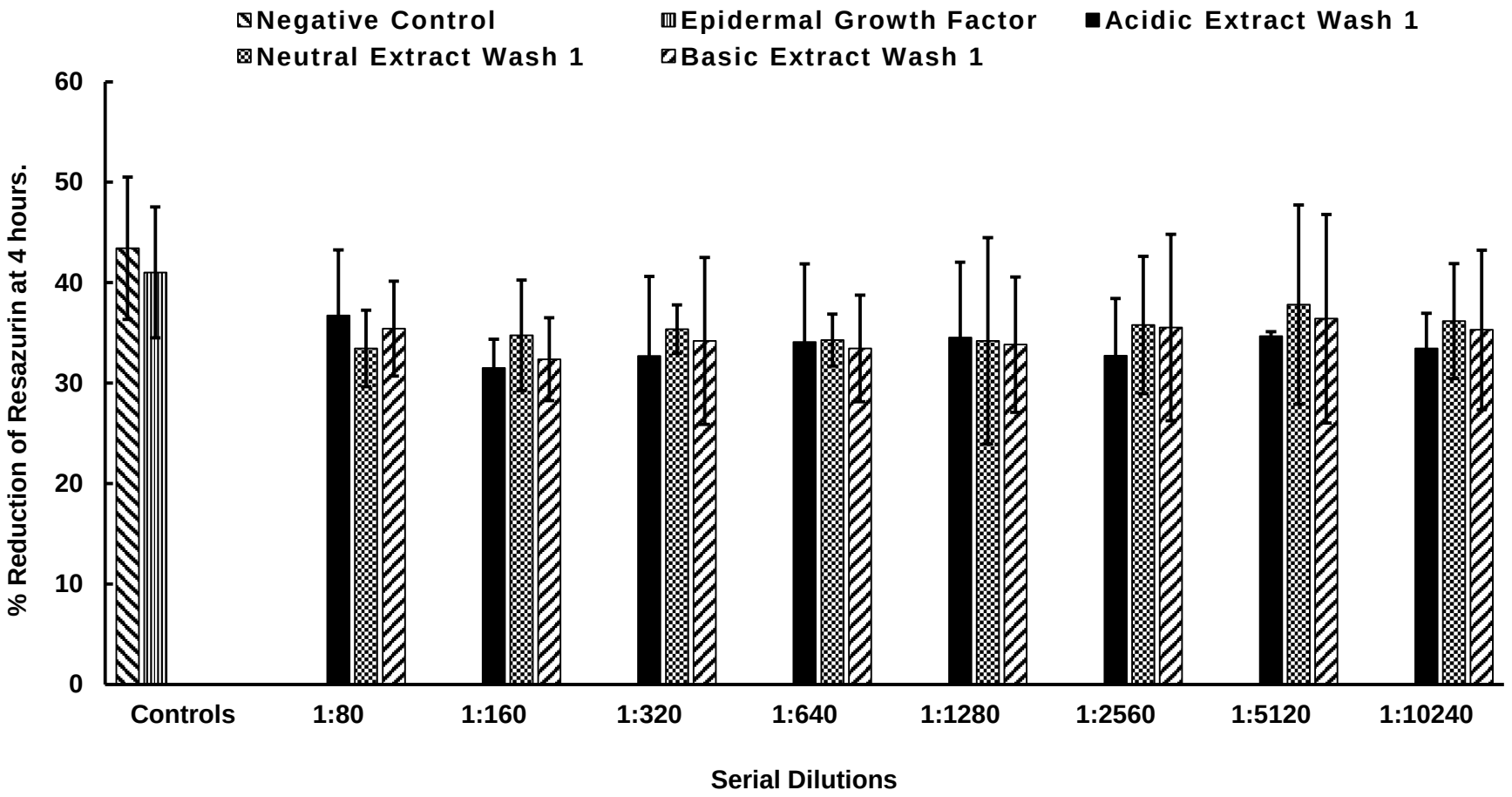


Figure 4.5. Graphical representation of the percentage reduction of the Wash 1 fraction at 4 hours post treatment. Each bar represents mean % reduction and the error bars represent the SD. *No significant differences were detected. Each bar represents mean % reduction and the error bars represent the standard deviation.*

Table 4.7. Percentage reduction of Wash 2 fraction of the acidic, neutral and basic extracts. Data are presented as mean ± SD (n). Corresponding comparisons between the negative control and EGF control were shown with p –values.

Extraction	Dilution	% Reduction	Negative Control Comparison *p* - value	Epidermal Growth Factor Comparison *p* - value
Controls	Negative Control	43.42 ± 7.09 (48)		
	Epidermal Growth Factor	41.01 ± 6.52 (48)		
Acidic Extract	1:80	37.03 ± 10.20 (4)	0.991	1.000
	1:160	34.09 ± 6.44 (4)	0.540	0.900
	1:320	34.35 ± 9.13 (4)	0.670	0.949
	1:640	36.40 ± 8.45 (4)	0.942	0.999
	1:1280	34.90 ± 6.40 (4)	0.735	0.970
	1:2560	37.88 ± 5.39 (4)	0.987	1.000
	1:5120	36.48 ± 7.68 (4)	0.987	1.000
	1:10240	45.52 ± 6.80 (4)	1.000	0.998
Neutral Extract	1:80	40.03 ± 7.52 (4)	1.000	1.000
	1:160	35.98 ± 5.43 (4)	0.843	0.993
	1:320	33.89 ± 6.39 (4)	0.595	0.917
	1:640	36.10 ± 6.67 (4)	0.922	0.998
	1:1280	37.64 ± 5.93 (4)	0.982	1.000
	1:2560	39.99 ± 9.41 (4)	1.000	1.000
	1:5120	36.78 ± 11.44 (4)	0.991	1.000
	1:10240	35.63 ± 8.67 (4)	0.813	0.988
Basic Extract	1:80	37.82 ± 9.76 (4)	0.997	1.000
	1:160	34.18 ± 8.96 (4)	0.556	0.908
	1:320	31.09 ± 4.27 (4)	0.200	0.529
	1:640	31.91 ± 2.71 (4)	0.349	0.718
	1:1280	31.90 ± 3.90 (4)	0.270	0.642
	1:2560	36.12 ± 4.62 (4)	0.890	0.996
	1:5120	36.77 ± 5.18 (4)	0.991	1.000
	1:10240	34.97 ± 3.84 (4)	0.715	0.967

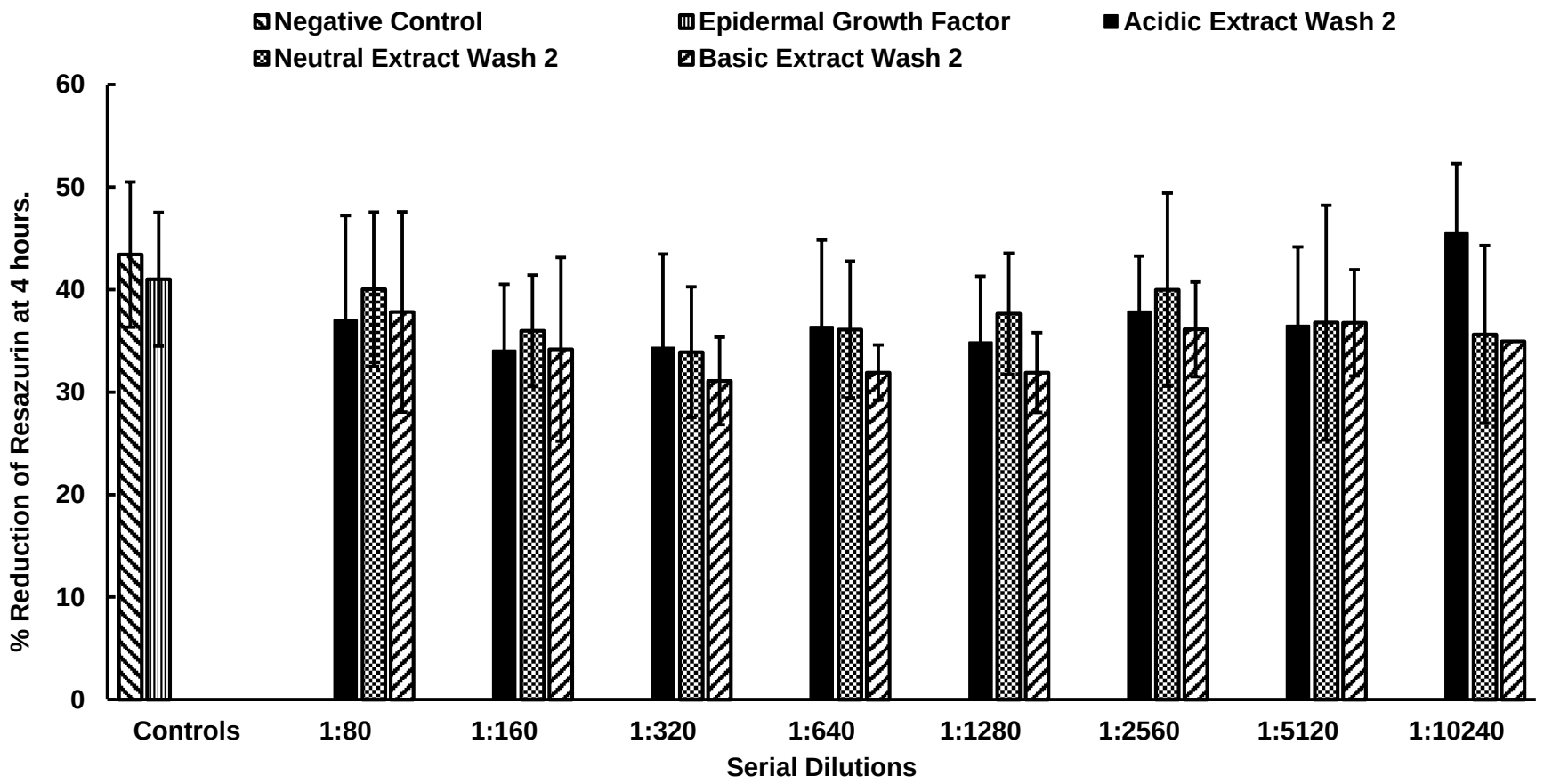


Figure 4.6. Graphical representation of the percentage reduction of the Wash 2 fraction at 4 hours post treatment. Each bar represents mean % reduction and the error bars represent the SD. *No significant differences were detected. Each bar represents mean % reduction and the error bars represent the standard deviation.*

Table 4.8. Percentage reduction of Elution 1 fraction of the acidic, neutral and basic extracts. Data are presented as mean ± SD (n). Corresponding comparisons between the negative control and EGF control were shown with p –values.

Extraction	Dilution	% Reduction	Negative Control Comparison *p* - value	Epidermal Growth Factor Comparison *p* - value
Controls	Negative Control	43.42 ± 7.09 (48)		
	Epidermal Growth Factor	41.01 ± 6.52 (48)		
Acidic Extract	1:80	37.85 ± 5.84 (4)	0.998	1.000
	1:160	35.02 ± 8.52 (4)	0.700	0.965
	1:320	36.11 ± 12.42 (4)	0.900	0.997
	1:640	35.35 ± 7.79 (4)	0.852	0.990
	1:1280	34.79 ± 4.86 (4)	0.718	0.966
	1:2560	34.62 ± 11.89 (4)	0.689	0.957
	1:5120	35.46 ± 3.58 (4)	0.957	0.998
	1:10240	38.59 ± 4.53 (4)	0.996	1.000
Neutral Extract	1:80	39.89 ± 6.58 (4)	1.000	1.000
	1:160	33.63 ± 5.96 (4)	0.461	0.850
	1:320	35.16 ± 5.42 (4)	0.792	0.982
	1:640	35.99 ± 9.27 (4)	0.913	0.997
	1:1280	34.89 ± 6.84 (4)	0.735	0.970
	1:2560	42.32 ± 11.98 (4)	1.000	1.000
	1:5120	35.73 ± 4.84 (4)	0.967	0.999
	1:10240	39.54 ± 3.96 (4)	1.000	1.000
Basic Extract	1:80	37.93 ± 7.08 (4)	0.998	1.000
	1:160	35.98 ± 4.09 (4)	0.842	0.992
	1:320	30.47 ± 9.30 (4)	0.145	0.430
	1:640	34.18 ± 2.49 (4)	0.697	0.953
	1:1280	36.46 ± 2.86 (4)	0.921	0.998
	1:2560	35.92 ± 14.94 (4)	0.869	0.994
	1:5120	33.69 ± 2.56 (4)	0.832	0.978
	1:10240	36.67 ± 10.14 (4)	0.925	0.999

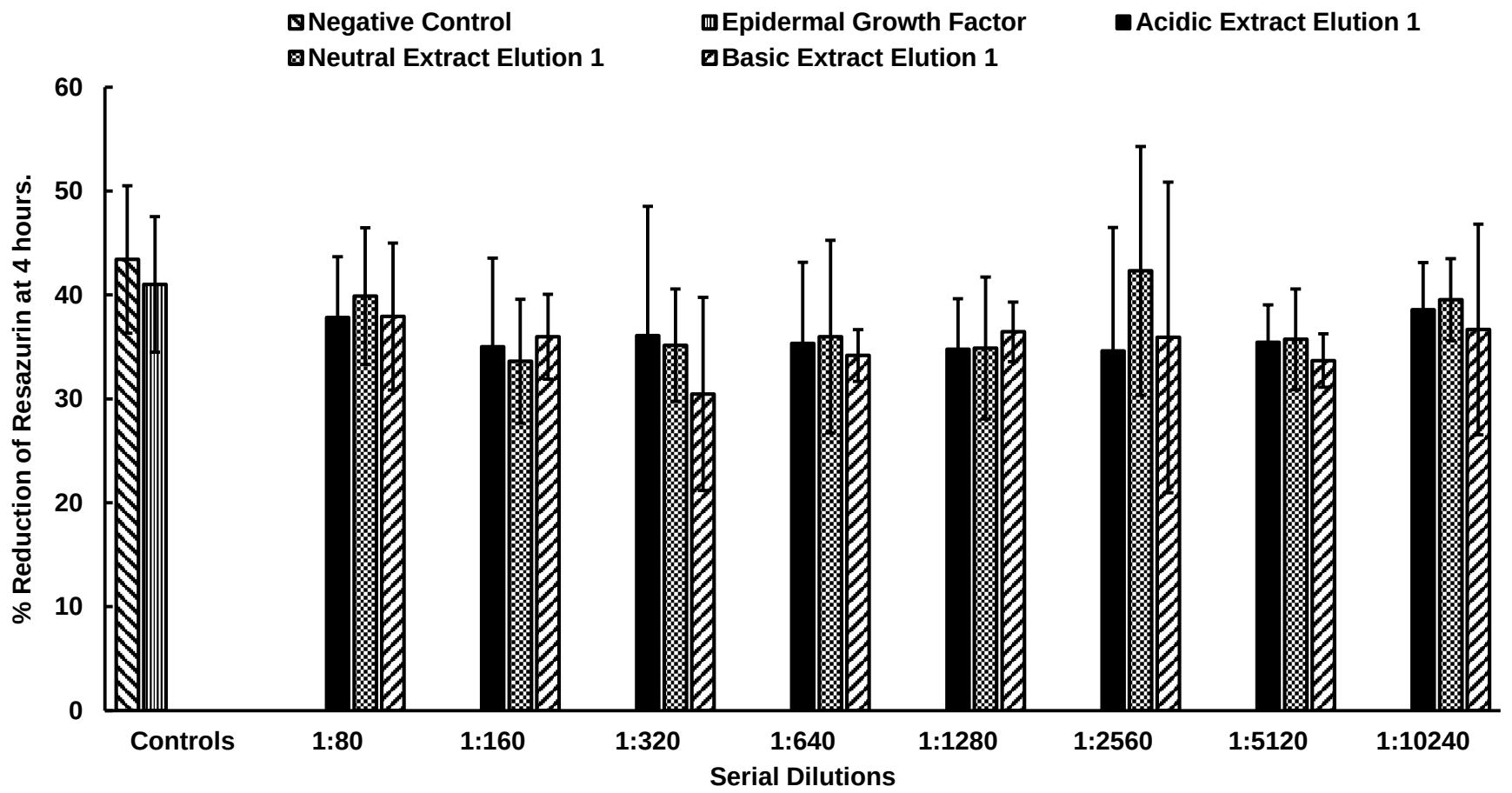


Figure 4.7. Graphical representation of the percentage reduction of the Elution 1 fraction at 4 hours post treatment. Each bar represents mean % reduction and the error bars represent the SD. No significant differences were detected. Each bar represents mean % reduction and the error bars represent the standard deviation.

Table 4.9. Percentage reduction of Elution 2 fraction of the acidic, neutral and basic extracts. Data are presented as mean ± SD (n). Corresponding comparisons between the negative control and EGF control were shown with p –values. Underlined p – values were significant.

Extraction	Dilution	% Reduction	Negative Control Comparison *p* - value	Epidermal Growth Factor Comparison *p* - value
Controls	Negative Control	43.42 ± 7.09 (48)		
	Epidermal Growth Factor	41.01 ± 6.52 (48)		
Acidic Extract	1:80	36.73 ± 4.51 (4)	0.581	0.875
	1:160	31.50 ± 3.96 (4)	0.030	0.136
	1:320	32.70 ± 5.68 (4)	0.098	0.324
	1:640	34.08 ± 4.10 (4)	0.191	0.501
	1:1280	34.52 ± 3.69 (4)	0.263	0.632
	1:2560	32.73 ± 6.14 (4)	0.257	0.625
	1:5120	34.66 ± 3.57 (4)	0.752	0.954
	1:10240	33.46 ± 5.27 (4)	0.247	0.619
Neutral Extract	1:80	39.69 ± 4.12 (4)	1.000	1.000
	1:160	64.10 ± 3.98 (4)	0.000	0.000
	1:320	63.29 ± 4.48 (4)	0.001	0.000
	1:640	57.25 ± 4.94 (4)	0.160	0.042
	1:1280	52.15 ± 4.68 (4)	0.389	0.123
	1:2560	59.14 ± 6.12 (4)	0.999	0.944
	1:5120	62.14 ± 9.48 (4)	0.998	0.949
	1:10240	50.14 ± 5.23 (4)	0.980	0.766
Basic Extract	1:80	55.25 ± 6.02 (4)	0.539	0.244
	1:160	57.01 ± 5.86 (4)	0.136	**0.029**
	1:320	51.28 ± 5.06 (4)	0.585	0.235
	1:640	54.52 ± 6.66 (4)	0.560	0.228
	1:1280	47.03 ± 6.70 (4)	1.000	0.993
	1:2560	51.96 ± 3.33 (4)	0.962	0.705
	1:5120	50.43 ± 6.50 (4)	1.000	0.996
	1:10240	46.90 ± 5.11 (4)	1.000	0.997

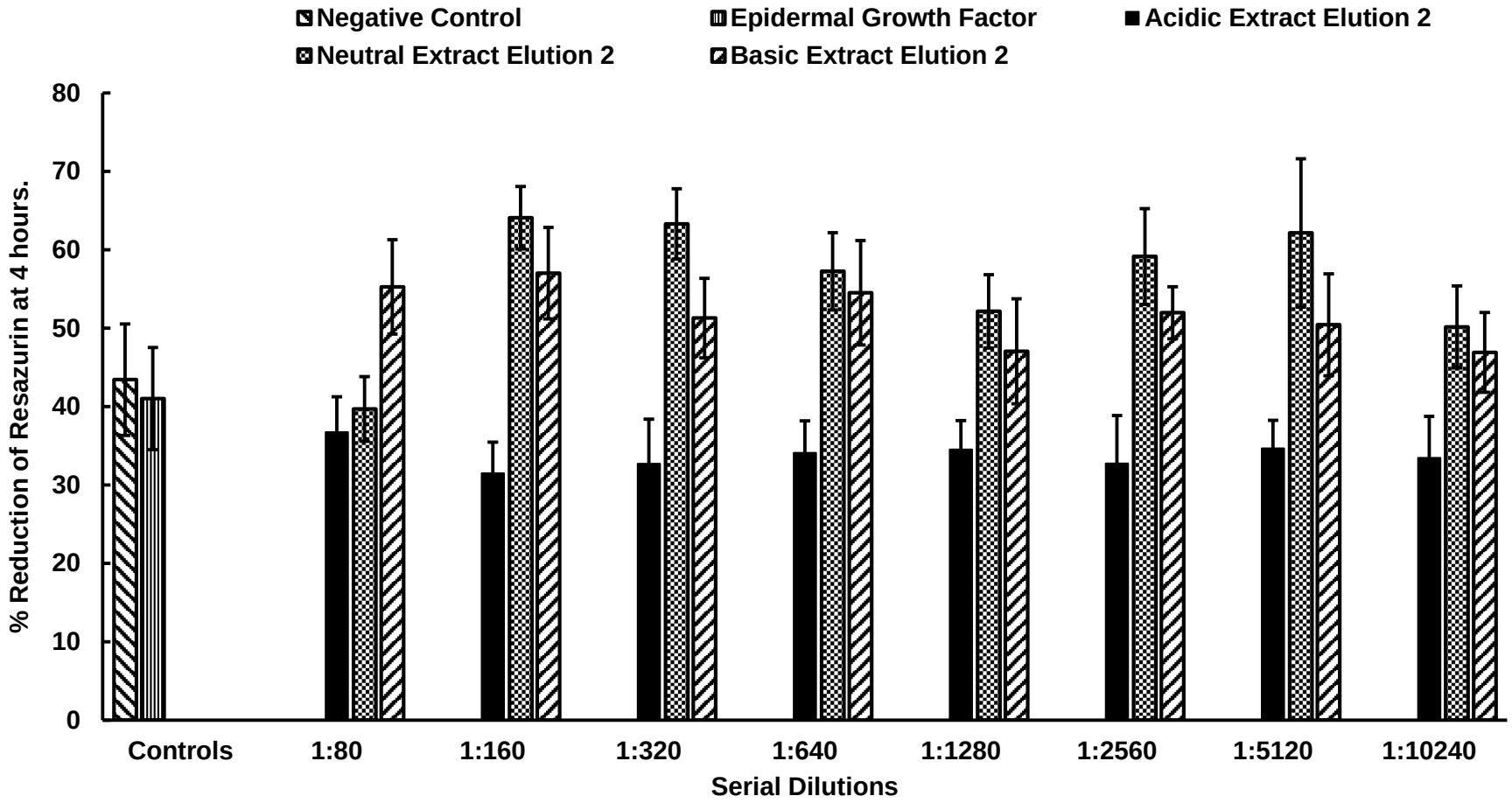


Figure 4.8 Graphical representation of the percentage reduction of the Elution 2 fraction. Each bar represents mean % reduction and the error bars represent the SD. No significant differences were detected. Each bar represents mean % reduction and the error bars represent the standard deviation. Significant differences were seen at the dilutions 1: 160, 1:320 and 1:640.

4.4.4 Real Time Proliferation Assay

The real time assay results (Table 4.11 and Figure 4.10) shows that the two fractions identified as potential leads have a significantly greater percentage reduction when compared to the controls at 4 hours. From the point of treatment (0 hours) the controls exhibit a period of delay after which at 2 hours the percentage proliferation starts to increase. The lead fractions exhibit no delay period and immediately start to increase. The lead fractions show a change in the rate of percentage reduction at 4 hours to reach an eventual end point at 12 hours equal to that of the controls.

When considering the first 4 hours and specifically the rate at which the cells are proliferating (Figure 4.11 and Table 4.12), the neutral and basic fractions have greater rates of proliferation when compared to the negative control (353% and 264% respectively) and the epidermal growth factor (383% and 286% respectively).

Table 4.10. Real time assay with the two fractions where activity was shown at 4 hours. Data are presented as mean ± SD (n). Corresponding comparisons between the negative control and EGF control were shown with p –values. Underlined p – values were significant.

Time			Basic Extract Elution 2			Neutral Extract Elution 2		
	Negative Control % Reduction	Epidermal Growth Factor % Reduction	% Reduction	Negative Control Comparison *p* = value	Epidermal Growth Factor Comparison *p* = value	% Reduction	Negative Control Comparison *p* = value	Epidermal Growth Factor Comparison *p* = value
0	29.22 ± 4.74 (6)	27.93 ± 3.98 (6)	19.48 ± 7.02 (4)	0.990	0.539	13.87 ± 2.18 (4)	0.690	0.170
2	31.69 ± 2.11 (6)	30.88 ± 2.82 (6)	35.68 ± 5.86 (4)	0.697	0.926	40.63 ± 2.42 (4)	0.689	0.930
4	43.42 ± 7.20 (6)	41.01 ± 6.21 (6)	57.01 ± 10.80 (4)	<u>0.001</u>	<u>0.001</u>	64.10 ± 1.38 (4)	0.136	<u>0.050</u>
8	63.96 ± 13.84 (6)	62.87 ± 13.24 (6)	74.07 ± 1.15 (4)	0.691	0.751	73.23 ± 3.20 (4)	0.750	0.493
12	89.70 ± 10.46 (6)	88.49 ± 10.96 (6)	91.38 ± 1.70 (4)	0.615	0.822	91.76 ± 3.98 (4)	0.570	0.783

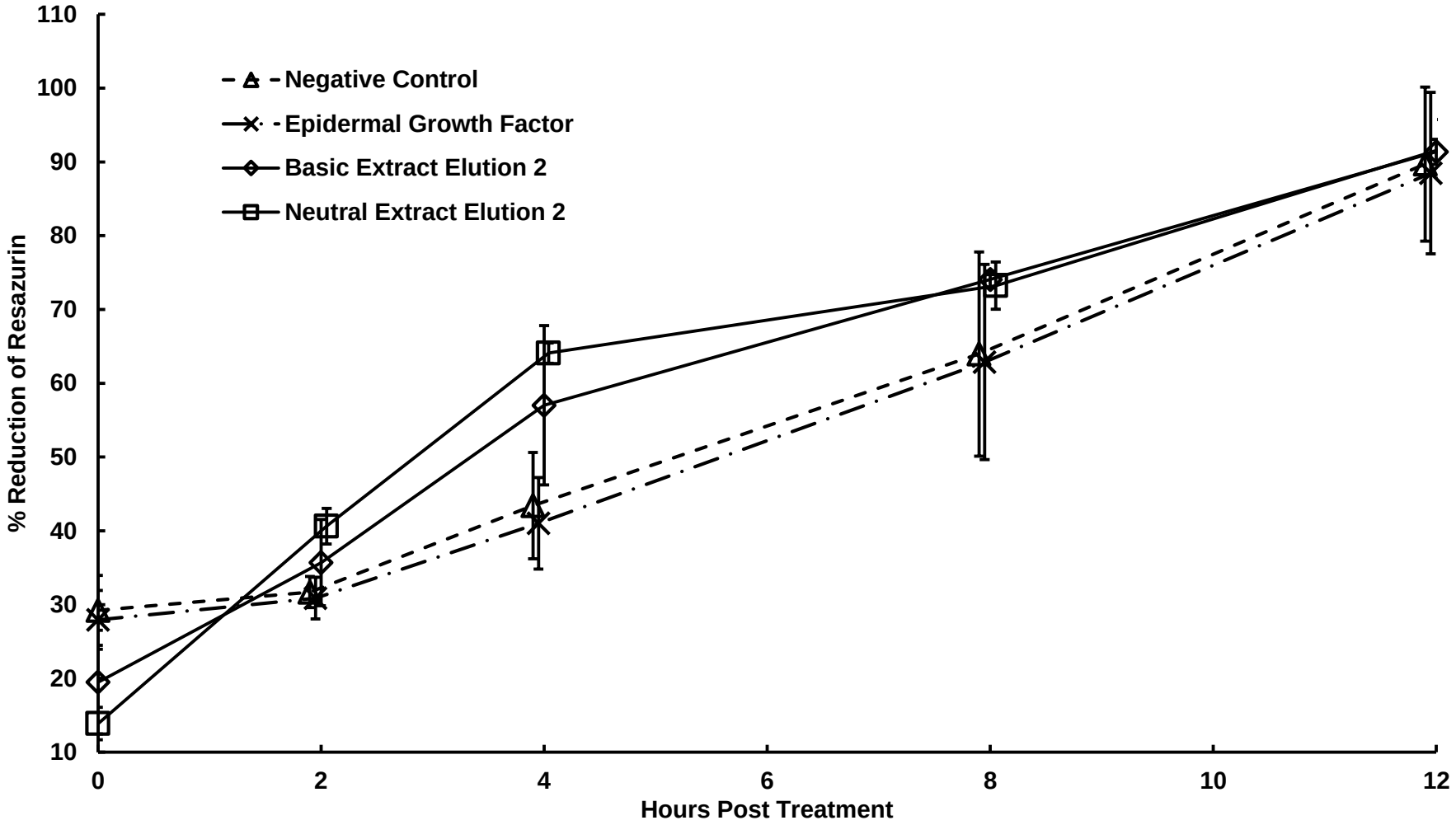


Figure 4.9. Real time assay of the two lead fractions compared to the controls. Means were plotted against hours post treatment. Markers represent the mean percentage reduction and the error bars represent the SD.

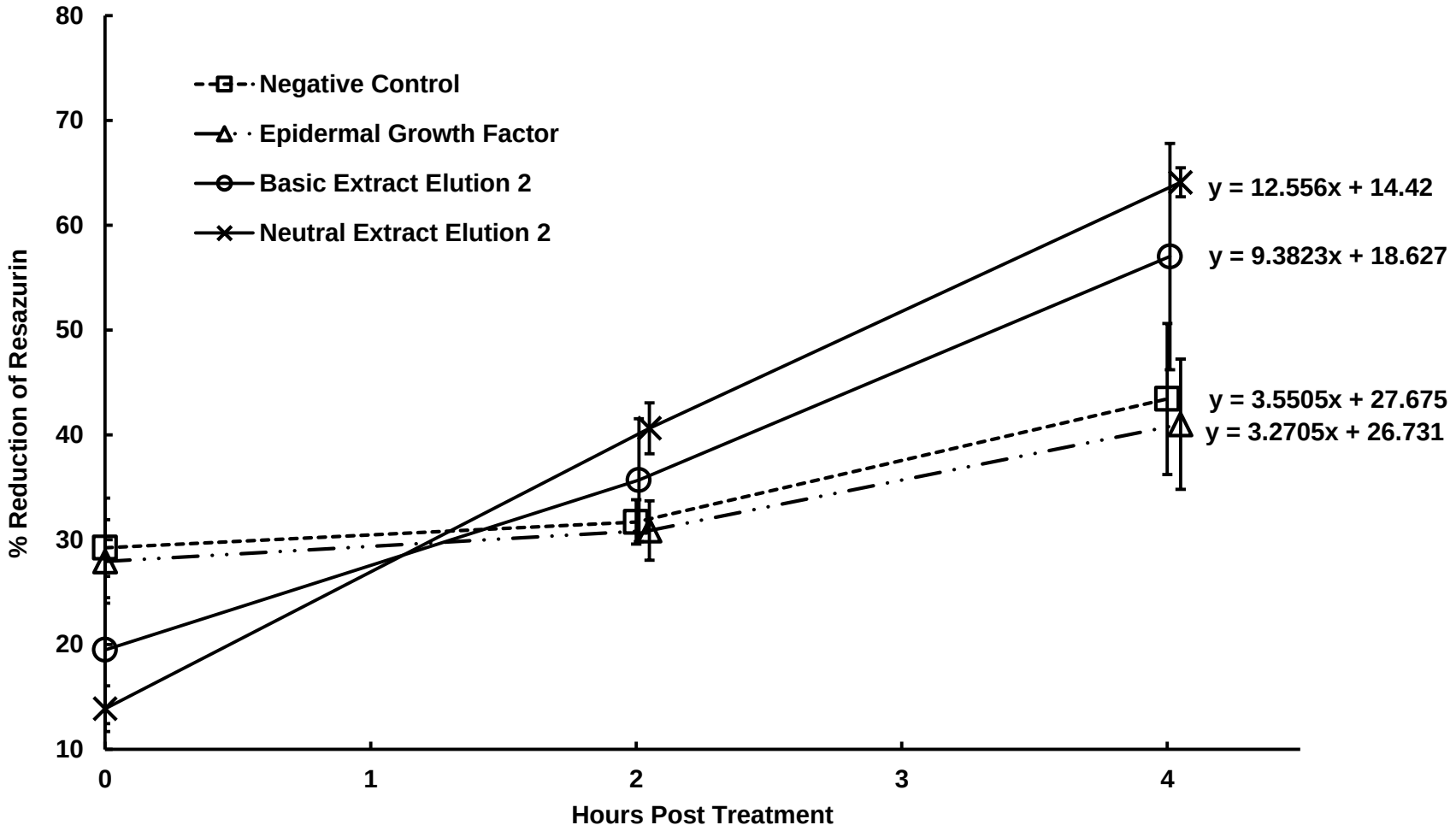


Figure 4.10. Analysis of the first 4 hours of the real time proliferation assay. Means were plotted against hours pot treatment. Markers represent the mean percentage reduction and the error bars represent them SD. Corresponding linear equations for each treatment are shown for further evaluation.

Table 4.11. Gradient and rate comparison of the fractions where activity was seen. The gradients shown here depict the rate of proliferation. Rates of proliferation were compared to both the negative control and epidermal growth factor and expressed as percentage of the relevant control.

Treatment	Equation	Gradient	Gradient Comparison of Extracts Compared to Controls (% of Control)	
			Negative Control	Epidermal Growth Factor
Negative Control	y = 3.5505x + 27.675	3.551		
Epidermal Growth Factor	y = 3.2705x + 26.731	3.271		
Neutral Extract Elution 2	y = 12.556x + 14.42	12.556	353.640	383.917
Basic Extract Elution 2	y = 9.3823x + 18.627	9.382	264.253	286.877

4.4.5 Gas Chromatography and Mass Spectrometry

The two fractions identified by the proliferation assays being the 2nd elution's of the neutral and basic extractions were further analysed by gas chromatography coupled with mass spectrometry. Gas chromatograms are seen in Figure 4.11 and Figure 4.12. Fragmentation patterns are seen in Table 4.12.

With the same GCMS run conditions, the neutral extract produced better peak separation and peak abundances when compared to the basic extract. In the neutral extract fraction, five peaks were identified as being significant and are labelled 1-5 in Figure 4.11. Corresponding peaks (based on retention time) of the basic extract fraction were labelled 6-8 in Figure 4.12 but peaks 3 and 5 were not identifiable in the basic extract fraction. Significant peak abundances in the neutral extract fraction ranged from 2×10^6 to 9×10^6 units compared to the basic extract fraction which ranged from 4×10^5 to 8×10^5 units.

The similarities between the 2 fractions were identified between the retention times of 18 and 25 minutes. The data produced for the parent ions (M) shows masses of 534.9, 539.3, 537.1, 538.9, 539.4, 493.0, 538.0 and 544.4 *m/z* for peaks 1 to 8 respectively. For simplification the

similar peaks were assessed based on base ions, similarities in the detected peaks, and parent ion indicated by the largest mass ion on the spectra.

At the retention time of 18.821 minutes, both peaks 1 and 6 have base ions of 199 *m/z*. Further similarities in the peak abundance (relative to base ion) are seen at 230, 135, 104, 76, 50 *m/z*. An additional peak at 253 *m/z* was noted in the basic extract fraction. The parent masses for these peaks are at 534.9 and 493.0 *m/z* for the neutral and basic extracts respectively indicating a difference of 41.9 *m/z*. Important fragmentation patterns are seen in peaks 1 and 6 with significant ions seen at 50, 76, 104 and 135 m/z with base ions at 199 m/z detected in both peaks.

At the retention time of 19.522 minutes, in peaks 2 and 7 both have base ions of 253 *m/z*. Similar peaks in the mass spectra can be seen at the ions 191, 64, and 48 *m/z* although the relative abundances are greater in the basic extract fraction at the ions 64 and 48 *m/z*. Additional peaks were noted in the basic extract at the ions 493, 346.1, 331.1, 301.1 and 269 *m/z*. The neutral extract had an additional ion at 207 *m/z*. The parent masses for these peaks are at 539.3 and 538.0 *m/z* for the neutral and basic extracts respectively indicating a difference of 1.3 *m/z*.

At the retention time of 20.047 minutes, peak 3 was detected in the neutral extract fraction but not the basic extract fraction. The fragmentation pattern here was the same as that of peak 2 with a base ion of 253 *m/z*. Differences were noted in the parent mass of 537.1 *m/z* and the abundance of the ion 207 m/z relative to the base ion was greater than that of peaks 2 and 7. Additional ions were detected here at 347.1 and 281 *m/z*.

At the retention time of 22.325 minutes peaks 4 and 8 were detected but were different. The base ions of the neutral extract was detected at 405 *m/z* and the basic extract detected at 301 *m/z*. The prominent ions in both fractions were detected at 405, 343.1, 64 and 48 m/z. In the neutral extract additional ions were detected at 373, 223, 131 and 119 *m/z* which were not present in the basic extract. The basic extract had additional ions detected at 389.1, 253, 191 and 135 *m/z*. The basic extract fraction had additional ions at 301 (base peak) and 156 *m/z*. The parent masses for these peaks were 538.9 and 544.4 *m/z* for the neutral and basic extracts respectively with a difference of 5.5 *m/z*.

At the retention time of 26.247 minutes peak 5 was seen in the neutral extract but not in the basic extract. Prominent base ions at 207 and 135.1 *m/z* were seen with a prominent ion at 472 *m/z*. Other significant ions were detected at 417. 64 and 48 *m/z*. The total parent mass ion was at 539.4 *m/z*.

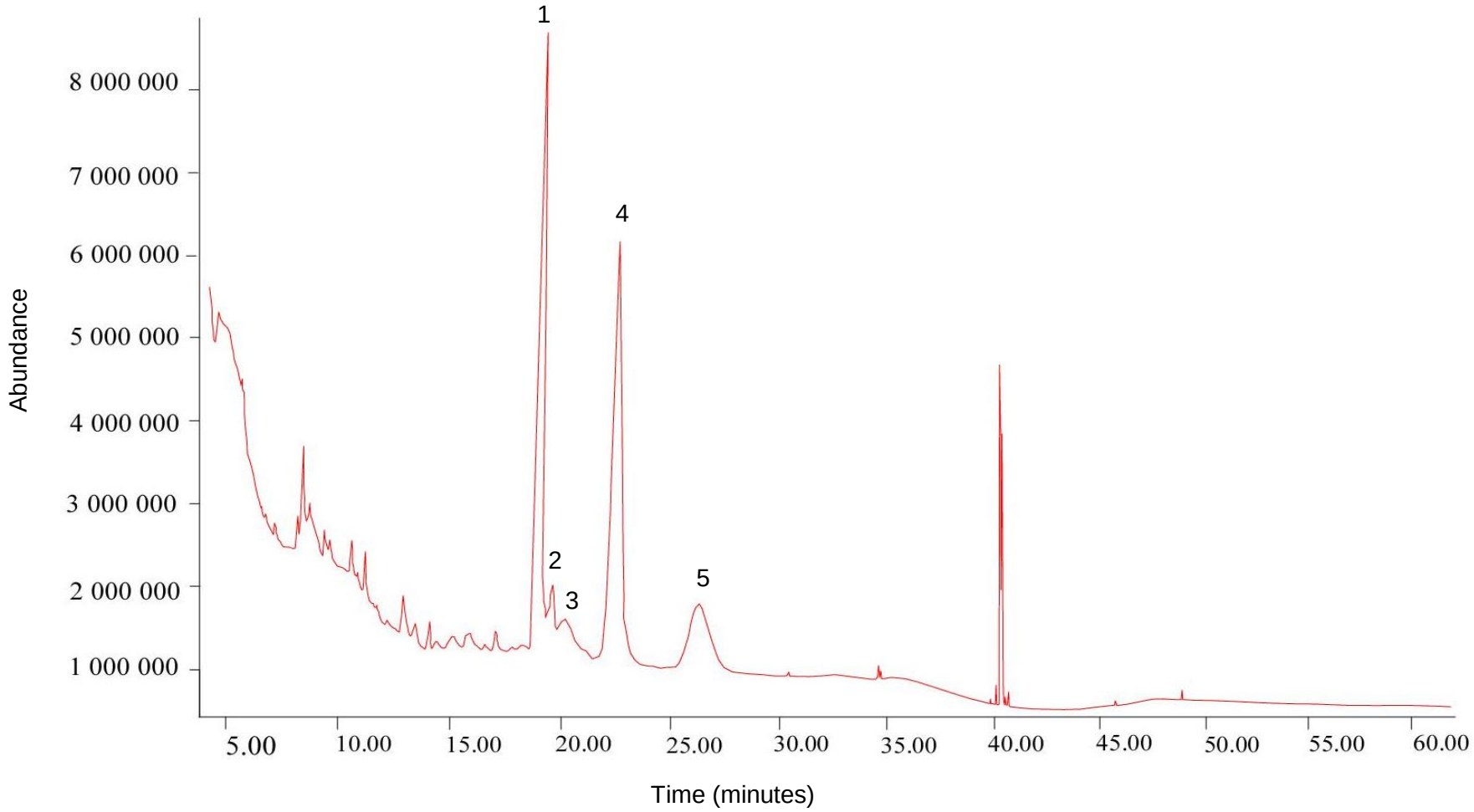


Figure 4.11. Gas chromatogram of the 2nd elution of the neutral extract. Significant peaks are labelled 1 – 5 on the chromatogram.

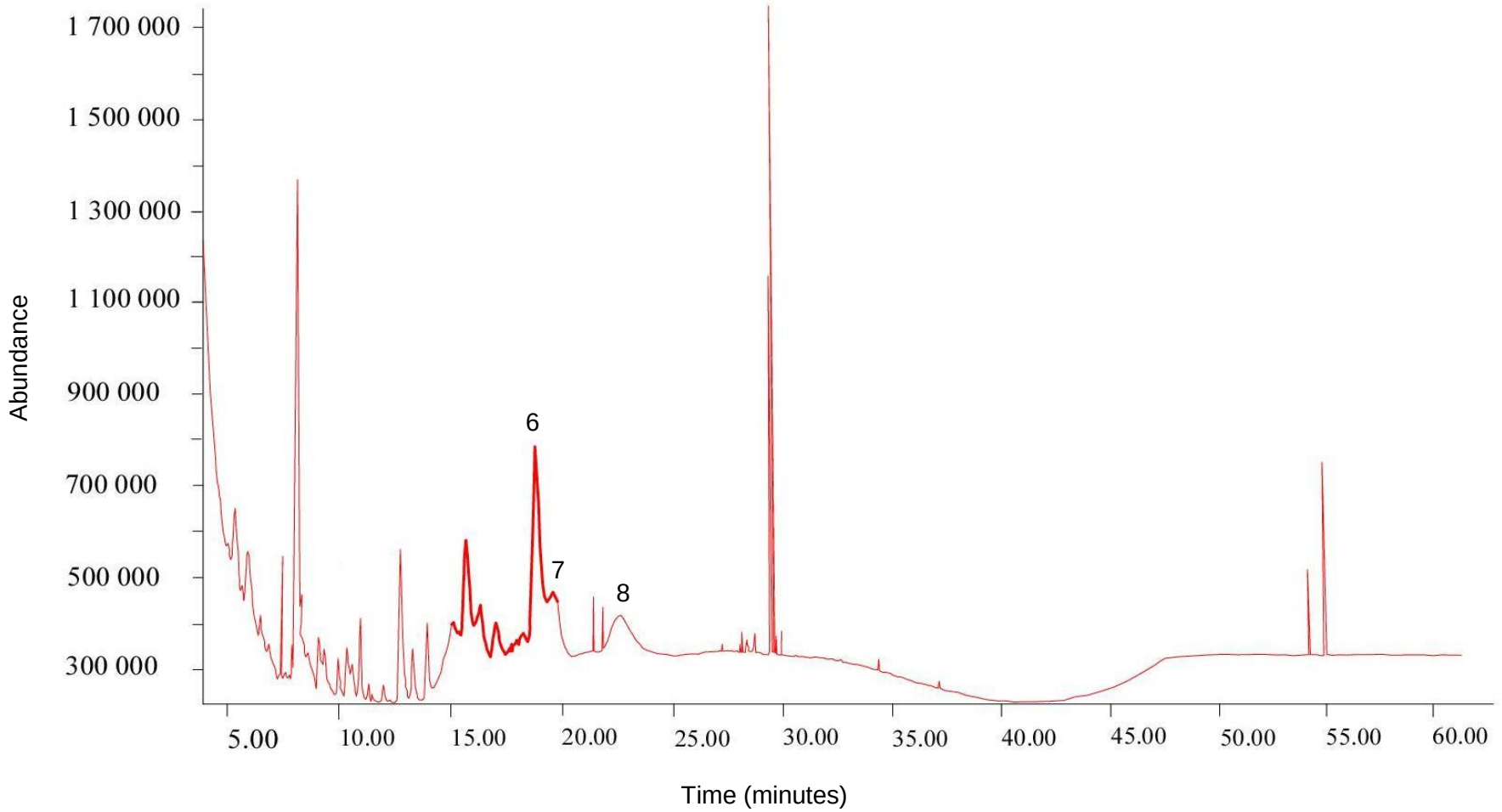


Figure 4.12. Gas chromatogram of the 2nd elution of the basic extract. Peaks labelled 6 – 8 are those correspond with the peaks identified in neutral extract. Peak 6 correlates with peak 1, peak 7 correlates with peak 2 and peak 8 correlates with peak 4. Peak 3 and 5 seen in the neutral extract were not detectable.

Table 4.12. GCMS results. Data presented – Extract either neutral or basic, Peak number corresponding to the labelled peaks in Figure 4.12 and Figure 4.13, Retention Time, Absolute Abundance, M or parent ion, and fragmentation pattern with the base ion bolded and underlined. M and fragmentation masses reported correspond with m/z. The fragmentation pattern for the pyrrolizidine and Isoquinoline type alkaloids are taken from the NIST database.

Extract	Peak Number	Retention Time (min)	Absolute Abundance	M	Fragmentation Pattern (Base ion is bolded and underlined)	(M+) - Base Ion
Neutral Extraction	1	18.821	9000000	*534.9*	*534,9 , 230 , **199** , 135 , 104 , 76 , 50,1*	335.9
	2	19.522	2200000	*539.3*	*539,3 , **253** , 207 , 191 , 64 , 48*	286.3
	3	20.047	1600000	*537.1*	*537,1 , 347,1 , 331,1 , 281,1 , **253** , 165,1 , 64 , 48*	284.1
	4	22.325	6300000	*538.9*	*538,9 , **405,1** , 389,1 , 343,1 , 253 , 191 , 135,1 , 64 , 48*	133.9
	5	26.247	2000000	*539.4*	539,4 , 417,2 , **207** , **135,1** , 64 , 48	332.4 / 404.4
Basic Extraction	6	18.821	800000	*493.0*	*493 , 253 , 230 , **199** , 135 , 104 , 76,1 , 50,1*	340.0
	7	19.522	500000	538.0	*538 , 493 , 346,1 , 331,1 , 301,1 , 269 , **253** , 191 , 165,1 , 91 , 64 , 48*	285.0
		20.047	Not detected			
	8	22.325	400000	544.4	544,4 , 405,1 , 343,1 , **301** , 156 , 64 , 48	243.4
		26.247	Not detected			
Pyrrolizidine Alkaloid Base Comparison					93-98 , 80-85 (**83**) , 67-70 , 52-58 (**55**) , 39-44 (**42**) , 27-30 (**28**)	
Isoquinoline Alkaloids Base Comparison					100-103 (**102**) , 74-78 (**76)** , 61-64 (**63**) , 50-52 (**51**) , 38-39	

4.5 Discussion

4.5.1 Cell Proliferation Assay

The extraction protocol followed here yielded multiple fractions based on the pH and relative solubilities of the wash and elution steps. Of the twelve fractions collected, two were seen to be efficacious based on the resazurin proliferation assay. The identified fractions were from the second elution steps of the neutral and basic extractions. Compared to the controls at 4 hours after treatment of the culture wells, the neutral extracts showed significantly greater percentage reductions of 64.1 ± 3.98% and 63.29 ± 4.48% (dilutions of 1:160 and 1:320 respectively) and the basic extracts showing percentage reductions of 57.01 ± 5.86% and 57.25 ± 4.94% (dilutions of 1:160 and 1:320 respectively) which was almost 20% greater than the controls.

With further experimentation over an extended observational period interesting differences were seen. The controls show a delayed response in that the percentage reductions here only increased appreciably after 2 hours. Compared to the identified fractions, the delay was not present and the treated cells exhibited an immediate increase in the reduction of the dye thereby bypassing the "lag" phase. Additionally, when the rate of proliferation was calculated, it was noted that the plant fractions increased the rate of proliferation by up to 380% when compared to the controls.

At the end of the observational period the percentage reductions were however equal but this is in keeping with the animal based assays where similar results were seen. Equal end points in experimental and controls was also seen in the work by Nagappan, *et al.* (31) which establishes the importance sequential measurements in a real time based assay which was achieved here.

Development of this assay was conducted with multiple controls to account for possible confounding factors. To establish the optimal time point for observation in mass experimentation, the negative control was run separately over a 12 hour observational period with a sequential increase in the percentage reduction noted. From this an optimal time period was identified at 4 hours after the cells where treated with a percentage reduction of 43.42 ± 7.2% close to 50% of the total amount of resazurin reduction that was possible.

The possibility of the plant fractions acting as possible reducing agents of the dye was also considered. At this optimisation stage, the fractions were shown not to affect the reduction of the dye. With the wells not having been seeded with cells, the percentage reduction was maintained at 30%. As there were no cells in the wells it was expected that the reduction of the dye should be 0% but this was not the case as was stated before however all the wells regardless of treatment and cells started at roughly the same point of around 20-30% reduction

and therefore the plant fractions were assessed as not being the cause of the reduction of the dye but rather the response of the cells to the plant fractions. It is currently unclear why the percentage reductions all started at 30% could be found.

With the confounding factors in mind, the assay results seen at 4 hours was sensitive enough to identify two lead fractions which were then followed up with further experimentation over a longer period of time converting the assay to a real time assay. With the evidence seen previously as being a good identification of the lead fractions, the real time assay revealed interesting trends which was seen with the loss of the lag phase. To our knowledge this has not been described before and is an interesting possibility when considering wound healing. It is also a possibility that the significant differences in percentage reduction seen at 4 hours was a product of the immediate proliferation induced by the plant fractions.

Importantly to the aims of this Chapter, the process of extraction and fractionation described here was found to be reproducible with scaling up of the procedure with large quantities of isolates being the eventual goal. Additionally an important aim achieved here is that 2 similar fractions were identified with the only difference being the pH at which they were initially extracted, all conditions were otherwise the same. For reasons unknown the acidic extracts second elution step did not show any activity.

Deductively any similar compounds identified between the active fractions should be the eventual molecules of interest. Here we have identified a number of similarities between the two fractions but the abundance obtained from each extraction differed and may be the reason for the differing proliferation assay results. It was shown that the neutral extract performed better compared to the basic extract but may be due to a concentration effect of the potential compounds. This is substantiated by a higher percentage reduction at the higher dilution of 1:180 of the basic extract (however not significant) compared to the neutral extract at the same dilution (55.25 ± 6.02 compared to 39.69 ± 4.12 respectively). At lower dilutions the neutral extract performed better (see dilutions 1:160 and 1:360) but at greater dilutions no effect was noted. This may be a toxic effect and further experimentation is warranted.

The assay developed here is not routinely performed for investigations concerning wound healing. As was previously stated, the most widely used approach is scratch assays, which are labour intensive and characterise the cell migration aspect of wound healing. The assay developed here is simple to perform making it highly reproducible, allows for real time applications and importantly can be applied to automated platforms for further development into a high-throughput assay.

Multiple advantages of conversion to a high-throughput assay exist. Firstly, by virtue of the fact that plants contain numerous potential lead compounds, they may be assessed quickly and efficiently with quantification of the effect as opposed to subjective assessments commonly seen in wound healing investigations. Secondly, there exists a possibility that other previously documented compounds existing in extensive databases may produce a similar effect which could be assessed singularly, in combination with other known compounds or used to augment the effects of the plant compounds that have been identified here.

4.5.2 Gas Chromatography and Mass Spectrometry

It is well known that members of the *Senecio* genus are known to contain pyrrolizidine alkaloids which prompted the search for a possible lead compound of this class. Significantly the report by Toma, *et al.* (144) identified this class as having a potential to promote healing however this was shown in the gastric mucosa of a rodent ulcer model. Additionally throughout the extraction process, the fractions where activity was shown where assessed for the presence of alkaloid type compounds by the use of Dragendorff's reagent. There is therefore a strong possibility that a pyrrolizidine-type alkaloid may be the reason for the beneficial effects noted in *Senecio* based therapy assessed here. The possibility that another compound type may also be of interest should not be ignored and therefore the extraction protocol followed here are not specifically aimed at isolating pyrrolizidine alkaloids but rather compounds with similar properties.

The choice of extraction and chromatographic techniques has varied considerably when alkaloids are concerned and even vary as to the various plant components from which they are isolated. Early descriptions of generic protocols were based on extractions performed with a chosen solvent followed by evaporation and protonation of the extract. From here the extracts were made basic with an alkali solution rendering the compound of interest insoluble in water. From here liquid-liquid extractions could be performed dissolving the compounds into a solvent with differing densities and polarities to that of the original extract and dichloromethane was commonly used.

Solid phase extraction protocols are now seen to be superior when isolating compounds from complex biological mixtures. Compared to the original liquid-liquid extraction techniques, solid phase extraction allows for faster processing times and higher isolate yields compared to the former but cost and extensive sorbent possibilities tend to be complicating factors (217). The use of this approach has mostly been seen in samples where the compound of interest was known and were used to identify and quantify the relevant compounds in samples. For

pyrrolizidine alkaloids specifically the packing sorbent material of the SPE cartridges is mostly strong cation exchange resins. This was used by Colgate, *et al.* (218) and Boppre, *et al.* (219) to identify pyrrolizidine alklaoids in food sources. Interestingly, Yoshimatsu, *et al.* (220) made use of the same cartridges that were used in this investigation, namely the hydrophobic-lipophilic (HLB) reverse phase based sorbent.

Ideally the sorbent material of the cartridges is selected based on the properties of the compounds of interest. An algorithm described by Zwir-Ference and Bizuik (221) shows that ideally water based extractions are best processed using cation or anion exchange resins once the extract is either acidified or alkalinised whereas neutral water and organic solvent extractions are mostly processed using phase dependent sorbent materials. Otherwisely described as separation based on polarity being more suited to phase dependent sorbent materials and charged based separations more suited ion exchange sorbent materials. The extractions of *Senecio* here*,* being either acidic, neutral or basic produced both of the previously mentioned scenarios. The acidic and basic extractions were most likely charged and therefore the ideal sorbent material should have been the relevant ion exchange resins. The neutral extract therefore performed better on the HLB reverse phase material and this may be a reason for the differing results obtained from the gas chromatography and mass spectrometry.

In theory, selection of the appropriate sorbent material is based on prior knowledge of the analyte of interest making the use of solid phase extraction controversial when used in the context of this investigation. To counteract this problem the use of the HLB cartridges allowed for a wider range of polarities to be isolated. According to the manufacturers insert, protocols have been designed to accommodate acidic, neutral and basic extractions. Also important to these experiments was the ability of the packing materials to tolerate water as the mobile phase for loading the samples. As the initial extractions were water based, there was no necessity to evaporate the samples to suspend them in organic solvents thus minimising sample processing steps and losses.

Literature concerning the chromatographic separation of plant extractions describe liquid chromatography as the technique of choice. This was seen in the study of *Murraya koenigii* (31) which is one of the few reports concerning alkaloid isolation for the use of wound healing. Again the work concerning *Daphne oleoides* (44) also employed the use of liquid chromatography to identify potential lead compounds. The use of chromatography with regards to wound healing has led to significant compound identification and so was considered ideal for the work described here.

This investigation included gas chromatography and mass spectrometry to characterise the compounds present in the extract fractions. Gas chromatography was preferred due to its advantages over liquid chromatography when analysing complex unknown mixtures but may not be the best option for pyrrolizidine alkaloids detection as further derivitisation techniques may be indicated (222). Nevertheless, reports of the use of gas chromatography for pyrrolizidine alkaloids have been reported in identification of toxic PA's in *Senecio cineraria* (223) and selected *Senecio* species from Egypt (224). In these instances a crucial step was included which was the reduction of the extracts using zinc powder which results in the reduction of the N-oxide form (which cannot be analysed on GCMS) to the free base form. The importance of this step is seen in the relative concentrations of these forms being roughly 90% of the N-oxide form and 10% of the free base form therefore allowing greater detection of pyrrolizidine alkaloids (225). As the fractions analysed here were largely unknown, omission of the derivitisation step was permissible.

The identification of potential compounds present in the plant was a partial success. Firstly as it was theorised that if multiple fractions elicite a certain reaction (i.e. keratinocyte proliferation), then the compounds that are similar within those fractions should be the compounds of interest. In these experiments, the compounds that were most similar were those seen in peaks 1 and 6. The similarities recorded here was the retention time, base ion, and fragmentation patterns. No other similarities were noted between the other identified peaks and therefore the possibility that peaks 1 and 6 contained the compound/s of interest was greatly supported.

Investigations of this nature typically aim to characterise the compounds with a molecular formula and structure as the end point. However mass spectrometry is not sufficient to achieve this and therefore further investigation such as nuclear magnetic resonance would be indicated. The goal of mass spectrometry would be to identify a compound based on reference spectra but as discussed previously this may be problematic when unknown samples are investigated. The mass spectra produced here were not identifiable on the NIST database, which may be advantageous as unknown compounds are promising for potential patents.

Possibly the most important question here is whether the compounds/peaks identified here are in fact pyrrolizidine alkaloids. As was previously stated, the pyrrolizidine alkaloids have characteristic mass spectra with a characteristic ion at 80/82 *m/z* depending on the saturation of the necine base with additional features that include the triplet fragments of 93-95, 119-121 and 136-138, none of which were evident in any of the identified peaks which suggests that the compound of interest may not be a pyrrolizidine alkaloids.

An important feature seen here was that the parent mass ions identified in the peaks where in the order 500 + *m/z*. The potential that the molecular mass of the compounds could be a general indicator as to the possibility that these compounds are not pyrrolizidine alkaloids was not substantiated as selected reports have shown a wide range in the parent masses of pyrrolizidine alkaloids. Witte, *et al.* (1993) reported extensively on about 100 different pyrrolizidine alkaloids with a range in parent masses extending from 155 *m/z* up to 483 *m/z*. Colgate, *et al*. (218) identified pyrrolizidine alkaloids in *Crotalaria juncea* with mass ions of up to 360 *m/z* with the presence of the characterisitc fragmentation ions. Boppre, *et al.* (219) characterised multiple pyrrolizidine alkaloids from commerically available honey extracts and showed that the masses of these compounds ranged from 380 *m/z* up to 500 *m/z*.

The work by Witte, *et al.* (226) documents of pyrrolizidine alkaloids extensively, based on separation by gas chromatography and identification by mass spectrometry, based on the retention time and mass ions. These important features provided adequate comparison here. Additionally they documented the use of a DB-5 column, which was used in the experiments reported here. In comparing retention times and mass ions, no similarities in any of the peaks were identified thereby reducing the possibility of the presence of pyrrolizidine alkaloids in the plant fractions analysed here.

The fragmentation patterns obtained here do provided information as to the potential class of compounds. From the peaks identified here it was seen that peaks 2, 3, 4 and 8 did not show any similarities with the alkaloid base fragmentation paterns identified in the NIST database but their potential as compounds of interest cannot be excluded.

Peaks 1 and 6 display similar fragmentation patterns with the potential that these are the same compounds. Additionally examination of the fragmentation patterns is not in keeping with any data consistent with pyrrolizidine alkaloids. The possibility therefore is that that the peaks identified here may be another type of alkaloid and comparrisons with the NIST data (table 1 and again in table 8) shows similarities with the isoquinolone type alkaloid bases, an important class due to the examples here being morphine and codeine normally extracted from the *Papaveraceae* family (227).

Although the bases show significant similarities between each other and with the bases identified in the NIST database, it was difficult to compare published data, as other mass spectrometric approaches were employed. Wu-Nan and Cheng-Hong (228) used ion spray tandem mass spectrometry to assess the various isoquinolone, benzylisoquinoline, aporphine and phenanthrene alkaloids. Schmidt, *et al.* (227) used tandem mass spectrometry to analyse these types of alkaloids but with atmospheric pressure photoionisation. Although the

experiments here did not use tandem mass spectrometry, similarities could be seen in the base peak ions occuring in the 180-200 ranges similar to what was seen in this investigation but the base ion of 199 *m/z* and mass ions could not be found in published reports concerning alkaloids.

With the speculation as to the possible types of compounds that have been identified, it is not certain as to what class of alkaloid could be exerting the effects seen in the *in-vitro* assays. It is clear that further isolation of the identified peaks is necessary and from this point the *in-vitro* assays would need to be repeated to identifiy the compound/s of interest. Further characterisation of the compound can be done using other modalities such as nuclear magnetic resonance.

4.6 Conclusion

The approach adopted here is different to that reported in the literature. In this investigation we used a porcine model to establish if efficacy indeed existed. *In-vitro* experiments were then used to further establish the efficacy and serve as an assay when fractionating the plant. The use of keratinocytes allowed for the development of an *in-vitro* assay that led to the identification of two potential active fractions. Furthermore the assay described here has the potential for high throughput applications. Analysis of these lead fractions by gas chromatography and mass spectrometry did not identify the pyrrolizidine alkaloids reported in the literature, but another class of alkaloids was identified which requires further characterisation.

With the aims of this project defined in Chapter 1, it was clear that multiple questions needed to be answered in order to accomplish the aims. It was clear that minimal information was present regarding the plant and moreover the effect that it could potentially have on the process of wound healing was largely if not completely unknown. Additionally, the wound healing process is extremely complex with multiple variables present and important at different phases throughout the process. This makes it particularly challenging to identify a mechanism through which potential agents may work. The project was therefore divided into Chapters dealing with: 1) efficacy and safety, 2) mechanistic investigation and 3) plant fractionation and assay development.

5.1 Efficacy and Safety

It was therefore decided that the first phase in this project would establish efficacy and safety; key concepts that needed to be proven as motivation for subsequent experimentation. This phase required *in-vivo* experimentation, mostly due to the complexities of wound healing being poorly translated into *in-vitro* experimentation. A porcine model was used with deep partial thickness and full thickness wounds created on the animal's dorsum. The reason for using deep partial thickness wounds lies in the traditional healer's indication being for superficial cuts and abrasions. However the addition of full thickness wounds was to provide important information that could not be obtained from the deep partial thickness wounds.

The information obtained from the deep partial thickness wounds included wound pH and epidermal thickness. The information obtained from the full thickness wounds included keratinocyte migration and wound contraction. An image analysis algorithm was also devised to assess the collagen production within both kinds of wounds, with a method which is believed to be novel, as opposed to the traditional colorimetric approaches.

The plant under investigation here is known colloquially as the "*2 day cure*" but its potential was only seen at day 5 post-operative by gross inspection. With clear differences seen at this time point it was necessary to quantify these differences in the most objective approach possible hence the development of the algorithms employed to describe and quantitate the elements of the wounds. It is believed that this is still a general approach to assess the efficacy of the plant but it was necessary to determine the viability of further investigations.

The wound pH was seen as a variable that describes the overall functionality of the regenerated skin. This concept is based on the presumption that normal intact skin maintains a specific pH. In general there were no major differences noted between the treatment groups

but interestingly, the wound pH in all treatment modalities stabilized at a later time point compared to when the epidermis was in situ. This suggests that that the physiological functionality of the skin was established at a time point later than when the perceived anatomical integrity was established.

The only difference in wound pH was at day 2 post-operative where the plant had a significantly lower pH as compared to the controls and the reason for this is not quite clear. Catabolic events may have contributed to this altered pH, but without objective evidence for this, the issue remains unsolved and may be a potential point of interest for further investigation. The advantage of the wound pH measurement lies in its simplicity and minimal invasiveness of the approach which may have both experimental and clinical applications.

Assessment of the epidermal thickness has not been commonly determined in wound healing investigations. Furthermore in this investigation a novel parameter, epidermal thickness ratio was determined to compare the epidermal thickness relative to the unwounded skin. In this instance it was necessary as the model included deep partial thickness wounds and minimal wound contraction would be expected. Interestingly the scenario that came to light included the epidermal thickness, which showed extensive thickening of the epidermis in the *Senecio* and activated carbon treated wounds but not in the negative control treated wounds. However, when the wounds were adjusted for regional variation of the thickness of the dorsal skin, this was not evident.

Controlling for regional skin thickness appears to have a great effect on the data as it could be seen that in the negative control treatment group, the epidermis did not thicken compared to the other treatments. It would therefore suggest that normal wound healing without the application of any therapy would not show the thickening followed by thinning of the epidermis. When the epidermal thickness ratio was considered, the process of thickening and thinning was more apparent in the negative control treated wounds. It is possible that the normal skin in the negative control groups was just naturally thinner. Important in this evaluation was the time point at which the skin thickness peaked which was 2 days before that of the controls. This therefore suggests that proliferative events occurred at an earlier point in time compared to the control groups.

The collagen content of the wounds was assessed which was seen to be similar within all treatment groups and regardless of the wound type. However the approach devised here was novel and requires further validation, but it could be seen as more sensitive when compared to the previously reported colorimetric and histological approaches reviewed in Chapter 1. Furthermore it is not subject to observer error as in the score based histological approaches

and secondly the potential for assaying normal skin is reduced as compared to the colorimetric approaches.

The issue of whether the plant is safe as a topical agent for wound healing was partially addressed here with liver function tests throughout the observational period and liver biopsies one month after the observation period. The liver function tests were deranged at some points in the observation period but histologically no evidence of hepato-toxicity could be detected. The topical administration of the plant is possibly the reason for why there was no toxicity detected histologically. Topical application of the plant compounds bypasses the gastro-intestinal system where the acidic pH of the stomach converts pyrrolizidine alkaloids to their free n-oxide bases, which are the molecules responsible for hepatotoxicity. It is however possible that the quantity of plant material that the pigs were exposed to was insufficient to elicit a toxic response and would require further investigation, but with the lead fractions or compounds.

5.3 Mechanistic Investigation

Attempts were made to identify a pathway by which the plant exerted it activity on the keratinocytes that were identified from the experiments in Chapter 2. In terms of the phases of wound healing, the phases that theoretically coincide with the differences noted in Chapter 2 (around days 5 -7) are the inflammatory and proliferative phases. Although this narrows down the potential targets for investigation, it is still extremely broad due to the multiple factors seen in each of these phases.

Assessment of the inflammatory phase focused on the inflammatory cytokines with the addition of the anti-inflammatory cytokine, IL-10. A limitation of this study was that few of these factors were determined. They only represent the messengers present within the wound and not the cellular components that react to or produce the messengers. However they may identify the state of the wound being either pro-inflammatory or anti-inflammatory. This designation should be made relative to the negative control treated wounds, as this is the natural course a wound should follow.

Compared to the negative control treated wounds at day 5 post-operative, it appeared that the activated carbon treated wounds displayed more of a pro-inflammatory status with elevated levels of IL-8, 1β and 6 together with an increase in the anti-inflammatory interleukin-10, but these concentrations were not significantly different. In the *Senecio* treated wounds, a similar picture was seen but the anti-inflammatory interleukin-10 was not as raised, suggesting the elevated pro-inflammatory cytokines may be necessary to the wound healing process. However in the case of the *Senecio* treated wounds a significantly raised interleukin-1β

concentration was seen compared to the negative control treated wounds. Interestingly interleukin-1β is known to play roles in induction of keratinocyte and fibroblast proliferation, fibroblast synthetic functions and keratinocyte migration. The above mentioned roles associated with interleukin-1β added to the possibility that the *Senecio* based therapy exerted its effects through keratinocyte proliferation.

Important to this investigation was the effects that pyrrolizidine alkaloids have on epidermal growth factor (EGF) that was shown by the work of Toma, *et al.* (134). Again the role of this growth factor is significant but it is well known that multiple growth factors beneficially affect wound healing to the extent that certain factors are currently approved for human therapeutic intervention. Of significance is that many of these growth factors, including various cytokines bind to their respective receptors and induce tyrosine phosphorylation, thereby identifying a common link to many of the factors.

The levels of tyrosine phosphorylation and resultant keratinocyte proliferation were assayed through immunofluorescence staining techniques. It was seen that the plant induced sustained cellular proliferation through increased tyrosine phosphorylation although. Additionally the initial increase from day 5 to 7 was much greater in the *Senecio* treated wounds compared to the controls. The possibility remains that other signalling events may also play a role in the sustained proliferation reported here due to the fact that the difference between the plant and negative control group was negligible. Again there is also the possibility that interleukin-1β is playing a role here.

The effects of ligand tyrosine phosphorylation are mostly mediated through various signalling cascades which were not assessed. Future investigations will be aimed at identifying the possible pathways that are activated by the plant in question through micro-array based assays. These can identify multiple signalling cascades which are important as the activation of many of these cascades simultaneously is a very real possibility. This may allow for future interventions where the cascades may be preferentially activated within a wound.

The level of proliferation from day 5 to day 9 post-operative was seen to decrease in the control treated wounds but in the *Senecio* treated wounds the levels were sustained which may be the reason for the increased epidermal thickness and ratio seen in Chapter 2. The reason for the decrease seen in the controls is unknown at this point but because the assumption that the negative control represents the normal wound healing process, this may be the normal response of keratinocytes.

The fact that at day 2 post-operative the epidermis was absent and but present by day 5 shows that important time points were missed. In the initial efficacy experiments in Chapter 2, this was not seen to be of any significance but at this stage there was a deficiency in the tyrosine

phosphorylation and cellular proliferation data. This is a point to be addressed in future investigations but is more appropriate once an active or lead compound is identified and isolated. However the investigations here did help identify a target for the identification and isolation of potential compounds.

5.4 Plant Extraction and Culture

It was clear that keratinocyte proliferation was the target that needed to be exploited to identify potential lead fractions/compounds. The prior experiments conducted, looked at broad events seen in wound healing from where was possible to narrow down to a quantifiable target. Additionally the advantage of this was that high-throughput assay modalities could be considered. This was due to the nature of plant-based investigations leading to multiple potential compounds/fractions. Additionally, compound databases could be accessed to produce the same effects or augment the effects of other compounds.

Initially it was suspected that pyrrolizidine alkaloids may be the class of compounds of interest to this investigation, but isolating only these compounds may be extremely naïve as previous plant based investigations by a number of authors have shown that many different compounds are beneficial to wound healing. It was therefore decided that extraction protocols employed should not be specific for pyrrolizidine alkaloids but should allow for extraction of multiple potential compounds. For this reason the extraction procedure used here with the chosen solid phase extraction cartridges allowed for the fractionation of the plant extracts based on chromatographic principles and provided extracts with as many potential compounds as possible. Additionally this approach was seen to be easily reproducible through commonly established protocols.

Once multiple fractions are produced, it is commonplace to analyse these fractions for the possible compounds that are present. It was decided that a more goal directed approach to optimize time and resources was to identify the fractions that show proliferative activity and thereafter analyse the fractions for possible lead compounds. With keratinocyte proliferation identified as the target for further investigation, the assay chosen to conduct these experiments was real time, resazurin-based proliferations. With the introduction of real time assays it was shown that two fractions were able to significantly increase the level and rate of cellular proliferation, up to 380%, an observation that would quite likely have been missed had traditional approaches been used.

The advantage of developing this assay for this application is that it is highly amenable to high-though put assays for the reasons previously mentioned. Additionally the resazurin-based assay demonstrated here is extremely compatible with automated culture systems. It is

important to state that the culture experiments conducted here were not high-throughput assays by strict definition, but did provide the framework for further development and application.

Analysis of the identified fractions was conducted using gas chromatography and mass spectrometry allowed for the identification of a potential alkaloid class. Additionally these compounds were not identifiable on the NIST database. The presence of pyrrolizidine alkaloids in this plant was not confirmed and still needs to be considered in future investigations.

The identification of two active fractions allowed for comparison between the fractions. An assumption was made that similar compounds would be present in both of the fractions were potentially the compounds of interest. Here a compound was identified in both fractions based on retention time and spectral fragmentation patterns. The fragmentation pattern of the lower mass to charge ratios was more in keeping with the Isoquinoline type alkaloids than to the pyrrolizidine type alkaloids and may be class of compounds of interest.

Future investigations will focus on the identified peaks seen here. These would be isolated further and tested using the developed proliferation assay. Animal models would be required to confirm the efficacy of the lead compounds. Furthermore the isolated compounds would be further characterized using physicochemical techniques.

1. Landro L. The burgeoning market for wound care. [Online].; 2012 [cited 2012 December 27. Available from: http://blogs.wsj.com/health/2012/04/16/a-burgeoning-market-for-wound-care/.

2. Sen C, Gordillo G, Roy S, Kirsner R, Lambert L, Hunt T, et al. Human skin wounds: A major and snowballing threat to public health and the economy. *Wound Repair and Regeneration*. 2009; 17(6): p. 763-771.

3. Muthu C, Ayyana M, Raja N, Ignacimuthu S. Medicinal plants used by traditional healers in Kancheepuram district of Tamil Nadu, India. *Journal of Ethnobiology and Ethnomedicine.* 2006; 2(43): p. online publication: http://www.ncbi.nlm.nih.gov/pmc/articles/PMC1615867/.

4. Calixto J. Efficacy, safety, quality control, marketing and regulatory guidelines for herbal medicines. *Brazilian Journal of Medical and BIological Research*. 2000; 33(2): p. 179-189.

5. Andrade-Cetto A. Effects of medicinal plant extracts on gluconeogenesis. *Botanics:* Targets and Therapy. 2012; 2: p. 1-6.

6. Mukherjee P, Ponnusankar S, Venkatesh P. Synergy in herbal medicinal products: concept to realisation. *Indian Journal of Pharmaceutical Education and Research.* 2011; 45(3): p. 210-217.

7. Accesswire-TNW. Investment ideas in the expanding wound care market. [Online].; 2013 [cited 2013 December 26. Available from: http://www.marketwatch.com/story/investment-ideas-in-the-expanding-wound-care-market-2013-05-17.

8. Kumar B, Vijayakumar M, Govindarajan R, Push S. Ethnopharmacological approaches to wound healing – exploring medicinal plants of India. J*ournal of Ethnopharmacology.* 2007; 114: p. 103-113.

9. Pather N, Viljoen A, Kramer B. A biochemical comparison of the in vivo effects of *Bulbine frutescens* and *Bulbine natalensis* on cutaneous wound healing. J*ournal of Ethnopharmacology*. 2011; 133: p. 364-370.

10. Pather N, Kramer B. *Bulbine Natalensis* and *Bulbine Frutescens* promote cutaneous wound healing. *Journal of Ethnopharmacology.* 2012; 144: p. 523-532.

11. Wong V, Sorkin M, Glotzbach J, Longaker M, Gurtner G. Surgical approaches to create murine models of human wound healing. *Journal of Biomedicine and Biotechnology*. 2010; 2011.

12. Galiano R, Michaels J, Dobryansky M, Levine J, Gurtner G. Quantitative and reproducible murine model of excisional wound healing. *Wound Repair and Regeneration.* 2004; 12: p. 485-492.

13. Sullivan T, Eaglstein W, Davis S, Mertz P. The pig as a model for human wound healing. *Wound Repair and Regeneration.* 2001; 9: p. 66-76.

14. Fikru A, Makonnen E, Eguale T, Debella A, Mekonnen G. Evaluation of in vivo wound healing activity of methanol extract of *Achyranthes aspera L. Journal of Ethnopharmacology.* 2012; 143: p. 469-474.

15. Annan K, Houghton P. Anti-bacterial, antioxidant and fibroblast growth stimulation of aqueous extracts of *Ficus asperifolia Miq.* and *Gossypium arboreum L.*, wound healing plants of Ghana. *Journal of Ethnopharmacology.* 2008; 119: p. 141-144.

16. Olugbuyiro J, Abo K, Leigh O. Wound healing effect of *Flabellaria paniculata l*eaf extracts. *Journal of Ethnopharmacology.* 2010; 127: p. 786-788.

17. Steenkamp V, Mathivha E, Gouws M, van Rensburg C. Studies on antibacterial, antioxidant and fibroblast growth stimulation of wound healing remedies from South Africa. *Journal of Ethnopharmacology.* 2004; 95: p. 353-357.

18. Ogwang P, Moses A, Omujal F, Tumusiime H, Kyakulaga A. Preclinical efficacy and safety of herbal formulation for management of wounds. *African Health Sciences.* 2011; 11(3): p. 524-529.

19. Mawera G, Mutseeka D, Nyazema N, Asala S. Effects of an ashed (MEND) powder on deep wound healing: a prelimenary study in guinea pigs. *East African Medical Journal*. 1997; 74(8): p. 495-498.

20. Zhao D, Shi W, Zhang P, Zhang C. Effects of Shibao powder on promoting the expression of b-FGF and TGF-beta1, in the repair of soft tissue injuries. *Zhongquo Gu Shang*. 2008; 21(9): p. 667-668.

21. Wang J, Ruan J, Cai Y, Luo Q, Xu H, Wu Y. In vitro and in vivo evaluation of the wound healing properties of *Siegesbeckia pubescens*. *Journal of Ethnopharmacology*. 2011; 134: p. 1033-1038.

22. Shailajan S, Menon S, Pednekar S, Singh A. Wound healing efficacy of *Jatyadi Talia*: In vivo evaluation in rat using excision wound model. *Journal of Ethnopharmacology.* 2010;: p. 99-104.

23. Ganeshkumar M, Ponrasu T, Krithika R, Iyappan K, Subramani Gayathri V, Suguna L. Topical application of *Acalypha indica* accelerates rat cutaneous wound healing by up-regulating the expression of type 1 and 3 collagen. *Journal of Ethnopharmacology*. 2012; 142: p. 14-22.

24. Lingaraju G, Krishna V, Joy Hoskeri H, Pradeepa K, Suresh Babu P. Wound healing activity of stem bark extract of *Semecarpus anacardium* using rats. *Natural Producs Research*. 2012; 26(24): p. 2344-2347.

25. Udupa S, Udupa A, Kulkarni D. Influence of *Tridax procumbens* on lysyl oxidase activity and wound healing. *Planta Medica.* 1991; 54(7): p. 325-327.

26. Goyal M, Nagori B, Sasmal D. Wound healing activity of latex of *Euphorbia caducifolia*. *Journal of Ethnopharmacology.* 2012; 144: p. 786-790.

27. Shivhare Y, Singour P, Patil U, Pawar R. Wound healing potential of methanolic exracts of *Trichosanthes dioca Roxb* (fruits) in rats. *Journal of Ethnopharmacology*. 2010; 127: p. 614-619.

28. Silambujanaki P, Bala Tejo Chandra C, Anil Kumar K, Chitra V. Wound Healing activity of *Glycosmis arborea* leaf extract in rats. *Journal of Ethnopharmacology*. 2011; 134: p. 198-201.

29. Mukherjee P, Verpoorte R, Suresh B. Evaluation of in-vivo wound healing activity of *Hypericum patulum* (Family: *Hypericacaea*) leaf extract on different wound model in rats. *Journal of Ethnopharmacology.* 2000; 70: p. 315-321.

30. Saha K, Mukherjee P, Das J, Pal M, Saha B. Wound healing activity of *Leucus lavandulaefolia Rees*. *Journal of Ethnopharmacology.* 1997; 56: p. 139-144.

31. Nagappan T, Chandra Segaran T, Wahid M, Ramasamy P, Vairappan C. Efficacy of carbazole alkaloids,essential oils and extract of *Murraya koenigii* in enhancing subcutaneous wound healing in rats. *Molecules.* 2012; 17: p. 14449-144463.

32. Singh M, Govidarajan R, Nath V, Rawat A, Mehrotra S. Antimicrobial, wound healing and antioxidant activity of *Plagiochasma appendiculatum Lehm. et Lind. Journal of Ethnopharmacology.* 2006; 107: p. 67-72.

33. Shenoy R, Sudheendra A, Nayak P, Paul P, Kutty N, Mallikarjuna Rao C. Normal and delayed wound healing is improved by sesamol, an active constituant of *Sesamum indicum (L.)* in albino rats. *Journal of Ethnopharmacology.* 2011; 133: p. 608-612.

34. Prasad V, Dorle A. Evaluation of ghee based formulation for wound healing activity. *Journal of Ethnopharmacology*. 2006; 107: p. 38-47.

35. Rane M, Mengi S. Comparitive effect of oral administration and topical application of alcoholic extract of *Terminalia arjuna* on incision and excision wounds in rats. *Fitoterapina.* 2003; 74: p. 553-558.

36. Pattanayak S, Sunita P. Wound healing, anti-microbial and anti-oxidant potential of *Dendrophthoe falcata (Lf) Ettingsh*. *Journal of Ethnopharmacology.* 2008; 120: p. 241-246.

37. Reddy B, Reddy R, Naidu V, Mudhusudhana K, Agwane S, Ramakrishna S, *et al.* Evaluationof anti-microbial, antioxidant and wound healing potentials of *Holoptelea integrifolia*. *Journal of Ethnophamocology.* 2008; 115: p. 249-256.

38. Shirwaikar A, Somashekar A, Udupa A, Udupa L, Someshekar S. Wound healing studies of *Aristolochia bracteolata Lam*. with supportive action of antioxidant enzymes. *Phytomedicine*. 2003; 10: p. 558-562.

39. Kim H, Kim J, Park J, Kim S, Uchida Y, Holleran W, *et al.* Water extract of Gromwell (*Lithospermum erythrorhizon*) enhances migration of human keratinocytes and dermal fibroblasts with increased lipid synthesis in an invitro wound scratch model. *Skin Pharmacology and Physiology.* 2012; 25: p. 57-64.

40. Sadaf F, Saleem R, Ahmed M, Ahmed S, Zafar N. Healing potential of cream containing extract of *Sphaeranthus indicus* on dermal wounds in Guinea pigs. *Journal of Ethnopharmacology.* 2006; 107: p. 161-163.

41. Park E, Chun M. Wound healing activity of *Opuntia ficus-indica*. *Finoterpia.* 2001; 72: p. 165-167.

42. Nualkaew S, Rattanamanee K, Thongpraditchote S, Wongkrajang Y, Nahrstedt A. Anti-inflammatory, analgesic and wound healing activities of the leaves of *Memecylon edule Roxb*. *Journal of Ethnopharmacology.* 2009; 121: p. 278-281.

43. Tumen I, Akkol E, Suntar I, Keles H. Wound repair and anti-inflammatory potential of essential oils from cones of *Pinaceae*: Preclinical experimental research in animal models. *Journal of Ethnopharmacology.* 2011; 127: p. 1215-1220.

44. Suntar I, Akkol E, Keles H, Yesilada E, Sarkar S, Arroo R, *et al*. Efficacy of *Daphne oleides subsp. kurdica* used for wound healing: Identification of active compounds through bioassay guided isolation technique. *Journal of Ethnopharmacology*. 2012; 141: p. 1058-1070.

45. Akkol E, Suntar I, Erdogan T, Keles H, Gonec T, Kivcak B. Wound healing and anti-inflammatory properties on Rananculus pedatus and *Rananculus constantinapolitanus*: A comparitive study. *Journal of Ethnophamacology.* 2012; 129: p. 478-484.

46. Guvenc A, Akkol E, Mesud Hurkul M, Suntar I, Keles H. Wound healing and anti-inflammatory activities of the *Michauxia L'Herit* (*Campanulaceae*) specie native to Turkey. *Journal of Ethnophamacology.* 2012; 139: p. 401-408.

47. Suntar I, Tumen I, Ustun O, Keles H, Akkol E. Appraisal on the wound healing and anti-inflammatory activities of the essential oils obtained from the cones and needles of Pinus species by in vivo and in vitro experimental models. *Journal of Ethnophamcology*. 2012; 139: p. 533.

48. Suntar I, Akkol E, Senol F, Keles H, Orhan I. Investigating wound healing, tyrosinase inhibitory and anti-oxidant activities of the ethanol extracts of *Salvia cryptantha* and *Salvia cyancescens* using in vivo and in vitro experimental models. *Journal of Ethnopharmacology.* 2011; 125: p. 71-77.

49. Suntar I, Tatli E, Akkol E, Keles H, Kahraman C, Akdemir Z. An ethnopharmacological study on *Verbascum* species: From conventional wound healing use to scientific verification. *Journal of Ethnopharmacology.* 2010; 132: p. 408-413.

50. Watkins F, Pendry B, Sanchez-Medina A, Corcoran O. Anti-microbial assays of three native british plants used in Anglo-Saxon medicine for wound healing formulations in the 10th century England. *Journal of Ethnopharmacology.* 2012; 144: p. 408-415.

51. Agyare C, Lechtenburg M, Deters A, Petereit F, Hensel A. Ellagitannins from P*hyllanthus muellerianus (Kuntze) Exell*.: Geranin and furosin stimulate cellular activity, differentiation and collagen synthesis of human skin keratinocytes and dermal fibroblasts. *Phytomedicine*. 2011; 18: p. 617-624.

52. Fronza M, Heinzmann B, Hamburger M, Laufer S, Merfort I. Determination of the wound healing effect of *Calendula* extracts using the scratch assay with 3TC fibroblasts. *Journal of Ethnopharmacology.* 2009; 126: p. 463-467.

53. Noormohamed S, Ray T. Effect of 'Compound R" on thermal burn and full-deapth wound contracture in fuzzy rats. *Journal of Burn Care and Rehabilitation.* 1998; 19(3): p. 213-215.

54. Malveira Cavalcanti J, Henrique Leal-Cardosa J, Diniz L, Gomes Portella V, Oliveira Costa C, Linard C, *et al.* The essential of of Croton zehntneri and trans-anethole improves cutaneous wound healing. *Journal of Ethnophamacology.* 2012; 144: p. 240-247.

55. Leite S, Palhano G, Almeida S, Biavatti M. Wound healing activity and sytemic effects of *Vernonia scorpioides* extract in guinea pigs. *Fitoterpia.* 2002; 73: p. 496-500.

56. Schmidt C, Fronza M, Goettert M, Geller F, Luik S, Flores E, *et al*. Biological studies on Brazillian plants used in wound healing. *Journal of Ethnopharmacology.* 2009; 122: p. 523-532.

57. Jorge M, Madjarof C, Ruiz A, Fernandes A, Rodrigues R, Sousa I, *et al*. Evaluation of wound healing properties of *Arrabidaea chica Verlot* extract. *Journal of Ethnopharmacology*. 2008; 118: p. 361-366.

58. Villegas L, Fernandez I, Maldonado H, Torres R, Zavaleta A, Vaisberg A, *et al*. Evaluation of the wound-healing activity of selected traditional medicinal plants from Peru. *Journal of Ethnopharmacology.* 1997; 55: p. 193-200.

59. Moura-Letts G, Villegas L, Marcalo A, Vaisberg A, Hammond G. In Vivo Wound-Healing Activity of Oleanolic Acid Derived from the Acid Hydrolysis of *Anredera diffusa*. *Journal of Natural Products.* 2006; 69: p. 978-979.

60. Gomez-Beloz A, Rucinski J, Balick M, Tipton C. Double incision wound heling bioassay using *Hamelia patens* from El Salvador. *Journal of Ethnopharmacology.* 2003; 88: p. 169-173.

61. Medscape. Experimental animal wound models. [Online].; 2001 [cited 2013 December 5. Available from: http://www.medscape.com/viewarticle/407568_2.

62. Billingham R, Russell P. Studies on wound healing, with special reference to the phenomenon of contracture in experimental wounds in rabbits' skin. *Annals of Surgery*. 1956; 144(6): p. 961-981.

63. Olsen L, Sherratt JA, Maini PK. A mechanochemical model for adult dermal wound contraction. *Journal of Biological Sysytems.* 1995; 3(4): p. 1021-1031.

64. Li J, Chen J, Kirsner R. Pathophysiology of acute wound heling. *Clinics in Dermatology*. 2007; 25: p. 9-18.

65. Howes E, Sooy J, Harvey S. The healing of wounds as determined by their tensile strength. *JAMA*. 1929; 92(1): p. 42-45.

66. White W, Brody G, Glaser A, Marangoni R, Beckwith T, Must J, *et al.* Tensiometric studies of unwounded and wounded skin: results using a standardised testing method. *Annals of Surgery*. 1971; 173(1): p. 19-25.

67. Rovee D, Lowell J, Miller C. A tensiometric analysis of epidermal healing in the plantar skin of guinea pigs. *The Journal of Investigative Dermatology.* 1967; 48(3): p. 266-267.

68. Akkol EK, Koca U, Pesin I, Yilmazer D. Evaluation of the wound heling potential of *Achillea biebersteinii Afan. (Asteraceae)* by In Vivo excision and incision models. *Evidence Based Complimentary and Alternative Medicine.* 2011; 2011: p. 7.

69. Mukherjee P, Mukherjee K, Rajesh Kumar M, Pal M, Saha B. Evaluation of wound healing activity of some herbal formulations. *Phytotherapy Research.* 2003; 17: p. 265-268.

70. Enoch S, Leaper D. Basic science of wound healing. *Surgery*. 2007; 26(2): p. 31-37.

71. Singer A, Clark R. Cutaneous wound healing. *New England Journal of Medicine*. 1999; 341(10): p. 738-746.

72. Eming S, Werner S, Bugnon P, Wickenhauser C, Siewe L, Utermohlen O, et al. Accelerated wound closure in mice deficient for interleukin 10. *The American Journal of Pathology.* 2007; 170(1): p. 188-202.

73. Hanna J, Giacopelli J. A review of wound healing and wound dressing products. *The Journal of Foot and Ankle Surgery.* 1997; 36(1): p. 2-14.

74. Robson M, Steed D, Franz M. Wound healing: biologic features and approaches to maximise healing trajectories. *Current Problems in Surgery*. 2001; 38(2): p. 72-140.

75. Beldon P. Basic science of wound healing. *Surgery.* 2010; 28(9): p. 409-412.

76. Baum C, Arpey C. Normal cutaneous wound healing: Clinical correlation with cellular and molecular events. *Dermatologic Surgery.* 2005; 31(6): p. 674-686.

77. Harrison P, Cramer E. Platelet a-granules. *Blood Reviews.* 1993; 7(1): p. 52-62.

78. Laurens N, Koolwijk P, Maat M. Fibrin structure and wound healing. *Journal of Thrombosis and Haemostasis*. 2006; 4: p. 932-939.

79. Martin P. Wound healing - aiming for perfect skin regeneration. *Science.* 1997; 276: p. 75-81.

80. Werner S, Grose R. Regulation of wound healing by growth factors and cytokines. *Physiology Reviews.* 2003; 83: p. 835-870.

81. Schreier T, Degen E, Baschong W. Fibroblast migration and proliferation during in vitro wound healing. A quantitative comparrison between various growth factors and a low molecular weigth blood dialysate used in clinic to normalise impaired wound healing. *Respiratory Experimental Medicine.* 1993; 193(4): p. 195-205.

82. Ware M, Wells A, Lauffenburger A. Epidermal growth factor alters fibroblast migration speed and directional persistance reciprocally and in a matrix dependent manner. *Journal of Cell Science*. 1998; 111: p. 2423.

83. Usui M, Mansbridge J, Carter W, Fujita M, Olerud J. Keratinocyte migration, proliferation and differentiation in chronic ulcers from patients with diabetes and normal wounds. *Journal of Histochemistry and Cytochemistry*. 2008; 56(7): p. 687-696.

84. O'Toole E. Extracellular matrix and keratinocyte migration. *Clinical and Experimental Dermatology*. 2001; 26: p. 525-530.

85. Paladini R, Takahashi K, Bravo N, Coulombe P. Onset of Re-epithelialisation after skin injury correlates with a reorganisation of keratin filaments in wound edge keratinocytes: Defining a potential role for Keratin 16. *The Journal of Celll Biology.* 1996; 132(3): p. 381-397.

86. Di Marco E, Mathort M, Bondanza S, Cutuli N, Marchisio P, Cancedda R, et al. Nerve growth factor binds to normal human keratinocytes through high and low affinity receptors and stimulates their growth by a novel autocrine loop. *The Journal of Biological Chemistry.* 1993; 268(30): p. 22838-22846.

87. Naldini L, Narsimham R, Guadino G, Zarnegar R, Michaelopoulos G, Comoglio P. Hepatocyte growth factor (HGF) stimulates tyrosine kinase activity of the receptor encoded by the proto-oncogene c-MET. *Oncogene.* 1991; 6(4): p. 501-504.

88. Young A, McNaught C. The physiology of wound healing. *Surgery.* 2011; 29(10): p. 475-479.

89. Faler B, Macsata R, Plummer D, Mishra L, Sidaway A. Transforming growth factor B and wound healing. *Perspectives in Vascular Surgery and Endovascular Therapy*. 2006; 18(1): p. 55-62.

90. Schweigerer L. Basic fibroblast growth factor as a wound healing hormone. *TIPS*. 1988; 9: p. 427-428.

91. McGee G, Davidson J, Buckley A, Sommer A, Woodward S, Aquino A, *et al.* Recombinant basic fibroblast growth factor accelerates wound healing. *Journal of Surgical Research*. 1988; 45: p. 145-153.

92. Bao P, Kodra A, Tomic-Canic M, Golinko S, Ehrlich H, Brem H. The role of vascular endothelial growth factor in wound healing. *Journal of Surgical Research.* 2009; 153(2): p. 347-358.

93. Colwell A, Beanes S, Dang C, TIng K, Longaker M, Atkinson J, *et al*. Increased angiogenesis and expression of vascular endothelial growth factor during scarless repair. *Plastic and Reconstructive Surgery.* 2005; 115(1): p. 204-212.

94. Berg D, Leach M, Kuhn R, Rajewsky K, Muller W, Davidson N. Interleukin 10 but not interleukin 4 is a natural suppressant of cutaneous inflammatory responces. *Journal of Experimental Medicine.* 1995; 182(1): p. 99-108.

95. Sato Y, Ohshima T, Kondo T. Regulatory role of endogenous interleukin 10 in cutaneous inflammatory responce of murine wound healing. *Biochemical and Biophysical research communications.* 2002; 265(1): p. 194-199.

96. Ashcroft G, Jeong M, Ashworth J, Hardman M, Jin W, Moutsopoulos N, et al. Tumor necrosis factor-alpha (TNF-a) is a therapeutic target for impaired cutaneous wound healing. *Wound Repair and Regeneration.* 2012; 20(1): p. 38-49.

97. Rapala K. The effect of tumor necrosis factor alpha on wound healing. An experimental study. *Annals of Chirig and Gynaecology Supplementary.* 1996; 211: p. 1-53.

98. Feiken E, Romer J, Eriksen J, Lund L. Neutrophils express tumor necrosis factor - a during mouse skin wound healing. *Journal of Investigative Dermatology.* 1995; 105: p. 120-123.

99. Steenfos H, Hunt T, Scheuenstuhl H, Goodson W. Selective effects of tumor necrosis factor-alpha on wound healing in rats. *Surgery.* 1989; 106(2): p. 171-175.

100. Shinozaki M, Okada Y, Kitano A, Ikeda K, Saika S, Shinozaki M. Impaired cutaneous wound healing with excess granualtion tissue formation in TNF alpha-null mice. *Archives for Dermatological Research.* 2009; 301(7): p. 531-537.

101. O'Driscoll S, Marx R, Beaton D, Miura Y, Gallay S, Fitzsimmons J. Validation of a simple histological-histochemical cartilage scoring system. *Tissue Engineering.* 2001; 7(3): p. 313-320.

102. Kesava Reddy G, Enwemeka C. A simplified method for the analysis of hydroxyproline in biological tissues. *Clinical Biochemistry.* 1996; 29(3): p. 225-229.

103. Henriques A, Jackson S, Cooper R, Burton N. Free radical production and quenching in honeys with wound healing potential. *Journal of Antimicrobial Chemotherapy*. 2006; 58: p. 773-777.

104. Gordillo G, Sen C. Revisiting the essential role of oxygen in wound healing. *The American Journal of Surgery.* 2003; 186(3): p. 259-263.

105. Houghton P, Hylands P, Mensah A, Hensel A, Deters A. In vitro tests and ethnopharmacological investigations: wound healing as an example. *Journal of Ethnopharmacology.* 2005; 100(1-2): p. 100-107.

106. Sen C, Khanna S, Gordillo G, Bagchi D, Bagchi M, Roy S. Oxygen, oxidants and anti-oxidants in wound healing. *Annals of the New York Acadamy of Sciences.* 2002; 957: p. 239-249.

107. Rasik A, Shukla A. Anti-oxidant status in delayed healing type of wounds. *International Journal of Experimental Pathology*. 2000; 81(4): p. 257-263.

108. Ulrich-Merzenich G, Panek D, Zeitler H, Vetter H, Wagner H. Drug development from natural products: Exploiting synergistic effects. *Indian Journal of Experimental Biology.* 2010; 48: p. 208-219.

109. Ilodigwe E, Ndunganu L, Ajaghaku D, Utoh-Nedosa U. Evaluation of the wound healing of a polyhermal remedy. *Annals of Biological Research*. 2012; 3(11): p. 5393-5398.

110. Evans W. Trease and Evans Pharmacognosy London: Elsevier; 2009.

111. Hutchings A. Zulu Medicinal Plants – An Inventory. 1st ed. Durban: University of Natal Press; 1996.

112. Van Wyk B, Van Oudtshoorn B, Gericke N. Medicinal Plants of South Africa. 1st ed. Johannesburg: Briza Publications; 1997.

113. Fawole O, Amoo S, Ndhlala A, Light M, Finnie J, van Staden J. Anti-inflammatory, anticholinesterase, antioxidant, and phytochemical properties of medicinal plants used for pain-related ailments in South Africa. *Journal of Ethnopharmacology*. 2010; 127(2): p. 235-241.

114. Steyn D. Vergifting van mens en dier. 1st ed. Pretoria: Van Skyk Publishing; 1949.

115. Rose E. Senecio Species: Toxic Plants used as food and Medicine in the Transkei. *South African Medical Journal.* 1972; 46: p. 1039-1043.

116. McLean E. The toxic actions of pyrrolizidine (senecio) alkaloids. *Pharmacological Reviews*. 1970; 22(4): p. 429-483.

117. Deinzer M, Thomson P, Burgett D, Isaacson D. Pyrrolizidine Alkaloids: their occurance in honey from tansy ragwort (*Senecio jocobaea L*.). *Science.* 1977; 195(4277): p. 497-499.

118. Elgorashi E, Taylor J, Maes A, van Staden J, De Kimpe A, Verschaeve L. Screening of medicinal plants used in South African traditional medicine for genotoxic effects. *Toxicology Letters.* 2003; 143: p. 195-207.

119. Cheeke P. Toxicity and metabolism of pyrrolizidine alkaloids. *Journal of Animal Science*. 1988; 66: p. 2343-2350.

120. Oh T, Shinogi Y, Lee S, Choi B. Utilization of biochar impregnated with anaerobically digested slurry as slow-release fertilizer. *Journal of Plant Nutrition and Soil Science.* 2013; 000: p. 1-7.

121. McMullen R, Bauza E, Gondran C, Oberto G, Domloge N, Dal Farra C, et al. Image analysis to quantifiy histological and immunofluorescent staining of ex vivo skin and skin cell cultures. *International Journal of Cosmetic Science.* 2010; 32: p. 143-154.

122. Cuttle L, Kempf M, Phillips G, Mill J, Hayes M, Fraser J, *et al.* A porcine deep dermal partial thickness burn model with hypertrophic scarring. *Burns*. 2006; 32(7): p. 806-820.

123. Geever E, Levenson S, Manner G. The role of noncollagenous substances in the breaking strength of experimental wounds. *Surgery*. 1966; 60(2): p. 343-351.

124. Schmid-Wendtner M, Korting H. The pH of the skin surface and its impact on the barrier function. *Skin Pharmacology and Physiology.* 2006; 19(6): p. 296-302.

125. Hachem J, Crumrine D, Fluhr J, Brown B, Feingold K, Elias P. pH directly regulates epidermal permeability barrier homeostasis, and stratum corneum integrity/cohesion. *Journal of Investigative Dermatology.* 2008; 121(2): p. 345-353.

126. Lynch S, Nixon J, Colvin R, Antoniades H. Role of platelet-derived growth factor in wound healing: Synergistic effects with other growth factors. *Proceedings of the National Academy of Science.* 1987; 84: p. 7696-7700.

127. Lynch S, Colvin R, Antoniades H. Growth factors in wound healing. Single and synergistic effects on partial thickness porcine skin wounds. *Journal of Clinical Investigation*. 1989; 84(2): p. 640-646.

128. Abercrombie M, Flint M, James D. Wound contraction in relation to collagen formation in scorborotic guinea-pigs. *Journal of Embryology and Experimental Morphology*. 1956; 4(2): p. 167-175.

129. Nimni M, De Guia E, Bavetta L. Collagen, hexosamine and tensile strength of rabbit skin during aging. *The Journal of Investigative Dermatology.* 1960; 47(2): p. 156-158.

130. Nayak B, Pinto Pereira L. Catharanthus roseus flower extract has wound-healing activity in Sprague Dawley rats. *BMC Complementary and Alternative Medicine.* 2006; 6: p. 41.

131. Rasik A, Raghubir R, Gupta A, Shukla A, Dubey M, Srivastava S, *et al*. Healing potential of *Calotropis procera* on dermal wounds in Guinea pigs. *Journal of Ethnopharmacology*. 1999; 68: p. 261-266.

132. Suguna L, Singh S, Sivakumar P, Sampath P, Chandraksan G. Influence of *Terminalia chebula* on dermal wound healing. *Phytotherapy Research.* 2002; 16: p. 227-231.

133. Kokane D, More R, Kale M, Nehete M, Mehendale P, Gadgoli C. Evaluation of wound healing activity of root of *Mimosa pudica*. *Journal of Ethnopharmacology.* 2009; 124: p. 311-315.

134. Rich L, Whittaker P. Collagen and picrosirius red staining: a polarized light assessment of fibrillar hue and spatial distribution. *Brazillian Journal of Morphological Science*. 2005; 22(2): p. 97-104.

135. Borges LF, Taboga SR, Gutierrez PS. Simultaneous observation of collagen and elastin in normal and pathological tissues, analysis of Sirius-red-stained sections by fluorescence microscopy. *Cell Tissue Research*. 2005; 320: p. 551-552.

136. Junqueira L, Bignolas G, Brentani R. Picrosirius staining plus polarization microscopy, a specific method for collagen detection in tissue sections. *Histochemical Journal.* 1987; 11: p. 447-455.

137. Dolber P, Spach M. Conventional and confocal fluorescence microscopy of collagen fibers of the heart. *The Journal of Histochemistry and Cytochemistry.* 1993; 41(3): p. 465-469.

138. Madden J, Peacock E. Studies on the biology of collagen during wound healing. *Annals of Surgery*. 1971; 174(3): p. 511-518.

139. Kumana C, Hsiang J, Ko W, Wu P, Todd D. Herbal tea induced hepatic veno-occlusive disease: quantification of toxic alkaloid exposure in adults. *Gut.* 1985; 26: p. 101-104.

140. Schoental R. Toxicology and Carcinogenic action of pyrrolizidine alkakloids. *Cancer Research.* 1968; 28: p. 2237-2246.

141. Zuckerman M, Steenkamp V, Stewart M. Hepatoc veno-occlusive disease as a result of a traditional remedy: confirmatio of toxic pyrrolizidine alkaloids as the cause, using an in vitro technique. *Journal of Clinical Pathology*. 2002; 55: p. 676-679.

142. Mattocks A, White I. Pyrrolic metabolites from non-toxic pyrrolizidine alkaloids. *Nature - New Biology.* 1971; 231: p. 114-115.

143. Brauchli J, Luthy J, Zweifel U, Schlatter C. Pyrrolizidine alkaloids from Symphytum officinale L. and their percutaneous absorption in rats. *Experientia*. 1982; 24: p. 466-468.

144. Toma W, Trigo J, de Paula A, Brito A. Modulation of gastrin and epifermal growth factor by pyrrolizidine alkaloids obtained from Senecio brasiliensis in acute and chronic induced gastric ulcers. *Canadian Journal of Physiology and Pharmacology.* 2004; 82: p. 319-325.

145. Dinh T. Emerging treatments in Diabetic Wound Care. [Online].; 2002 [cited 2014 April 21. Available from: http://www.medscape.com/viewarticle/430888_3.

146. Robson M, Mustoe T. The future of recombinant growth factors in wound healing. *The American Journal of Surgery.* 1998; 176(Suppl 2A): p. 80S-82S.

147. Carter C, Jolly D, Warden Sr C, Hendren D, Kane C. Platelet-rich plasma gel promotes differentiation and regeneration during equine wound healing. *Experimental and Molecular Pathology.* 2003; 74: p. 244-255.

148. Okumura K, Kiyohara Y, Komada F, Iwakawa S, Hirai M, Fuwa T. Improvement in wound healing by epidermal growth factor (EGF) ointment. I. Effect of Nafamostat, Gabexate, or Gelatin on stabilization and efficacy of EGF. *Pharmaceutical Research*. 1990; 7(12): p. 1289-1293.

149. Dogan S, Demirer S, Kepenekci I, Erkek B, Kiziltay A, Hasirci N, *et al.* Epidermal growth factor-containing wound closure enhances wound healing in non-diabetic and diabetic rats. *International Wound Journal.* 2009; 6(2): p. 107-115.

150. Hardwicke J, Schmaljohann D, Boyce D, Thomas. Epidermal growth factor therapy and wound healing – past, present and future perspectives. *The Surgeon.* 2008; 6(3).

151. Tsuboi R, Rifkin D. Recombinant basic fibroblast growth factor stimulates wound healing in healing-impaired db/db mice. *Journal of Experimental Medicine.* 1990; 172: p. 245-251.

152. Fu X, Shen Z, Chen Y, Xie J, Guo Z, Zhang M, et al. Recombinant bovine basic fibroblast growth factor accelerates wound healing in patients with burns, donor sites and chronic dermal ulcers. *Chinese Medical Journal.* 2000; 113(4): p. 367-371.

153. Uhl E, Barker J, Bondar I, Galla T, Leiderer R, Lehr H, *et al*. Basic fibroblast growth factor accelerates wound healing in chronically ischaemic tissue. *British Journal of Surgery.* 1992; 80(8): p. 977-980.

154. Oda Y, Kagami H, Ueda M. Accelerating effects of basic fibroblast growth factor on wound healing of rat palatal mucosa. *Journal of Oral and Maxillofacial Surgey.* 2004; 62: p. 73-80.

155. Kawai K, Suzuki S, Tabata Y, Nishimura Y. Accelerated wound healing through the incorporation of basic fibroblast growth factor-impregnated gelatin microspheres into artificial dermis using a pressure-induced decubitus ulcer model in genetically diabetic mice. *Journal of Plastic and Aesthetic Surgery.* 2005; 58(8): p. 1115-1123.

156. Suh D, Hunt T, Spencer E. Insulin-like growth factor-I reverses the impairment of wound healing induced by corticosteroids inrats. *Endocrinology.* 131: 2399-2403. 1992; 131: p. 2399-2403.

157. Todorović V, Peško P, Micev M, Bjelović M, Budeč M, Mićić M, *et al.* Insulin-like growth factor-I in wound healing of rat skin. *Regularory Peptides*. 2008; 150: p. 7-13.

158. Pierce G, Mustoe T, Senior R, Reed J, Griffin G, Thomason A, *et al*. In vivo incisional wound healing augmented by platelet-derived growth factor and recombinant c-sis gene homodimeric proteins. *Journal of Experimental Medicine.* 1988; 167: p. 974-987.

159. Beer H, Longaker M, Werner S. Reduced expression of PDGF and PDGF receptors during impaired wound healing. *Journal of Investigative Dermatology.* 1997; 109(2): p. 132-138.

160. Deuel T. Growth factors, wound healing, and neoplasia platelet-derived growth factor as a model cytokine. *The International Journal of Cell Cloning.* 1991; 9(S1): p. 60-71.

161. Todd R, Donoff B, Chiang T, Chou M, Elovic A, Gallagher G, *et al.* The eosinophil as a cellular source of transforming growth factor alpha in healing cutaneous wounds. *American Journal of Pathology.* 1991; 138(6): p. 1307-1313.

162. Hakvoort T, Altun V, van Zuijlen P, de Boer W, van Schadewij W, van der Kwast T. Transforming growth factor-beta(1), -beta(2), -beta(3), basic fibroblast growth factor and vascular endothelial growth factor expression in keratinocytes in burn scars. *European Cytokine Network*. 2000; 11(2): p. 233-239.

163. Theoret C. Update on Wound Repair. *Clinical Techniques in Equine Practice.* 2004; 3: p. 110-122.

164. Mercado A, Padgett D, Sheridan J, Marucha P. Altered kinetics of IL-1α, IL-1β, and KGF-1 gene expresson in early wounds of restrained mice. *Brain, Behavior, and Immunity*. 2002; 16: p. 150-162.

165. Bai R, Wan L, Shi M. The time-dependant expressions of IL-1β, COX-2, MCP-1, mRNA in skin wounds of rabbits. *Forensic Science International.* 2008; 175: p. 193-197.

166. Bryan D, Walker K, Ferguson M, Thorpe R. Cytokine expression in a murine wound healing model. *Cytokine.* 2005; 31: p. 429-438.

167. Lemmon M, Schlessinger J. Cell signalling by receptor tyrosine kinases. *Cell*. 2010; 141: p. 1117-1134.

168. Monteiro H, Arai R, Travassos L. Protein tyrosine phosphorylation and protein tyrosine nitration in redox signalling. *Antioxidants and Redox Signalling.* 2008; 10(5): p. 843-889.

169. Schlessinger J. Cell signalling by receptor tyrosine kinases. *Cell.* 2000; 103: p. 211-225.

170. Fantl W, Johnson D, Williams L. Signalling by receptor tyrosine kinases. *Annual review of Biochemistry*. 1993; 62: p. 453-481.

171. Bennasroune A, Gardin A, Aunis D, Cremel G, Hubert P. Tyrosine kinase receptors as attractive targets of cancer therapy. *Critical Reviews in Oncology/Hematology.* 2004; 50: p. 23-38.

172. Marshall C. Specificity of tyrosine kinase signalling: Transient versus sustained extracellualr signal-regulated kinase activation. *Cell.* 1995; 80: p. 179-185.

173. Morrison D. MAP kinase Pathways. *Cold Spring Harbor Perspectives in Biology*. 2012; 4: p. a011254.

174. Sekiya F, Poulin B, Kim Y, Rhee S. Mechanism of tyrosine phosphorylation and activation of phospholipase C-y1. *The Journal of Biochemical Chemistry.* 2004; 279-31: p. 32181-32190.

175. Penneys N, Bogaert M, Serfing U, Sisto M. PCNA expression of cutaneous neoplasms and Verruca Vulgaris. *American Journal of Pathology.* 1992; 141(1): p. 139-142.

176. Wang S, Nakajima Y, Yu Y, Xia W, Chen C, Yang C, *et al.* Tyrosine phosphorylation controls PCNA function through protein stability. *Nature Cell Biology.* 2006; 8: p. 1359-1368.

177. Zhao H, Lo Y, Ma L, Waltz S, Gray J, Hung M, *et al.* Targeting tyrosine phosphorylation of PCNA inhibits prostate cancer growth. *Molecular Cancer Therapeutics.* 2011; 10(1): p. 29-36.

178. Lo Y, Ho P, Wang S. Epidermal growth factor receptor protects proliferating cell nuclear antigen from Cullin 4A protein-mediated proteolysis. *The Journal of Biological Chemistry.* 2012; 287(32): p. 27148-27157.

179. Hergott G, Kalnins V. Expression of proliferating cell nuclear antigen in migrating retinal pigmant epithelial cells during wound healing in organ culture. *Experimental Cell Research.* 1991; 195(2): p. 307-314.

180. Unemori E, Ehsani N, Wang M, Lee S, Mcguire J, Amento E. Inteleukin-1 and transforming growth factor-α: synergistic stimulation of metalloproteinases, PGE2, and proliferation in human fibroblasts. *Experimental Cell Research.* 1994; 210(2): p. 166-171.

181. Saunder D, Kilian P, Mclane J, Quick T, Jakubovic H, Davis S, et al. Interleukin-1 enhances epidermal wound healing. *Lymphokine Research*. 1990; 9(4): p. 465-473.

182. Wilson S, He Y, Weng J, Li Q, McDowall A, Vital M, *et al.* Epithelial injury induces keratinocyte apoptosis: hypothesized role for the interleukin-1 system in the modulation of corneal tissue organization and wound healing. *Experimental Eye Research.* 1996; 62(4): p. 325-338.

183. Berthier R, Rizzitelli A, Martinon-Ego C, Laharie A, Collin V, Chesne S, *et al.* Fibroblasts inhibit the production of interleukin-12p70 by murine dendritic cells. *Immunology.* 2003; 108(3): p. 391-400.

184. Stout R, Jiang C, Matta B, Tietzel I, Watkins S, Suttles J. Macrophages sequentially change their functional phenotype in response to changes in microenvironmental influences. *The Journal of Immunology.* 2005; 175: p. 342-349.

185. Verma N, Boyd R, Robinson C, Tran G, Hall B. Interleukin-12p70 prolongs allograft survival by induction of interferon gamma and nitric oxide production. *Transplantation.* 2006; 82(10): p. 1324-1333.

186. Mc Farland-Mancini M, Funk H, Paluch A, Zhou M, Giridhar V, Mercer C*, et al.* Diferences in wound healing in mice with deficiency of IL-6 versus IL-6 receptor. *The Journal of Immunology.* 2010; 184: p. 7219-7228.

187. Ebihara T, Matsuda A, Nakamura S, Matsuda H, Murakami A. Role of IL-6 classic and trans signalling pathways in corneal sterile inflammation and wound healing. *Cornea.* 2011; 52(12): p. 8549-8557.

188. Yoon K, Jeong I, Park Y, Yang S. Interleukin 6 and tumor necrosis factor-alpha levels in tears of patients with dry eye syndrome. *Cornea.* 2007; 26: p. 431-437.

189. Simon D, Denniston A, Tomlins P. Soluble gp130, an antagonist of IL-6 trans-signaling, is elevated in uveitis aqueous humor. *Investigative Opthalmology.* 2008; 49: p. 3988-3991.

190. Baggiolini M, Clark-Lewis I. Interleukin-8, a chemotactic and inflammatory cytokine. *FEBS letters.* 1992; 307: p. 97-101.

191. Kleinbeck K, Faucher L, Weiyuan K. Biomaterials modulate interleukin-8 and other inflammatory proteins during reepithelialisation in cutaneous partial thickness wounds in pigs. *Wound Repair and Regeneration*. 2010; 18: p. 486-498.

192. Han Y, Wu T, Hughes M, Garner W. TNF-alpha stimulates activation of pro-MMP2 in human skin through NF-(kappa) B mediated induction of MT1-MMP. *Cell Science*. 2001; 114: p. 131-139.

193. Barrientos S, Stojadinovic O, Golinko M, Brem H. Growth factors and cytokines in wound healing. *Wound Repair and Regeneration*. 2008; 16: p. 585-601.

194. Murphy L, Blenis J. MAPK signal specificity: the right place at the right time. *Trends in Biochemical Sciences.* 2006; 31(5): p. 268-275.

195. Miteva M. Signal transduction in keratinocytes. *Experimental Dermatology*. 1999; 8: p. 96-108.

196. Dotto G. Signal transduction pathways controlling the switch between keratinocyte growth and differentiation. *Critical Reviews in Oral Biology and Medicine.* 1999; 10(4): p. 442-457.

197. Bowman G, O'Donnell M, Kuriyan J. Structural analysis of a eukaryotic sliding sliding clamp-clamp loader complex. *Nature*. 2004; 429(6993): p. 724-730.

198. Wang S, Nakajima Y, Yu Y, *et al.* Tyrosine phosphorylation controls PCNA function through protein stability. *Nature Cell Biology.* 2006; 8(12): p. 1359-1368.

199. Barker J, Mitra R, Griffiths C, Dixit V, Nickoloff B. Keratinocytes as intiators of inflammation. *The Lancet*. 1991; 337: p. 211-214.

200. Singleton V, Rossi J. Colorimetry of total phenolics with phosphomolybdic-phosphotungstic acid reagents. *The American Journal of Enology and Viticulture.* 1965; 16: p. 144-158.

201. Suntar I, Akkol E, Keles H, Yesilada E, Sarkar S, Baykal T. Comparitive evaluation of the traditional prescriptions from *Cichorium intybus L.* for wound healing: Stepwise isolation of an active component by in vivo bioassay and its mode of activity. *Journal of Ethnopharmacology.* 2012; 143: p. 229-309.

202. NIST. National Institute of Standards and Technology (NIST). [Online].; 2011 [cited 2014 July. Available from: http://webbook.nist.gov/chemistry/name-ser.html#Top.

203. Dewhurst J, Kaminski J, Supple J. Mass spectra of some tropane and tropidine derivitives. *Journal of Heterocyclic Chemistry.* 1972; 9: p. 507-511.

204. Ruan J, Li N, Xia Q, Fu P, Peng S, Ye Y, et al. Charactersitic ion clusters as determinants for the identification of pyrrolizidine alkaloid N-oxides in pyrrolizidine alakloid-containg natural products using HPLC-MS analysis. *Journal of Mass spectrometry*. 2012; 47(3): p. 331-337.

205. Scheubert K, Hufsky F, Bocker S. Computational mass spectrometry for small molecules. Journal of Cheminformatics. 2013; 5(12): http://www.jcheminf.com/content/5/1/12.

206. Fales H, Lloyd H, Milne G. Chemical ionisation mass spectrometry of complex molecules. II. Alkaloids. *Journal of the American Chemical Society*. 1970; 92(6): p. 1590-1597.

207. Liang C, Park A, Guan J. In-vitro scratch assay: a convenient and inexpensive method for analysis of cell migration in vitro. *Nature Protocols.* 2007; 2: p. 329-333.

208. Al-Nasiry S, Geusens N, Hanssens M, Luyten C, Pijnenborg R. The use of Alamar blue assay for quantitative analysis of viability, migration and invasion of choriocarcinoma cells. *Human Reproduction.* 2007; 22(5): p. 1304-1309.

209. Byth H, Mchunu B, Dubery I, Bornman L. Assessment of a simple, non-toxic alamar blue cell survival assay to monitor tomato cell viability. *Phytochemical Analysis*. 2001; 12: p. 340-346.

210. Kawaii S, Tomono Y, Katase E, Ogawa K, Yano M. Anti-proliferative activity of flavonoids on several cancer cell lines. *Journal of Bioscience, Biotechnology and Biochemistry.* 1999; 63(5): p. 896-899.

211. Sevilmi-Gur C, Onbasilar I, Atilla P, Genc R, Cakar N, Deliloglu-Gurhan I, *et al.* In vitro growth stimulatroy and in vivo wound healing studies on cycloartane-type saponins of *Astogalus* genus. *Journal of Ethnopharmacology*. 2011; 134(3): p. 844-850.

212. Macarron R, Hertzberg R. Design and implementation of high throughput screening assays. *Springer Protocols - Methods in Molecular Biology*. 2002; 190: p. 1-29.

213. Yarrow J, Perlman Z, Westwood N, Mitchison T. A high-throughput cell migration assay using scratch wound healing, a comparison of image-based readout methods. *BMC Biotechnology.* 2004; 4(21): p. Open Access. http://www.biomedcentral.com/1472-6750/4/21.

214. Martis E, Radhakarishnan R, Badve R. High-throughput screenin: the hits and leads of drug discovery - an overview. *Journal of Applied Pharmaceutical Science.* 2011; 1(1): p. 2-10.

215. Inglese J, Johnson R, Simeonov A, Xia M, Zheng W, Austin C, *et al.* High-throughput screening assays for the identification of chemical compounds. *Nature - Chemical Biology.* 2007; 3(8): p. 466-479.

216. Hsu S, Bollag W, Lewis J, Huang Q, Singh B, Sharawy M, *et al*. Green tea polyphenols induce differentiation and proliferation in epidermal keratinocytes. T*he journal of pharacology and experimental therapeutics.* 2003; 306(1): p. 29-34.

217. Crews C, Berthlier F, Krska R. Update on analytical methods for toxic pyrrolizidine alkaloids. *Ananyltical and Bioanalytical Chemistry.* 2010; 396: p. 327-338.

218. Colgate S, Gardner D, Joy R, Betz J, Panter K. Dehydropyrrolizidine alkaloids, including monoesters with an unusual esterifying acid, from cultivated *Crotalaria juncea* (Sunn Hemp cv. "tropic sun"). *Journal of Agriculture and Food Chemistry.* 2012; 60: p. 3541-3550.

219. Boppre M, Colegate S, Edgar J. Pyrrolizidine alkloids of *Echium vulgare* honey found in pure pollen. *Journal of Agricultural and Food Chemistry.* 2005; 53: p. 594-600.

220. Yoshimatsu K, Kiuchi F, Shimomura K, Makino Y. A rapid and reliable solid-phase extraction method for high-performance liquid chromatographic analysis of opium alkaloids from *Papaver* plants. *Chemical and Pharmaceutical Bullitin*. 2005; 53(11): p. 1446-1450.

221. Zwir-Ference A, Bizuik M. Solid phase extraction technique - trends oppertunities and applications. *Polish Journal of Environmental Studies.* 2006; 15(5): p. 677-690.

222. Popl M, Fahnrich J, Tatar V. Chromatographic Analysis of Alkaloids, Chromatographic Science Series New York: CRC Press, Marcel Dekker Inc.; 1990.

223. Tundis R, Loizzo M, Statti G, Passalacqua N, Peruzzi L, Menichini F. Pyrrolizidine alkaloid profiles of the *Senecio cineraria* Group (*Asteraceae*). *Verlag der Zeitschrift fyr Naturforschung.* 2007; 62: p. 467-472.

224. El-Shazly A. Pyrrolizidine alkaloid profiles of some *Senecio* species from Egypt. *Verlag der Zeitschrift fur Naturforschung*. 2002; 57: p. 429-433.

225. Rizk A. Naturally Occuring Pyrrolizidine Alkaloids Florida: CRC Press Inc; 1990.

226. Witte L, Rubiolo P, Bicchi C, Hartmann T. Comparitive analysis of pyrrolizidine alakloids from natural sources by gas chromatography-mass spectrometry. *Phytochemistry*. 1993; 32(1): p. 187-196.

227. Schmidt J, Raith K, Boettcher C, Zenk M. Analysis of benzylisoquinoline-type alkaloids by electrospray tandem mass spectrometry and atmospheric pressure photoionisation. *Mass Spectrometry*. 2005; 11: p. 325-333.

228. Wu-Nan W, Cheng-Hong H. Structural Elucidation of Isoquinoline, Isoquinolone, Benzylisoquinoline, Aporphine, and Phenanthrene alkaloids using API-ionspray tandem mass spectrometry. *The Chinese Pharmaceutical Journal.* 2006; 58: p. 41-55.

UNIVERSITY OF THE WITWATERSRAND, JOHANNESBURG

STRICTLY CONFIDENTIAL

ANIMAL ETHICS SCREENING COMMITTEE (AESC)

CLEARANCE CERTIFICATE NO. 2008/15/ 4

APPLICANT: Mr. A Gould

SCHOOL: Surgery
DEPARTMENT:
LOCATION:

PROJECT TITLE: **Altered wound healing in the presence of Drimia robusta and Senecio serratuloides extracts**

Number and Species

3 large white pig for a pilot study

Approval was given for to the use of animals for the project described above at an AESC meeting held on 20080326. This approval remains valid until 20100326

The use of these animals is subject to AESC guidelines for the use and care of animals, is limited to the procedures described in the application form and to the following additional conditions:

Signed: _____ (Chairperson, AESC) Date: 02/04/08

I am satisfied that the persons listed in this application are competent to perform the procedures therein, in terms of Section 23 (1) (c) of the Veterinary and Para-Veterinary Professions Act (19 of 1982)

Signed: _____ (Registered Veterinarian) Date: 02/04/08

cc: Supervisor: Geoffrey Candy
Director: CAS

Works 2000/lain0015/AESCCert.wps